



Chalmers, Fiona (2016) Improving protein yield from mammalian cells by manipulation of stress response pathways. PhD thesis

<http://theses.gla.ac.uk/7666/>

Copyright and moral rights for this thesis are retained by the author

A copy can be downloaded for personal non-commercial research or study, without prior permission or charge

This thesis cannot be reproduced or quoted extensively from without first obtaining permission in writing from the Author

The content must not be changed in any way or sold commercially in any format or medium without the formal permission of the Author

When referring to this work, full bibliographic details including the author, title, awarding institution and date of the thesis must be given

Improving protein yield from mammalian cells by manipulation of stress response pathways

Fiona Chalmers (BSc Hons, MRes)

Supervised by Prof Neil Bulleid and Dr Katharine Cain

A thesis submitted in fulfilment of the requirements for the degree
of Doctor of Philosophy

Institute of Molecular, Cell and Systems Biology
College of Medical, Veterinary and Life Sciences
University of Glasgow

July 2016

Abstract

Monoclonal antibodies are a class of therapeutic that is an expanding area of the lucrative biopharmaceutical industry. These complex proteins are predominantly produced from large cultures of mammalian cells; the industry standard cell line being Chinese Hamster Ovary (CHO) cells. A number of optimisation strategies have led to antibody titres from CHO cells increasing by a hundred-fold, and it has been proposed that a further bottleneck in biosynthesis is in protein folding and assembly within the secretory pathway. To alleviate this bottleneck, a CHO-derived host cell line was generated by researchers at the pharmaceutical company UCB that stably overexpressed two critical genes: XBP1, a transcription factor capable of expanding the endoplasmic reticulum and upregulating protein chaperones; and Ero1 α , an oxidase that replenishes the machinery of disulphide bond formation. This host cell line, named CHO-S XE, was confirmed to have a high yield of secreted antibody.

The work presented in this thesis further characterises CHO-S XE, with the aim of using the information gained to lead the generation of novel host cell lines with more optimal characteristics than CHO-S XE. In addition to antibodies, it was found that CHO-S XE had improved production of two other secreted proteins: one with a simple tertiary structure and one complex multi-domain protein; and higher levels of a number of endogenous protein chaperones. As a more controlled system of gene expression to unravel the specific roles of XBP1 and Ero1 α in the secretory properties of CHO-S XE, CHO cells with inducible overexpression of XBP1, Ero1 α , or a third gene involved in the Unfolded Protein Response, GADD34, were generated. From these cell lines, it was shown that more antibody was secreted by cells with induced overexpression of XBP1; however, Ero1 α and GADD34 overexpression did not improve antibody yield. Further investigation revealed that endogenous XBP1 splicing was downregulated in the presence of an abundance of the active form of XBP1. This result indicated a novel aspect of the regulation of the activity of IRE1, the stress-induced endoribonuclease responsible for XBP1 splicing. Overall, the work described in this thesis confirms that the overexpression of XBP1 has an enhancing effect on the secretory properties of CHO cells; information which could contribute to the development of host cells with a greater capacity for antibody production.

Table of contents

Abstract	1
List of figures	5
List of tables	7
Acknowledgements	8
Author's declaration.....	9
Definitions/abbreviations	10
Chapter 1 Introduction	13
1.1 The biopharmaceutical industry.....	14
1.1.1 Therapeutic monoclonal antibodies	14
1.1.2 Overview of therapeutic antibody production	15
1.1.3 Optimisation of therapeutic antibody production.....	16
1.1.4 History of Chinese Hamster Ovary (CHO) cells in bioprocessing.....	18
1.2 Protein folding and disulphide bond formation	22
1.2.1 Structure and folding of antibodies	22
1.2.2 Role of Protein Disulphide Isomerase family members	26
1.2.3 Function and regulation of ER oxidoreductin 1	28
1.3 Quality control and the Unfolded Protein Response.....	30
1.3.1 Calnexin/calreticulin and the glycan code.....	30
1.3.2 ER associated degradation.....	32
1.3.3 The Unfolded Protein Response.....	33
1.3.4 PERK branch	35
1.3.5 ATF6 branch	36
1.3.6 IRE1 branch	37
1.4 Optimisation of protein production.....	40
1.4.1 Increasing productivity via genetic manipulation of folding factors.....	40
1.4.2 Increasing productivity via manipulation of the Unfolded Protein Response	41
1.5 Project aims and objectives	42
Chapter 2 Materials and methods	44
2.1 Materials.....	45
2.1.1 Sources of chemicals, reagents and equipment	45
2.1.2 Solutions.....	45
2.2 Cell culture methods.....	45
2.2.1 Maintenance of cell lines	45
2.2.2 Cell count and viability.....	46
2.2.3 Cryopreservation of cells	46
2.2.4 Thawing cells from frozen stocks	46
2.2.5 Generation of stable cell lines	46
2.2.6 Doxycycline treatment	47
2.2.7 Tunicamycin treatment	47

2.2.8	4 μ 8C treatment	47
2.2.9	Transient transfection.....	47
2.2.10	ER Tracker treatment.....	48
2.2.11	Flow cytometry	48
2.3	DNA methods	49
2.3.1	Subcloning of pTetOne vector.....	49
2.3.2	Plasmid prep.....	49
2.3.3	Agarose gel electrophoresis	49
2.3.4	XBP1 splice assay.....	50
2.4	Molecular methods	50
2.4.1	Cell lysis	50
2.4.2	Preparation of polyacrylamide gels	51
2.4.3	SDS PAGE	51
2.4.4	Western blot.....	51
2.4.5	Protein A affinity purification	52
2.4.6	TCA precipitation	53
2.4.7	Antibody capture ELISA	53
2.5	Statistical methods.....	54
Chapter 3	Characterisation of the high yield cell line CHO-S XE.....	55
3.1	Introduction	56
3.1.1	Generation of a high yield host cell line.....	56
3.1.2	Preliminary characterisation of CHO-S XE.....	57
3.1.3	Objectives.....	59
3.2	Results	61
3.2.1	CHO-S XE-D has a slower rate of growth than CHO-S	61
3.2.2	CHO-S XE-D has a high yield of secreted proteins.....	63
3.2.3	CHO-S XE-D has higher levels of transiently transfected GFP	66
3.2.4	CHO-S XE-D has high levels of endogenous proteins	69
3.2.5	CHO-S XE-D cells are larger than CHO-S	72
3.2.6	CHO-S and CHO-S XE-D have the same amount of ER membrane	73
3.2.7	CHO-S XE-D shows higher cell mortality when transiently transfected	74
3.3	Discussion.....	76
Chapter 4	Effect of inducible gene overexpression on antibody yield.....	82
4.1	Introduction	83
4.1.1	Rationale behind the use of an inducible gene system	83
4.1.2	Inducible CHO-S derived cell lines.....	83
4.2	Results	89
4.2.1	Screening for GOI expression in X1 cells.....	89
4.2.2	Screening for GOI expression in E1 cells.....	91
4.2.3	Screening for GOI expression in G1 cells.	93
4.2.4	Screening for GOI expression in X1-B cells.	94

4.2.5	Screening for GOI expression in EX1 cells.	96
4.2.6	Comparison of induction in XBP1s expressing cell lines	98
4.2.7	Determining altered antibody yield in induced cells.	100
4.2.8	Antibody yield in wild-type CHO-S cells	102
4.2.9	Antibody yield in X1 cells	104
4.2.10	Antibody yield in E1 cells	106
4.2.11	Antibody yield in G1 cells	108
4.2.12	Antibody yield in X1-B cells	110
4.2.13	Antibody yield in EX1 cells	112
4.3	Discussion	114
Chapter 5	Consequence of XBP1s overexpression	118
5.1	Introduction	119
5.1.1	Further investigation of CHO-S X1 and CHO-S X1-B	119
5.1.2	Quantification of XBP1 splicing	120
5.2	Results	122
5.2.1	ER size in XBP1s overexpressing CHO cell lines.	122
5.2.2	Investigation of the loss of BFP in induced X1-B cells	124
5.2.3	The loss of BFP in induced X1-B corresponds to a reduction in blue fluorescence	125
5.2.4	Proteasomal inhibition does not affect the loss of BFP in CHO-S X1-B....	127
5.2.5	Quantification of XBP1 splicing in the presence of tunicamycin	131
5.2.6	Quantification of XBP1 splicing during a transient transfection.....	137
5.2.7	XBP1 splicing in cells treated with the IRE1 inhibitor 4 μ 8C.....	139
5.2.8	Quantification of XBP1S protein in the presence of 4 μ 8C	143
5.2.9	ER amount in the presence of 4 μ 8C	145
5.2.10	Antibody productivity in the presence of 4 μ 8C	147
5.3	Discussion	149
Chapter 6	Discussion.....	153
6.1	Summary of objectives	154
6.1.1	Characterisation of CHO-S XE-D.....	154
6.1.2	Investigation of CHO-S cell lines with inducible gene overexpression	156
6.1.3	Investigation into the biochemistry of XBP1 signalling	161
6.2	Concluding remarks	162
Appendix		163
List of References		164

List of figures

Figure 1-1 - Cartoon of karyotypes from Chinese hamster and CHO DG44 cells.	19
Figure 1-2 - Structure of Immunoglobulin G (IgG).	23
Figure 1-3 - Folding of antibody chains and formation of the IgG tetramer	25
Figure 1-4 - Disulphide bond formation by PDI family members and the role of Ero1 α . .	27
Figure 1-5 - Regulation of Ero1 α activity.	29
Figure 1-6 - The calnexin/calreticulin quality control cycle.....	31
Figure 1-7 - Schematic of the Unfolded Protein Response.	34
Figure 1-8 - Generation of the transcription factor XBP1S by splicing of XBP1 transcripts.	39
Figure 3-1 - CHO-S XE-D has a slower rate of growth than CHO-S.....	62
Figure 3-2 - CHO-S XE-D has a high yield of secreted proteins	65
Figure 3-3 - CHO-S XE-D has higher levels of fluorescence from transiently transfected eGFP.....	68
Figure 3-4 - CHO-S XE-D has high levels of endogenous proteins.....	71
Figure 3-5 - CHO-S XE-D cells are larger than CHO-S.....	72
Figure 3-6 - CHO-S and CHO-S XE-D have the same size of ER membrane	73
Figure 3-7 - CHO-S XE-D shows higher cell mortality when transiently transfected.....	75
Figure 4-1 - Map of pTetOne vector showing activation by doxycycline.	85
Figure 4-2 - Generation of CHO-S derived inducible cell lines.....	88
Figure 4-3 - Screening for XBP1S expression in X1 cells.	90
Figure 4-4 - Screening for Ero1 α expression in E1 cells.....	92
Figure 4-5 - Screening for GADD34 expression in G1 cells.....	93
Figure 4-6 - Screening for XBP1s induction and BFP expression in X1-B cells.	95
Figure 4-7 - Screening for XBP1S and Ero1 α induction in EX1 cells.	97
Figure 4-8 - Comparison of XBP1 induction in X1, X1-B, XE-D and EX1 cells.....	99
Figure 4-9 - Schematic of antibody yield experiments.....	101
Figure 4-10 - Antibody yield from transiently transfected CHO-S cells.	103
Figure 4-11 - Antibody yield from transiently transfected X1 cells.	105
Figure 4-12 - Antibody yield from transiently transfected E1 cells.	107
Figure 4-13 - Antibody yield from transiently transfected G1 cells.....	109
Figure 4-14 - Antibody yield from transiently transfected X1-B cells.....	111
Figure 4-15 - Antibody yield from transiently transfected EX1 cells.....	113
Figure 5-1 - cDNA products generated by RT-PCR XBP1 splicing assay.	121
Figure 5-2 - ER expansion is triggered by doxycycline in XBP1s inducible cell lines.....	123
Figure 5-3 - BFP is depleted by XBP1s overexpression in X1-B cells.	124
Figure 5-4 - BFP fluorescence in CHO-S X1-B cells is reduced by XBP1s induction or treatment with tunicamycin.	126
Figure 5-5 - Proteasome inhibition does not block the depletion of BFP in induced X1-B cells.	128

Figure 5-6 - XBP1S protein levels with proteasome inhibition.	130
Figure 5-7 - Endogenous XBP1 splicing in tunicamycin treated cells.	132
Figure 5-8 - Total XBP1 transcripts in tunicamycin treated cells.	134
Figure 5-9 - Endogenous XBP1 splicing in CHO-S and CHO-S XE-D cells treated with tunicamycin.	136
Figure 5-10 - Endogenous XBP1 splicing in transiently transfected cells.	138
Figure 5-11 - Endogenous XBP1 splicing in X1-B cells treated with the IRE1 inhibitor 4 μ 8C.	140
Figure 5-12 - Total XBP1 transcripts in X1-B cells treated with the IRE1 inhibitor 4 μ 8C.	142
Figure 5-13 - XBP1S protein levels in cells treated with 4 μ 8C.	144
Figure 5-14 - ER size in 4 μ 8C treated cells.	146
Figure 5-15 - Antibody productivity in CHO-S X1-B cells treated with 4 μ 8C.	148

List of tables

Table 1 - Summary of differences between CHO-S and CHO-S XE-D.	81
Table 2 - Primers	163

Acknowledgements

This thesis represents three and a half years of work in the Bulleid lab towards achieving my PhD, work which could not have been accomplished without the support and contributions of others. I am indebted to my academic supervisor, Prof Neil Bulleid, first of all for giving me the opportunity to do this PhD, and for supporting me throughout with advice, encouragement, and generally being a good mentor. I am grateful to my industrial supervisor, Dr Katharine Cain, as well as Dr Paul Stephens and Dr David Humphreys at UCB, for their resources, support and invaluable discussions.

I would also like to thank Prof Bill Cushley for being my mock viva examiner and for teaching me flow cytometry, and Dr Jo Mountford and the members of lab 332 for letting me use their flow cytometer. I am grateful for the contribution of Dr Erik Snapp in donating the ER-BFP construct. I also thank the BBSRC Bioprocessing Research Industry Club (BRIC) for funding of my PhD, and for the opportunity to attend and present my work at BRIC dissemination events.

I've enjoyed my time in the Bulleid lab and I'm grateful for the support of fellow lab members, past and present: Chloe Stoye, Esraa Haji, Tomasz Szmaja, Dr Greg Poet, Dr Rachel Martin, Dr Phil Robinson, Dr Ojay Oka, Dr Marcel van Lith, Dr Zhenbo Cao and Donna McGow. Special thanks go to Marie Anne Pringle for cloning of the pTetOne vector and general technical wizardry throughout the project. All of the morning tea breaks, afternoon chats and Friday pub visits made the stress and hard work a lot more enjoyable.

Finally, I would like to thank my family for all their love and support throughout my PhD: my parents, Bob and Christine, and my brothers, Colin and Iain. I couldn't have done any of this without them.

Author's declaration

I declare that, except where explicit reference is made to the contribution of others, this thesis is the result of my own work and has not been submitted for any other degree at the University of Glasgow or any other institution.

Fiona Chalmers

July 2016

Definitions/abbreviations

4 μ 8C	8-formyl-7-hydroxy-4-methylcoumarin
α 1AT	Alpha 1 anti-trypsin
aa	Amino acid
Ab	Antibody
APS	Ammonium persulphate
ATF4	Activating transcription factor 4
ATF6	Activating transcription factor 6
ATP	Adenosine triphosphate
BiP	Heavy chain binding protein
BFP	Blue fluorescent protein
bp	Base pairs
cAMP	Cyclic adenosine monophosphate
CD CHO	Chemically defined CHO medium
cDNA	Complementary DNA
CH1	Constant heavy domain 1
CHO	Chinese hamster ovary
CHO-S	Chinese hamster ovary suspension
CHOP	CCAAT enhancer binding protein homologous protein
CL	Constant light domain
DEPC	Diethylpyrocarbonate
DHFR	Dihydrofolate reductase
DMEM	Dulbecco's modified eagle medium
DMSO	Dimethylsulfoxide
DNA	Deoxyribonucleic acid
Dox	Doxycycline
DTT	Dithiothreitol
E1	CHO-S Ero1-pTetOne
EDEM	ER degradation enhancing α -mannosidase like protein
EDTA	Ethylenediaminetetraacetic acid
eIF2 α	Eukaryotic translation initiation factor 2A
ELISA	Enzyme linked immunosorbent assay

ER	Endoplasmic reticulum
ERAD	Endoplasmic reticulum associated degradation
Ero1 α	Endoplasmic reticulum oxidoreductase alpha
ERp57	Endoplasmic reticulum protein 57
Fab	Antigen binding fragment
FACS	Fluorescence activated cell sorting
Fc	Crystallised fragment
FDA	Food and drug administration
FITC	Fluorescein isothiocyanate
G1	CHO-S GADD34-pTetOne (also, gap phase 1)
GADD34	Growth and DNA damage inducible protein 34
GAPDH	Glyceraldehyde 3-phosphate dehydrogenase
GFP	Green fluorescent protein
GPX7	Glutathione peroxidase 7
GS	Glutamine synthetase
GSH	Glutathione
GSSG	Glutathione disulphide
HBSS	Hank's balanced salt solution
HC	Heavy chain
HEK293	Human embryonic kidney 293
IgG	Immunoglobulin G
IRE1	Inositol requiring enzyme
kDa	Kilodalton
KDEL	Lysine - aspartic acid - glutamic acid - leucine
LB	Luria-Bertani broth
LC	Light chain
mRNA	Messenger RNA
MTX	Methotrexate
NaBu	Sodium butyrate
NEB	New England Biolabs
NEM	N-ethylmaleimide
OD	Optical density

ORF	Open reading frame
PBS	Phosphate buffered saline
PCR	Polymerase chain reaction
PDI	Protein disulphide isomerase
PERK	Protein kinase like endoplasmic reticulum kinase
PMSF	Phenylmethane sulfonyl fluoride
PP1	Protein phosphatase 1
PPIase	Peptidyl prolyl isomerase
PRDX4	Peroxiredoxin 4
RNA	Ribonucleic acid
S/MAR	Scaffold/matrix attachment region
SDS	Sodium dodecyl sulphate
SDS PAGE	SDS polyacrylamide gel electrophoresis
TAE	Tris, acetic acid, EDTA
TBS	Tris buffered saline
TBST	Tris buffered saline with tween
TEMED	Tetramethylethylenediamine
Tn	Tunicamycin
TNF α	Tumour necrosis factor alpha
tPA	Tissue plasminogen activator
tRNA	Translation RNA
UCB	United Chemicals Belgium
UDP	Uridine diphosphate
UGGT	UDP glucose glycoprotein glucosyltransferase
UPR	Unfolded protein response
UTR	Untranslated region
VKOR	Vitamin K epoxide reductase
X1	CHO-S XBP1-pTetOne
X1-B	CHO-S XBP1-pTetOne with BFP
XBP1	Xbox binding protein 1
XBP1s	XBP1 spliced
XBP1u	XBP1 unspliced

Chapter 1 Introduction

1.1 The biopharmaceutical industry

1.1.1 Therapeutic monoclonal antibodies

Monoclonal antibodies are large, multi-domain proteins which can be used therapeutically in a range of diseases, particularly in the treatment of auto-immune conditions and certain types of cancer (reviewed in (Ecker et al. 2015)). These therapeutic antibodies are delivered to patients intravenously, and can be used alone or in conjunction with other treatments such as small molecule pharmaceuticals or chemotherapy. Through their highly variable antigen binding domains, antibodies are theoretically capable of binding to any protein or small molecule target, and this binding action can be used to fight disease by a number of different molecular mechanisms. For instance, adalimumab is an antibody capable of binding to tumour necrosis factor alpha (TNF α), and can be used to alleviate the symptoms of a number of auto-immune conditions, including rheumatoid arthritis or Crohn's disease, by binding and blocking the activity of TNF α , which is dysregulated in these diseases (Scheinfeld 2003). Antibody binding can also be used to focus the immune response to a particular antigen target, similar to the natural mechanism of action for antibodies in the acquired immune response. Ofatumumab is an antibody which utilises this mechanism to treat chronic lymphocytic leukaemia by targeting natural killer cells to cancerous cells that express the CD20 antigen, which ofatumumab specifically binds to (Zhang 2009). Another mechanism for the therapeutic potential of antibodies is for them to be used as a vehicle for drug delivery. For instance, the radiolabelled antibody ibritumomab tiuxetan is used in the treatment of non-Hodgkin's lymphoma by bringing its conjugated radiation dose into the proximity of CD20 expressing cancerous cells, which focuses the efficacy of the treatment to where it is required while limiting the damage caused to healthy cells (Witzig 2000). Due to this targeted action, the side effects of antibody therapy for cancer treatment are generally considered to be less severe than conventional cancer treatments such as chemotherapy (Chung 2008).

With the development of human-mouse chimera antibodies in the 1990s, which could better evade the immune systems of patients and provide treatment without generating a dangerous immune reaction, therapeutic antibodies began to gain traction as both a viable treatment option for health services, and as a growing segment of the pharmaceutical market. Subsequent developments, reviewed in (Safdari et al. 2013), resulted in the generation of humanised antibodies, in which only a small, key component of the variable region is of non-human origin, and eventually in the production of fully human antibodies which are indistinguishable from an immunogenic perspective from the patient's own adaptive immune response.

These ground-breaking developments, together with the relative tolerability of side effects and the wide range of current and potential antigenic targets, have resulted in monoclonal antibodies being commercial successes as well as a therapeutic success. Global sales of monoclonal antibodies reached \$63 billion in 2013, and the market is expected to grow by 5% each year (Walsh 2014). However, the cost of development for antibodies, as for any drug, is extremely high, and was estimated to be \$2.6 billion per FDA approved drug in 2014 (DiMasi et al. 2016). This development cost has risen on an average of 8.2% each year due to a number of factors such as the increasing complexity and stringency of clinical trials, together with the increasingly high standards and low success rate for regulatory approval, where only 11.83% of drugs entering clinical trials will achieve approval for market (DiMasi et al. 2016). In order to compensate for these spiralling costs, and to ensure that drugs remain affordable for patients and health services, any drugs which make it to market must be as profitable as possible by having the highest yield for the lowest production cost.

Efforts made towards achieving this ideal yield have been largely successful, and production methods for monoclonal antibodies have been steadily optimised over the last two decades to obtain antibody titres 100 fold higher than those reported in the 1990s. Yields now routinely meet 1g/L, occasionally as much as 10g/L (Wurm 2004) and this substantial improvement in the rate of production has been achieved by a number of strategies to amplify and optimise the growth of cultured cell lines, as well as in improving mechanisms for enhancing transcription, translation and secretion of proteins. These strategies will be summarised and discussed below.

1.1.2 Overview of therapeutic antibody production

Generally, the industrial production of therapeutic antibodies is performed in large-scale suspension cultures of mammalian cells. These cells are preferentially used over prokaryotic or lower eukaryotic cell lines due to their innate capacity to secrete exogenous proteins in a bio-active form with the appropriate tertiary structure and glycosylation profile for use in human patients.

The procedure for producing a desired therapeutic protein in a mammalian host cell line, reviewed in (Jayapal et al. 2007), is a multi-step process that usually takes around three months. Firstly, the DNA sequence for the protein of interest must be known, and this is incorporated into an appropriate mammalian expression vector to be transfected into the cells. Generally the expression vector is stably incorporated into the host cell genome, though transient expression systems can be used for smaller, pilot scale production. In a stable integration, the specific site of transgene integration will vary

on a cell-by-cell basis to result in a mixed population of high expressing, low expressing and non-expressing cells, due to the presence of enhancing or repressing elements acting on the region of the chromosome where gene integration occurred. In order to obtain a homogenous population of high expressing cells, the mixed population must be subjected to clonal selection, where the presence of a co-transfected antibiotic resistance gene is used to isolate transgene expressing cells from non-expressing. Clonal populations derived from single expressing cells can then be obtained by limiting dilution.

The extent of antibody expression is then screened for. Clones with a high yield of antibody can be identified through labour-intensive methods such as antibody capture ELISA, or by high throughput methods like fluorescence activated cell sorting (FACS) to detect the presence of either secreted protein or a co-transfected fluorescent protein. Dedicated systems for the high throughput screening of clones are also available. One such system is ClonePix (Genetix), which uses a fluorescently-tagged antibody binding reagent to identify clones growing in the presence of an abundance of secreted antibody. To illustrate the timescales involved with clonal selection: capture ELISA can screen the productivity of 1000 clones in eight weeks, whereas the ClonePix system can screen 10,000 clones in three weeks (Dharshanan et al. 2011). After screening, high yield clones are expanded over many passages into a homogenous culture of high producing cells. Culture volumes of up to 10,000 L can be achieved in stirred-tank bioreactors, capable of producing kilograms of therapeutic protein.

1.1.3 Optimisation of therapeutic antibody production

The described process of generating an antibody producing cell line has been steadily optimised at each stage in a variety of experiments performed over many years in order to increase the final yield of antibody. Improvements to final product yield can be achieved by changes to the culture method, as well as in genetic manipulation of the cells and the design of expression vector used. For instance, it was observed that decreasing the temperature of growth from 37°C to 30°C resulted in an increase in the productivity of a model protein, secreted alkaline phosphatase (SEAP), by 1.7 - 3.4 fold (Kaufmann et al. 1999). This effect was attributed to an activation of a cold-specific signalling response that affected post-translation modifications, as two endogenous host cell line proteins were found to be phosphorylated after the culture temperature had been lowered to 30°C. The drop in temperature also caused cell cycle arrest in G1 phase.

Another strategy for increasing yield is the addition of sodium butyrate (NaBu) to cell cultures. This compound is known to improve yield of recombinant proteins, and reported increases have ranged from 2 fold to a 9 fold increase, depending on the protein expressed (Gorman et al. 1983; Palermo et al. 1991). Although the mechanism is not fully understood, it has been proposed that NaBu functions as an inhibitor of histone deacetylase to result in chromatin that is hyper-acetylated in treated cells (Kruh 1982). This hyper-acetylation locks chromatin into an open state which makes it more readily accessible by transcription factors and polymerases for gene expression. One detrimental effect of NaBu treatment is that it lowers the rate of growth and the viable cell density of treated cultures, although it has been reported that this can be alleviated by supplementation with N-acetylcysteine, which improves culture viability but does not compromise the improvements in yield resulting from NaBu treatment (Chang et al. 1999). It is thought that N-acetylcysteine functions as an antioxidant and improves viability by removing reactive oxygen species that are generated by NaBu (Oh et al. 2005).

Similar to the proposed mechanism of NaBu function, another commonly used mechanism for improving transgene expression through chromatin modification is in the use of scaffold/matrix attachment regions (S/MARs). These are DNA elements flanking a gene that bind to the nuclear scaffold/matrix and are used to hold the chromatin structure of the gene of interest in an open state, allowing for easier access by transcription factors and, therefore, faster gene transcription. These DNA elements are found in many endogenous genes to enhance expression, and S/MAR sequences can be incorporated into the transgene expression vector to improve the final yield of recombinant protein (Phi-Van et al. 1990; Zahn-Zabal et al. 2001).

Translation of exogenous proteins can also be improved by codon optimisation, where the sequence of the transgene is optimised at the nucleotide level to use codons more commonly found in the host cell line species. This optimisation does not alter the amino acid sequence of the protein, and its benefit is based on the alleviation of bottlenecks caused by differences in the abundance of tRNA molecules, where a certain tRNA molecule could be very commonly required in one species and therefore expressed at a high level, but is expressed at low levels in another species. For instance, it was reported that altering the DNA sequence of the human interferon gamma (INF γ) gene to use codons more commonly found in the Chinese hamster allowed for a ten-fold increase in the expression of INF γ from Chinese Hamster Ovary (CHO) cells than if the nucleotides of the native human DNA sequence were used (Chung et al. 2013).

1.1.4 History of Chinese Hamster Ovary (CHO) cells in bioprocessing

A number of cell line types have been used in the industrial production of monoclonal antibodies, such as the Human Embryonic Kidney line HEK293 and mouse myeloma-derived NS0 cells, but the industry standard is the Chinese Hamster Ovary (CHO) cell (Wurm 2004). This cell line accounts for 70% of all recombinant proteins produced, and sales of recombinant proteins produced in CHO cells are worth \$30 billion per year worldwide (Jayapal et al. 2007).

The history of the use of Chinese hamsters (*Cricetulus griseus*) in biological research and bioprocessing, reviewed in (Jayapal et al. 2007) and (Yerganian 1972), began with their use as a disease model organism since 1919, where they were used to study pneumonia. After the discovery that the hamster had a low chromosome number, with ten autosomal chromosome pairs and two sex chromosomes, and that these chromosomes were larger than for other model organisms, the species was used extensively in genomics, radiation and mutagenesis studies.

Ovary tissue was extracted from a female hamster in the late 1950s, and was trypsinised and grown by *in vitro* culture methods for use in genetic studies (Puck et al. 1964; Tjio and Puck 1958). These original Chinese hamster ovary cells appeared to be predominantly fibroblasts, and were maintained in continuous culture for ten months. As these cells did not display the normal senescence associated with multiple passages in long-term *in vitro* culture, it is thought that the cells were able to spontaneously immortalise by an unknown mechanism (Wurm 2013). After ten months in culture, it was published that the cells had changed from a recognisably fibroblast morphology to an 'epithelioid' shape, and proline auxotrophy was also reported in this early culture, suggesting that genomic mutations had occurred (Puck et al. 1964).

Although there were many poorly understood aspects to this early CHO cell line, there were also many advantages in their use over other cell models of the time, and CHO cells were soon gifted to a number of interested laboratories. The cells were known to be amenable to *in vitro* culture and had fast generation times, leading to their use becoming more established and widespread. Cultures were found to be relatively easy to synchronise through cell-cycle arresting drugs, leading to their use in cell proliferation studies, and their unstable genome made them useful for investigating chromosome abnormalities and mutagenesis (Chasin and Urlaub 1975; Kao and Puck 1967).

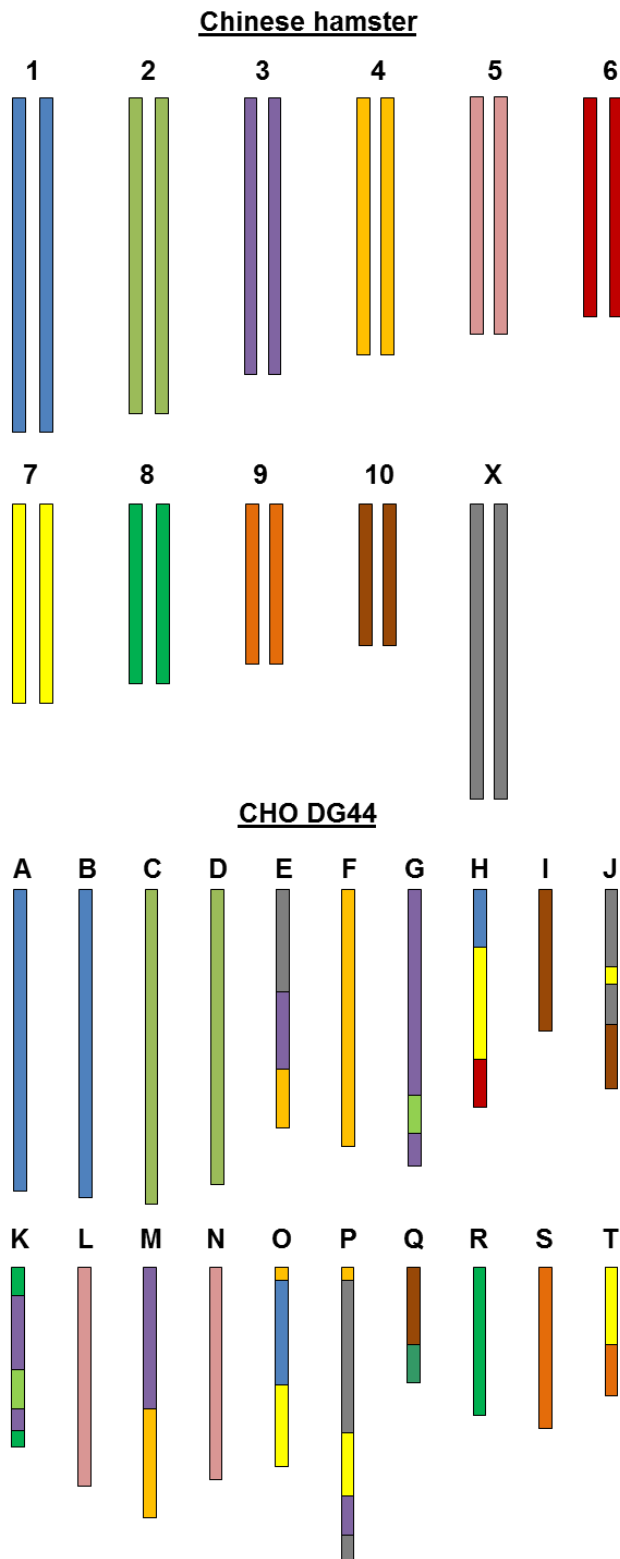


Figure 1-1 - Cartoon of karyotypes from Chinese hamster and CHO DG44 cells.

Inherent genomic instability in CHO cells led to the spontaneous translocation and deletion of chromosome sections, and to the generation of a 'quasi-diploid' karyotype. Autosomal Chinese hamster chromosome pairs are numbered from 1 to 10, whereas CHO chromosomes do not generally form recognisable pairs and are individually named from A to T. CHO chromosome sections are coloured according to their estimated Chinese hamster homologue. Adapted from (Cao et al. 2011) Figure 1.

Due to this well-documented genomic instability of CHO cells, the karyotype of modern CHO lineages differs greatly from that of the Chinese hamster, and gene inactivation and chromosomal arrangements have led to CHO cells being effectively 'quasi-diploid', as the majority of CHO chromosomes no longer form recognisable pairs (Cao et al. 2011). Decades of isolated *in vitro* culture of this notoriously unstable cell line led to the emergence of a variety of CHO subtypes (reviewed in (Wurm 2013)). The CHO-K1 lineage is believed to be the most closely related to the original CHO cells grown by Puck and Kao, and is one of the most widely used subtypes. Another notable subtype is the CHO-S lineage, used throughout this project, which is derived from cells grown at the University of Toronto after being adapted for suspension culture (Thompson and Baker 1973). CHO-S is advantageous over other CHO subtypes such as CHO-K1 when growing in large-scale suspension cultures, and is therefore a commonly used subtype in the bioprocessing industry.

Another subtype used in industrial scale recombinant protein production is CHO DG44, an auxotroph lineage that requires the addition of glycine, hypoxanthine and thymidine to the culture medium, in addition to the proline auxotrophy which is a characteristic of all CHO lineages (Wurm and Hacker 2011). The CHO DG44 subtype was purposefully engineered to lack the dihydrofolate reductase (DHFR) enzyme required for the synthesis of hypoxanthine and thymidine from folate (Urlaub and Chasin 1980), with the aim of co-transfecting the required DHFR gene alongside a gene of interest for stable protein expression. Clones with a high uptake of the gene of interest will have high uptake of DHFR, and better survival in a culture environment lacking glycine, hypoxanthine and thymidine. The addition of the folic acid analogue methotrexate (MTX) to this system reduces the activity of DHFR so that only clones with a high copy number of transfected DHFR, and consequently the gene of interest, will be able to survive, and is, therefore, used as a method of increasing gene of interest uptake. The DHFR system of stable gene transfection and the utilisation of MTX has resulted in an increase in antibody titres, and it is one of the main reasons why CHO cells are the industry standard in recombinant protein production today (Kaufman et al. 1985).

There are many other desirable qualities in CHO cells that make them preferred host cell lines in the modern bioprocessing industry (reviewed in (Kim et al. 2012) and (Mason et al. 2012)). For instance, CHO-S and CHO DG44 cells are easily adaptable to grow in large suspension cultures, allowing for high cell densities and higher yields of secreted protein. In addition to this, serum-free medium can be readily used in these cultures, which reduces potential sources of product contamination. Also, proteins made in CHO cells have a glycosylation profile similar to that of human proteins, due to 99% of human glycosylation enzymes having a homologue in CHO (Xu et al. 2011). This

allows the recombinant proteins from CHO cells to be safely and effectively used in human patients. Another benefit is that, due to its popularity and long history of use, it is relatively easy to be granted approval from regulatory bodies to license new products derived from CHO cells, saving time and money and reducing the risk of rejection (Kim et al. 2012). The rate of transgene expression can also be strongly amplified in CHO cells using the DHFR system, or the similar glutamine synthetase (GS) gene amplification system, to screen for transfected clones with the most favourable growth and secretion properties.

The productivity of high yield CHO lineages is now reported to be in the region of 40-50 pg of antibody per cell per day (Reinhart et al. 2015; Zboray et al. 2015). However, despite these advances in production methods, bottlenecks that limit the yield from CHO cells are still thought to exist, particularly in post translational steps in the secretory process such as protein folding and assembly (Bibila and Flickinger 1992; Reinhart et al. 2014). A number of strategies have been investigated to remove these hypothetical assembly bottlenecks and improve the rate of recombinant protein folding. These strategies are based on the structural details of the protein of interest and the mechanisms by which it folds.

1.2 Protein folding and disulphide bond formation

1.2.1 Structure and folding of antibodies

Antibodies are composed of two light chains (LC) and two heavy chains (HC) connected by disulphide bonds to form a Y-shaped tetramer. There are two types of light chain: κ and λ , and each of these chains is composed of one constant domain, CL, and one variable domain, VL. Each heavy chain is composed of four domains: three constant domains, CH1, CH2 and CH3, which form the constant region, and one variable domain, VH, which forms the antigen binding site together with VL (Huber et al. 1976). The structure of antibodies can be subdivided into two antigen binding fragments (F(ab)), consisting of the VH, VL, CH1 and CL domains, and one crystallised fragment (Fc), consisting of the CH2 and CH3 domains. The terms F(ab) and Fc are used to describe the structural fragments generated when IgG is treated with the protease pepsin.

There are five types of heavy chain constant region: μ , γ , α , δ and ϵ , and each of these can bond with either of the two light chain types (Alt et al. 1987). Depending on the type of CH region present, the Ig tetramer can be categorised into one of the isotypes IgM, IgG, IgA, IgD and IgE, which correspond to their CH region Greek letter equivalents. The number of disulphide bonds in these isotypes varies, and ranges from 16 to 28 bonds (Borth et al. 2005). Each isotype can also be further subdivided into subtypes, for example IgG has four subtypes named IgG1 - 4. These subtypes vary in both their amino acid sequence and in the positions of their disulphide bonds; factors which result in variation in their properties such as in their stability. This variation is of such significance that the IgG subtypes vary in their stability and have different functions within the immune system.

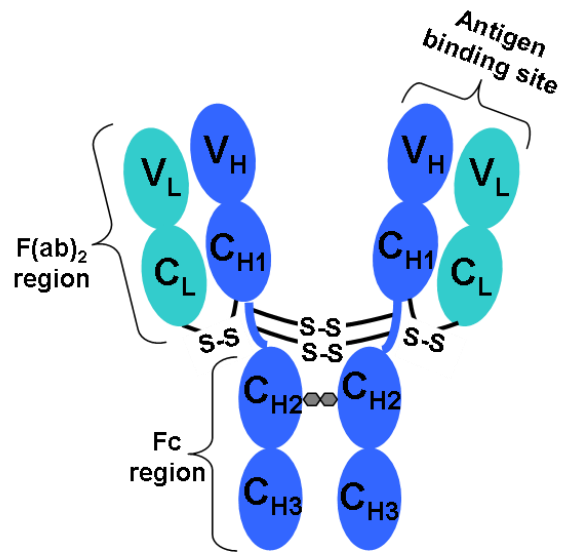


Figure 1-2 - Structure of Immunoglobulin G (IgG).

The structure of IgG consists of two heavy chains (blue) and two light chains (green) connected by interchain disulphide bonds. The highly specific antigen binding site is formed from the variable regions, V_H and V_L. The quaternary structure of IgG can be divided into two antigen binding fragments (F(ab)), consisting of the V_H, V_L, C_{H1} and C_L domains, and one crystallised fragment (Fc), consisting of the C_{H2} and C_{H3} domains. N-linked oligosaccharides are shown on the C_{H2} domain in grey. Adapted from (Feige et al. 2010) Figure 1A.

A high degree of variability in the antigen binding site is essential for the adaptability and function of all antibodies. This variability is generated by the shuffling of three genes: a variable, diversity and joining gene, which are combined at the DNA level to form a single allele (Early et al. 1980; Maki et al. 1980). The joining of these three genes is quite crude, which helps to introduce variations into the DNA sequence to result in an increase in the variability of the region (Alt et al. 1987). In addition, variability is increased by the process of class switching, where the VH region is removed from the IgM constant region and recombined to any of the other constant regions (Calame et al. 1980). While these processes are essential for the function of antibody molecules, they also increase the risk of generating non-functional proteins that cannot be folded or secreted correctly. Because of this, antibody production depends heavily on a strict quality control system in the ER to ensure that only correctly folded and functional antibodies leave the ER, and the misfolded molecules are disposed of by the 26S proteasome by the process of ER associated degradation (ERAD).

The folding of IgG is a multi-step process that involves the interaction of nascent HC and LC with the chaperone BiP; members of the Protein Disulphide Isomerase (PDI) family of oxidoreductases, which are responsible for the insertion of disulphide bonds into folding proteins; and Peptidyl-Prolyl Isomerase (PPIase), which catalyses the isomerisation of proline residues. Upon entering the ER, the HC and LC begin folding cotranslationally (Bergman and Kuehl 1979). Hydrophobic regions on these folding chains attract the binding of BiP, which retains the chain in the ER to allow sufficient time for complete folding (Haas and Wabl 1983). The folding of each domain of the HC and LC requires the isomerisation of a conserved proline residue from a *trans* to a *cis* conformation by PPIase (Lilie et al. 1995), and the formation of an intrachain disulphide by PDI family members (Roth and Pierce 1987). These two steps are sufficient for the folding of all antibody domains (Feige et al. 2004), with the exception of the CH1 domain, which remains unfolded and bound by BiP (Feige et al. 2009). When folding of the CH3 domain is completed, the HC forms a homodimer which is stabilised by an interchain disulphide bond at the hinge region (Baumal et al. 1971). The CL domain of the folded LC then displaces BiP from the CH1 domain and enables it to finish folding (Feige et al. 2009). The final step in the formation of the IgG tetramer is the insertion of an interchain disulphide bond between the LC and HC, at the CL and CH1 domains (Huber et al. 1976), and this process is now known to be performed by PDI (Roth and Pierce 1987). The completed, functional molecule can then be exported from the ER to the Golgi, from where it can be secreted from the cell.

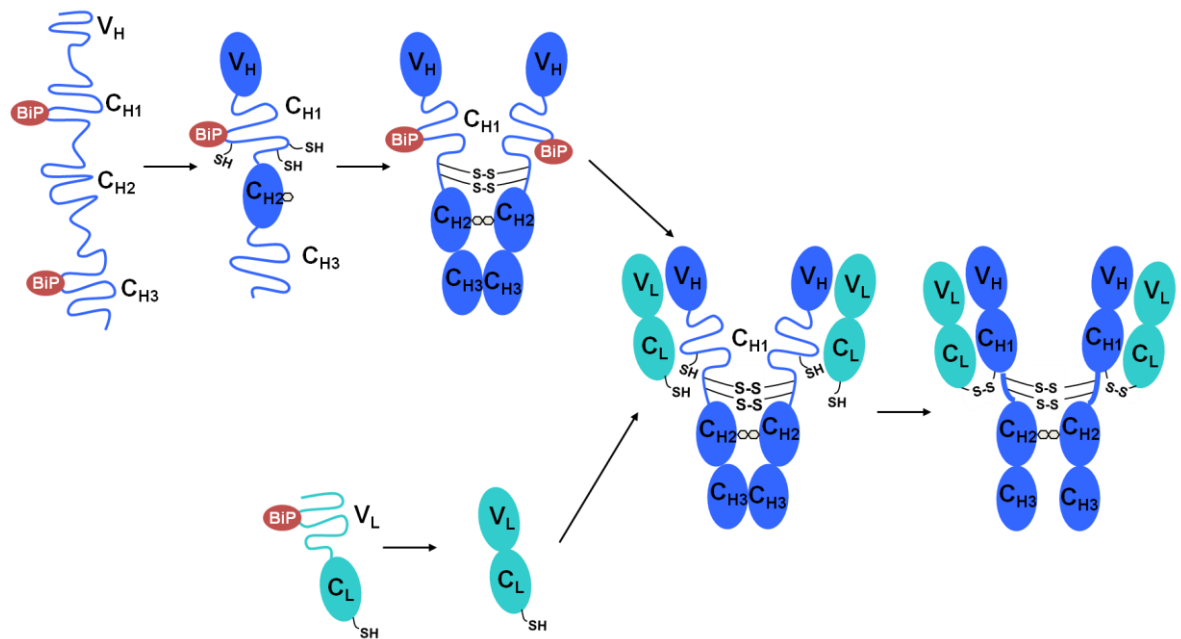


Figure 1-3 - Folding of antibody chains and formation of the IgG tetramer

IgG heavy chain (HC, shown in blue) and light chain (LC, shown in green) begin to fold co-translationally upon entering the ER. BiP attaches to hydrophobic regions on the CH1, CH3 and VL domains and retains the unfolded chains within the ER. The CL domain folds so rapidly that BiP does not bind. After a conserved proline residue on each of the domains is converted from a *trans* to a *cis* isomerisation, the VH, CH2 and CH3 domains finish folding and intrachain disulphide bonds are inserted by PDI family members to stabilise their structure. The folded CH3 domain induces HC dimerisation and an interchain disulphide bond is formed between HCs at the hinge region. The LC folds in parallel to the HC, and the CL domain of the folded LC is able to displace BiP from the unfolded CH1 domain. This brings LC and HC into close proximity, inducing the CH1 domain to finish folding, and enabling PDI to insert a final interchain disulphide bond between HC and LC. This completes the folding of the IgG tetramer, and the protein is then exported to the Golgi for secretion from the cell. Adapted from (Feige et al. 2010), Figure 4.

1.2.2 Role of Protein Disulphide Isomerase family members

Disulphide bonds are essential for the correct tertiary structure, and therefore the correct function, of the majority of secreted proteins including antibodies. While the secondary structure of a protein can usually form spontaneously alongside translation through the collapse of hydrophobic residues to the centre of a protein (Fedorov and Baldwin 1997), disulphide bond formation is an active process catalysed by members of the PDI family of proteins, the most studied of these ER-resident proteins being the eponymous PDI (Venetianer 1966). PDI family members are able to form disulphide bonds in newly synthesised proteins, break bonds in proteins about to be degraded, or rearrange bonds already formed. These processes involve the shuttling of electrons between the client protein and the active site of the thioredoxin-like domain(s) of PDI family members, which contain a conserved CYS-X-X-CYS (CXXC) motif (Chivers et al. 1996).

There are more than 20 known PDI family members (reviewed in (Okumura et al. 2015)). Although these members differ in their amino acid sequence and in the extent of their catalytic activity and function, they share a degree of domain structure homology, and all contain at least one thioredoxin-like domain. Some PDI family members are able to reduce and oxidise disulphide bonds equally well, such as the eponymous PDI, while others specialise in the reduction of disulphide bonds, such as ERdj5 (Oka et al. 2013). Others are catalytically inactive but assist with the activity of other family members, such as ERp27, which is thought to bind to and regulate the activity of ERp57 by competing with its binding to calreticulin (Kober et al. 2013). Another example of a catalytically inactive family member is ERp44, which retains a number of ER resident proteins which lack the usual KDEL retention motif within the ER, and has Ero1 α as a notable client protein (Anelli et al. 2003; Otsu et al. 2006). There is a degree of redundancy between the functions of the many PDI family members; however, some are more specific in their protein substrates than others. For instance, ERp57 specifically binds to glycoproteins (Jessop et al. 2007), and P5 forms a non-covalent complex with BiP and interacts with BiP client proteins, including IgG heavy chains (Jessop et al. 2009). Overall, the numerous PDI family members work in concert to ensure the efficiency and accuracy of disulphide bond formation.

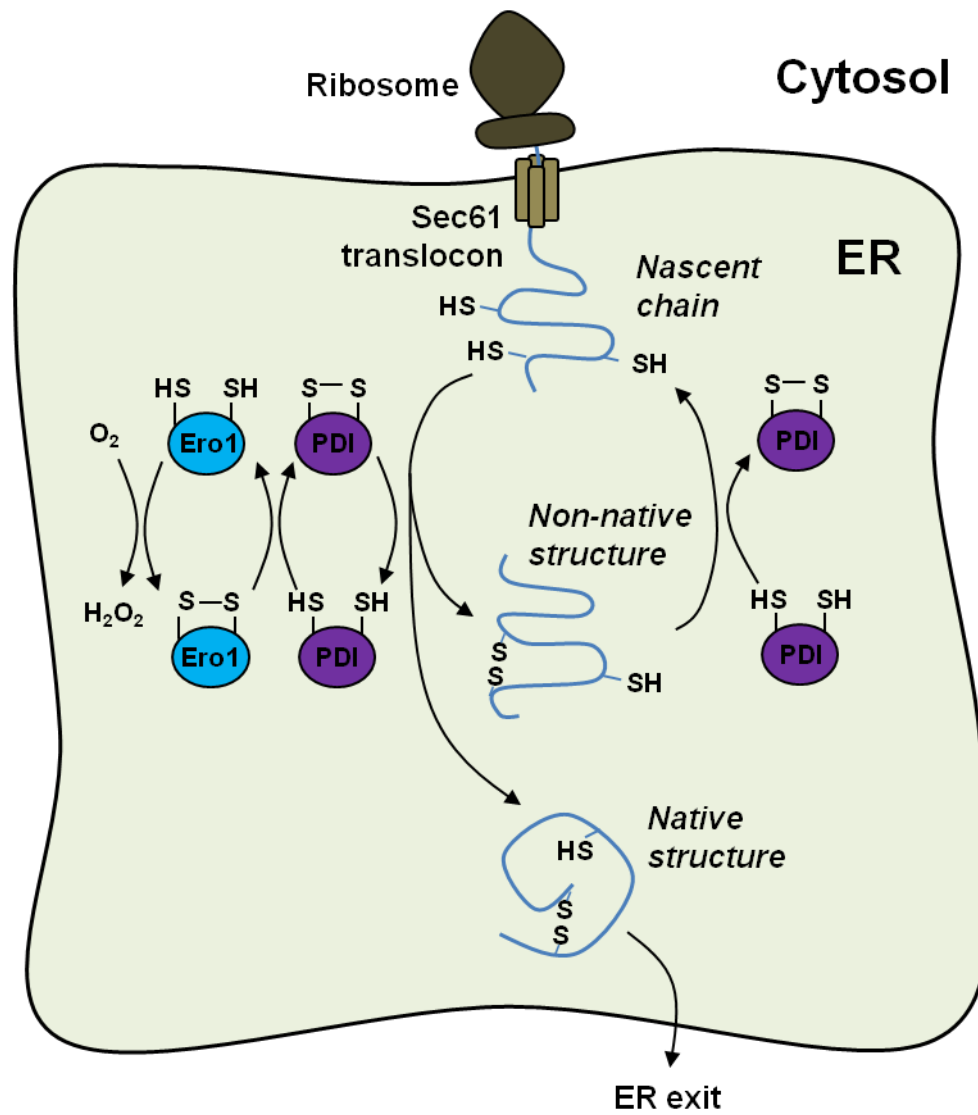


Figure 1-4 - Disulphide bond formation by PDI family members and the role of Ero1 α . Sulfhydryl groups on the cysteine residues of proteins can be converted into a disulphide bond in a reaction catalysed by oxidised PDI. Disulphide bonds that are not a component of the protein's native structure can also be reduced by PDI, and repeated rounds of sulfhydryl reduction and oxidation can occur before the protein's native structure is obtained. The oxidation of a client protein reduces the catalytic site of PDI, and this must be reoxidised before disulphide bond formation can occur again. The reoxidation of PDI is performed by Ero1 α , which generates a disulphide bond in its own active site through the conversion of molecular oxygen into hydrogen peroxide, and this bond is then transferred to PDI. Adapted from (Bulleid 2012) Figure 1.

1.2.3 Function and regulation of ER oxidoreductin 1

The formation of disulphide bonds is facilitated by the oxidising environment of the ER, which is maintained by an abundance of glutathione in the GSSG oxidised form, relative to its reduced GSH form (Chakravarthi and Bulleid 2004). However, this environment is not sufficient to recycle and reoxidise PDI after a disulphide bond is transferred into a client protein. In order to ensure that PDI is efficiently recycled and able to continually perform its functions, PDI is reoxidised by ER oxidoreductin 1 (Ero1). In mammalian cells, this reoxidation is performed by the Ero1 family members Ero1 α (Cabibbo et al. 2000) and Ero1 β (Pagani et al. 2000). Ero1 α is ubiquitously expressed in all tissues, whereas Ero1 β is only expressed in the pancreas and has a role in insulin synthesis and glucose homeostasis (Zito et al. 2010). Parallel pathways exist for the reoxidation of PDI family members that are mediated by quiescin sulfhydryl oxidase (QSOX), peroxiredoxin 4 (PRDX4), glutathione peroxidase 7 and 8 (GPX7 and GPX8) and vitamin K epoxide reductase (VKOR) (reviewed in (Bulleid and Ellgaard 2011)). These pathways operate independently of Ero1 α , and due to this redundancy, mammalian cells can survive the knockout of both Ero1 α and Ero1 β (Zito et al. 2010). However, in yeast cells the oxidation of PDI is performed solely by Ero1p, and the knockout of yeast Ero1p is lethal (Frand and Kaiser 1998).

The activity of mammalian Ero1 α is tightly controlled as its reaction results in the formation of hydrogen peroxide, a reactive oxygen species which is damaging to proteins and DNA (Tu and Weissman 2002). This regulation is controlled by the presence of disulphide bonds between catalytically active and inactive cysteines, which block the activity of the active site cysteines (Appenzeller-Herzog et al. 2008). A similar regulatory strategy exists for yeast Ero1p, however, in this case the presence of the regulatory disulphide bond presents a physical barrier to PDI entering the Ero1p active site (Sevier et al. 2007). It is thought that PDI is capable of sensing the oxidative state of the ER, and when a build-up of hydrogen peroxide causes the ER to become more oxidising, Ero1 α is inactivated by the PDI family members PDI and ERp46 by the formation of these regulatory disulphide bonds (Shepherd et al. 2014). As Ero1 α is required to oxidise and activate PDI, the two enzymes exist in a negative feedback loop to control the extent of each other's activity (Appenzeller-Herzog et al. 2010). When the activity of Ero1 α is required again the regulatory disulphides are reduced by PDI (Chambers et al. 2010; Inaba et al. 2010).

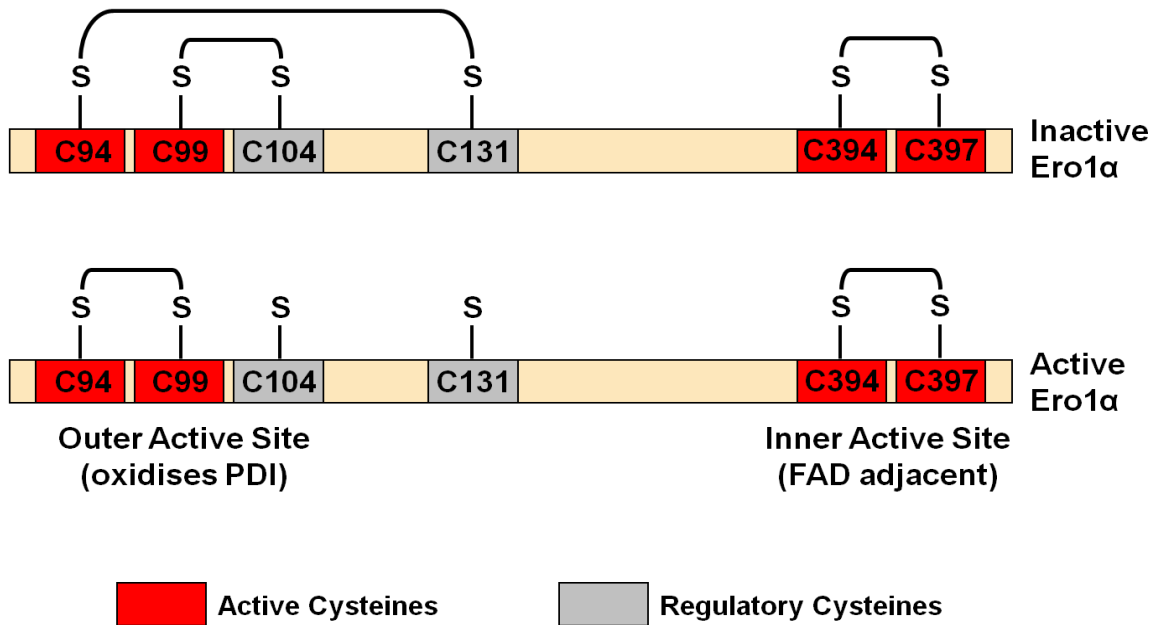


Figure 1-5 - Regulation of Ero1 α activity.

The outer active site of Ero1 α has two catalytic cysteines (C94 and C99) and two regulatory cysteines (C104 and C131). A disulphide bond is generated by the inner active site from molecular oxygen, and this is transferred to C94 and C99 in the outer active site. This bond can then be transferred to the substrate of Ero1 α , PDI. To regulate the activity of Ero1 α , disulphide bonds are formed between the active cysteines and the regulatory cysteines. These two bonds cannot be transferred to the PDI catalytic site, and the protein is therefore in an inactive form. Ero1 α is converted to and from its active form by PDI family members. Adapted from (Bulleid and Ellgaard 2011), Box 1, Figure 1.

1.3 Quality control and the Unfolded Protein Response

1.3.1 Calnexin/calreticulin and the glycan code

As the structure of a protein is essential for its correct function, a number of extensive quality control mechanisms exist within the ER which help to ensure the fidelity of protein folding; one of these mechanisms is the calnexin/calreticulin cycle. When nascent chains enter the ER through the Sec61 translocon (Matlack et al. 1998), an oligosaccharide group is added to an asparagine residue on a conserved Asn-X-Ser/Thr motif (Helenius and Aebi 2004). The presence of this oligosaccharide allows tracking of a protein within the ER, and modification of this group by the addition or cleavage of sugar molecules forms the basis of a 'glycan code', where a variety of fates can be specified depending on the 'code' of sugar molecules present on the protein (Hebert et al. 2005). The initial core glycan has the structure $\text{Glc}_3\text{Man}_9\text{GlcNAc}_2$, where 'Glc' is glucose, 'Man' is mannose and 'GlcNAc' is N-acetylglucosamine. When this glycan is trimmed to $\text{Glc}_1\text{Man}_9\text{GlcNAc}_2$ by glucosidase 1 and 2, the nascent protein is able to interact with the quality control lectins calnexin and calreticulin through the trimmed glucose moiety (Hammond et al. 1994). Calnexin is a transmembrane protein which can simultaneously bind to $\text{Glc}_1\text{Man}_9\text{GlcNAc}_2$ on client proteins via a carbohydrate binding domain, and the oxidoreductase ERp57 by a region called the P domain (Schrag et al. 2001), bringing the nascent chain into proximity with ERp57 and enabling this PDI family member to assist in client protein folding (Frickel et al. 2002). Calreticulin has shared functionality with calnexin, but is localised to the ER lumen as opposed to the ER membrane (Ellgaard et al. 2001).

The client protein is released after interaction with calnexin/calreticulin by further trimming of the core glycan to $\text{Man}_9\text{GlcNAc}_2$ by glucosidase 2. If the protein's native structure has not been achieved it can be sequestered for further interaction with calnexin/calreticulin following reglucosylation by Uridine Diphosphate (UDP) glucose glycoprotein glucosyltransferase (UGGT), an enzyme that preferentially interacts with partially folded glycoproteins (Caramelo et al. 2004; Trombetta 2003). Multiple rounds of the calnexin/calreticulin cycle can be achieved by the addition and removal of glucose from folding proteins, which ensures a prolonged period of time within the ER for the protein to interact with chaperones and oxidoreductases, and this should be sufficient to achieve the protein's native structure. If misfolding persists after multiple quality control cycles then further interaction with ERp57 is abandoned and the protein is instead targeted for ERAD.

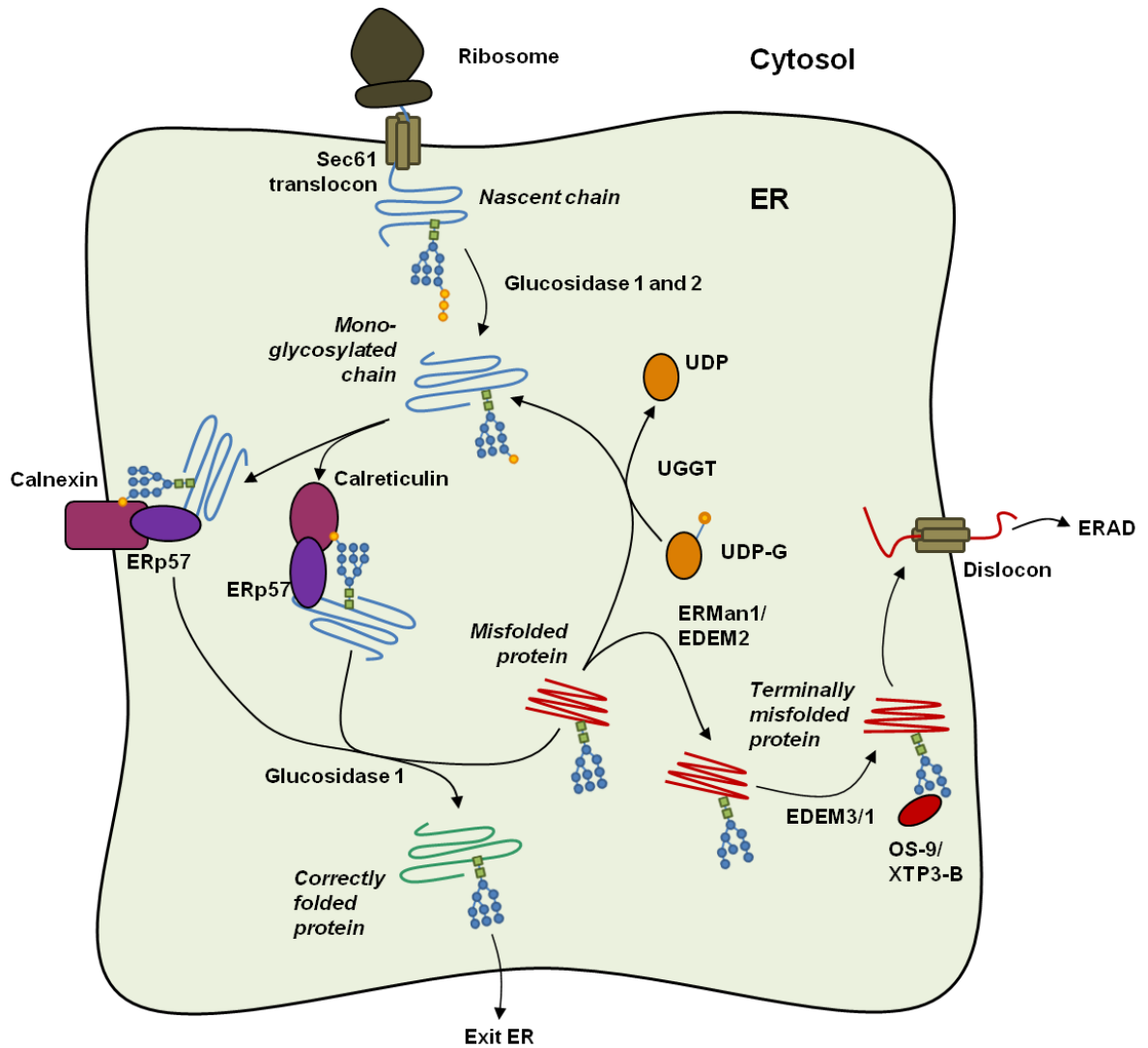


Figure 1-6 - The calnexin/calreticulin quality control cycle.

Nascent chains enter the ER through the Sec61 translocon complex, and a core glycan is attached to a conserved asparagine residue. Two glucose molecules (shown as yellow circles) are trimmed from the glycan by glucosidases 1 and 2 to enable recognition by calnexin and calreticulin. The binding of calnexin/calreticulin brings the unfolded protein chain into proximity with the oxidoreductase ERp57, which should lead to the protein achieving its native structure and its subsequent export from the ER. If this structure is not achieved, a glucose molecule can be reattached from UDP by UDP glucose-glycoprotein glycosyltransferase (UGGT) to allow additional exposure to ERp57 via calnexin/calreticulin binding. If the protein remains persistently misfolded, then mannose molecules (shown as a blue circle) are sequentially removed by ER mannosidase 1 (ERMan1) or EDEM2, and then EDEM3 or EDEM1. This trimming targets the protein for ERAD through interaction with OS-9/XTP3-B, leading to the eventual degradation of the protein in the 26S proteasome. Adapted from (Chakrabarti et al. 2011) Figure 1.

1.3.2 ER associated degradation

Protein misfolding and aggregation can be triggered by cellular stresses such as glucose starvation, hypoxia or a viral infection (Kaufman et al. 2002). Misfolded proteins can be distinguished from their normal, natively folded counterparts by the presence of hydrophobic residues on the outside of the protein, as these are normally embedded in the centre of the protein when folded correctly. These hydrophobic residues are recognised by BiP, a chaperone which stabilises and retains misfolded client proteins within the ER and assists in their refolding, which is mediated by other folding factors. If a protein remains persistently misfolded after multiple quality control and protein folding cycles, it is instead targeted for ERAD.

The degradation of terminally misfolded glycoproteins by ERAD is triggered by the sequential removal of two mannose groups from the core glycan. In mammalian cells, the trimming of $\text{Man}_9\text{GlcNAc}_2$ to $\text{Man}_8\text{GlcNAc}_2$ is performed by ER mannosidase 1 (ERMan1) or by ER degradation enhancing α -mannosidase like protein 2 (EDEM2) (Ninagawa et al. 2015; Ninagawa et al. 2014). A second cleavage event to convert $\text{Man}_8\text{GlcNAc}_2$ into $\text{Man}_7\text{GlcNAc}_2$ is performed by EDEM3, and to a lesser extent by EDEM1 (Ninagawa et al. 2015; Ninagawa et al. 2014). $\text{Man}_7\text{GlcNAc}_2$ is recognised by the mannose-specific lectins OS-9 and XTP3-B, which assist in the dislocation of the misfolded protein to the ER dislocon. OS-9 and XTP3-B both exhibit a mannose-6-phosphate receptor homology (MRH) domain, through which the binding to $\text{Man}_7\text{GlcNAc}_2$ is mediated, but display little other sequence homology (Satoh et al. 2010). Knockdown of either OS-9 or XTP3-B was shown to cause mild attenuation of ERAD but a double knockdown caused a greater reduction in the rate of degradation, suggesting that there is a degree of redundancy in their functions (Hosokawa et al. 2009). Regardless of the distinctions between these two lectins, both are thought to interact with the ER membrane protein Sel1, a component of the dislocon, through their MRH domains.

The interaction of OS-9/XTP3-B and Sel1 brings the misfolded protein into contact with the dislocon machinery (Jeong et al. 2016). In addition to Sel1, this complex of membrane and soluble proteins contains: ERp90 (Riemer et al. 2011) and ERdj5 (Ushioda et al. 2008), PDI family members which reduce any disulphide bonds in the partially folded amino acid chain; p97, which assists in 'threading' the unfolded protein through the dislocon channel and into the cytosol (DeLaBarre et al. 2006); and Hrd1, an E3 ubiquitin ligase also known as synoviolin (SYVN1) which forms a structural component of the channel alongside Derlin1 and also catalyses the addition of ubiquitin to the protein to target it for degradation in the 26S proteasome (Carvalho et al. 2010; de Virgilio et

al. 1999). This complex mediates the extraction of misfolded proteins from the ER, and their disassembly, ubiquitination and eventual degradation in the proteasome.

1.3.3 The Unfolded Protein Response

These procedures for quality control ensure that, under normal physiological conditions, misfolded proteins are efficiently recycled or disposed of and prevented from accumulating in the ER. However, under stress conditions the load of misfolded proteins can exceed the capacity of quality control and ERAD, allowing potentially toxic levels of protein accumulation and aggregation. Under these circumstances, the unfolded protein response (UPR) is triggered. This is an elaborate and extensive stress response utilised by the cell in order to remove aggregated proteins and restore the normal homeostasis of protein translation, degradation and secretion (reviewed in (Chakrabarti et al. 2011)).

The first strategy undertaken as part of the UPR is for the cell to degrade untranslated mRNA transcripts and halt further protein translation, which prevents nascent polypeptide chains from entering the already-overloaded ER. Secondly, the ER increases its protein folding capacity by overexpressing chaperones and by physically increasing in size, helping to clear the backlog of misfolded proteins. The process of ERAD is also upregulated and proteins that cannot be correctly folded are retained in the ER then sent to the 26S proteasome for degradation (Travers et al. 2000). If these two strategies are successful in clearing the build-up of aggregates then translation can resume and the stress response is brought to an end. However, if the backlog cannot be cleared then the cell must begin its third strategy and undergo autophagy before, finally, apoptosis.

The wide range of intricately-regulated functions of the UPR are mediated by three initial effector molecules in mammalian cells, and the downstream signalling from each of these three effectors form three distinct branches of activity. There is a degree of cross-talk between the branches, and each branch can lead to both pro-survival and pro-apoptotic functions that are activated under different circumstances. The three effectors of the mammalian UPR are named double-stranded RNA activated protein kinase (PKR)-like endoplasmic reticulum kinase (PERK), inositol requiring enzyme (IRE1), and activating transcription factor 6 (ATF6). In contrast, the UPR of lower eukaryotes is only mediated by a single effector, Ire1p (Ron and Walter 2007). Under normal physiological conditions, mammalian PERK, IRE1 and ATF6 are bound in an inactive form by BiP. In the presence of hydrophobic residues found on misfolded proteins, BiP detaches from the UPR effectors and binds instead to the aggregates, triggering the

activation of downstream signalling pathways (Kebache et al. 2004). When the stress response is no longer required, BiP reassociates with PERK, IRE1 and ATF6 to suppress their activity.

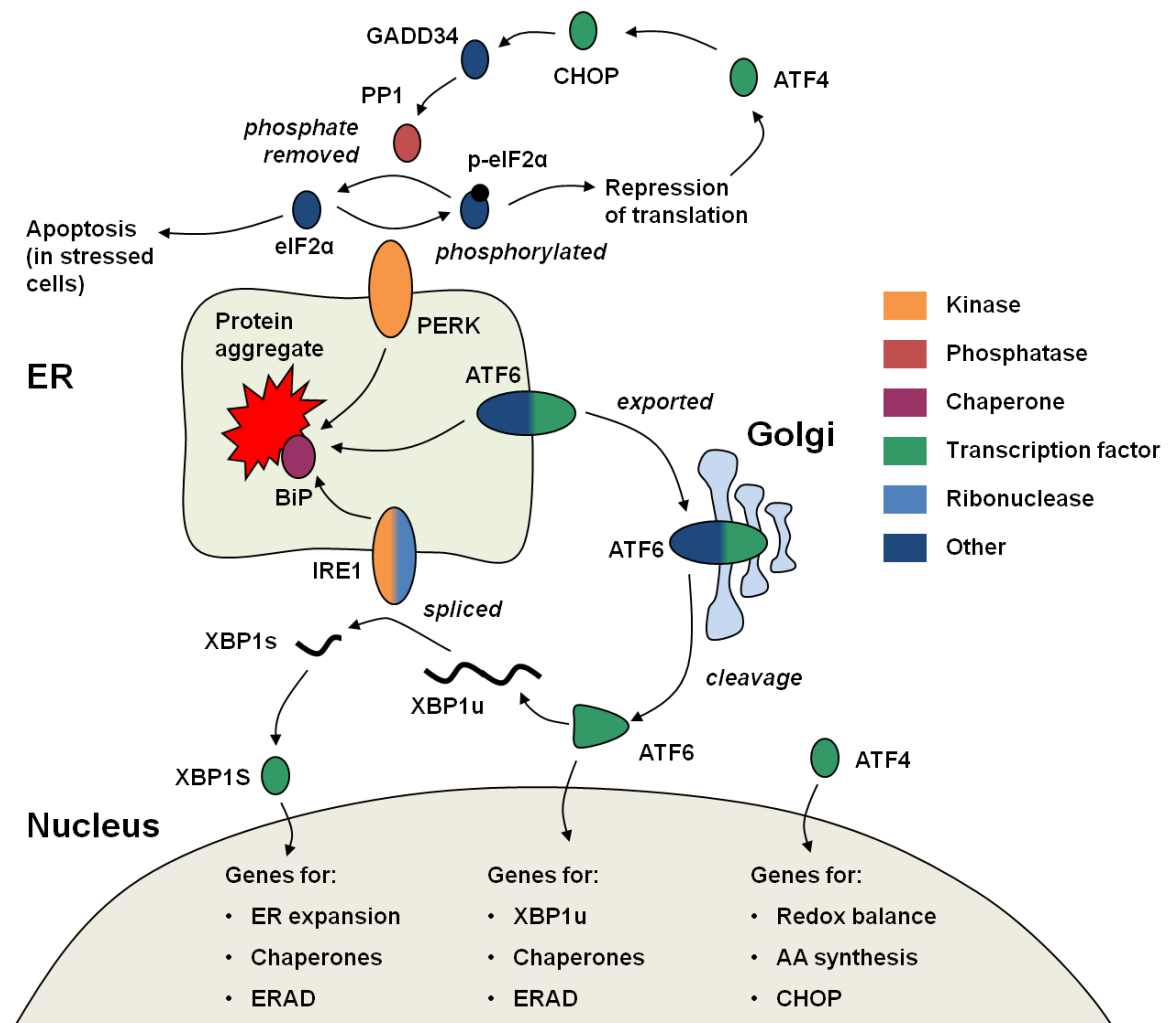


Figure 1-7 - Schematic of the Unfolded Protein Response.

In the presence of protein aggregates, BiP detaches from and activates PERK, ATF6 and IRE1. PERK phosphorylates eIF2α which leads to a global attenuation of protein translation. Under this circumstance, transcripts for the transcription factor ATF4 are more readily translated, and a number of targets downstream of ATF4 are upregulated. One of these targets is CHOP, which in turn upregulates GADD34. The phosphatase recruited by GADD34, PP1, has the function of dephosphorylating eIF2α and relieving the block on protein translation. In a second functional branch of the UPR, ATF6 is exported to the Golgi and cleaved to form a transcription factor, which transcribes XBP1u and other adaptive genes. XBP1u is spliced by IRE1 to generate XBP1s, which is translated into an active transcription factor. XBP1s upregulates chaperones, allowing for increased protein folding and ERAD with the aim of clearing the build-up of aggregates. If this strategy is unsuccessful, pro-apoptotic genes are triggered and the cell undergoes apoptosis. Adapted from Chakrabarti et al, 2011 Figure 2B.

1.3.4 PERK branch

PERK is a type 1 transmembrane protein consisting of an N-terminal ER stress sensing region that binds BiP, and a C-terminal cytosolic kinase. The dissociation of BiP from the N-terminus of PERK allows for the formation of a homodimer, and this is activated by subsequent autophosphorylation (Kebache et al. 2004). The activation of PERK triggers the upregulation of cellular inhibitor of apoptosis (cIAP), a pro-survival factor (Hamanaka et al. 2009), and also mediates the attenuation of translation by phosphorylation of eukaryotic translation initiation factor 2 (eIF2 α) (Gebauer and Hentze 2004). Phosphorylated eIF2 α is unable to form the eIF2-GTP-tRNA^{met} complex required for the initiation of translation.

The repression of protein translation is able to efficiently block the initiation of translation for the majority of mRNA transcripts. However, it is not ubiquitous, and one transcript which is known to be able to bypass the block is activating transcription factor 4 (ATF4). Transcripts for ATF4 are constitutively expressed, but are only translated under the circumstances of repressed translation induced by p-eIF2 α (Lu et al. 2004; Vattam and Wek 2004). ATF4 transcripts have two open reading frames in the 5'UTR. Under unstressed conditions, the ribosome complex will translate uORF1 and then the 60S ribosome subunit will dissociate. Due to the abundance of unphosphorylated eIF2 α , the 60S subunit will quickly reassociate with the 40S subunit to resume translation at the next available start codon. This codon initiates the inhibitory uORF2 frame, which translates to a truncated protein and also bypasses the coding region for ATF4. During stress conditions, the reinitiation of translation is less efficient due to phosphorylated eIF2 α , and the ribosome complex does not reform quickly enough to translate uORF2, leading to the resumption of translation at the next available start codon, which is the start codon for ATF4 translation.

ATF4 functions as a transcription factor, and a key UPR component that upregulates amino acid synthesis and transport, as well as the secretion of folded proteins, and also improves resistance to oxidative stress, all of which assist in alleviating the protein folding load of the stressed ER (Harding et al. 2003). In addition to these pro-survival effects, ATF4 upregulates a transcription factor known for its role in apoptosis, C/EBP homologous protein (CHOP) (Gachon et al. 2001). CHOP is thought to promote apoptosis on stressed cells by downregulating the pro-survival factor Bcl2 (McCullough et al. 2001), and by the upregulation of growth arrest and DNA damage inducible protein 34 (GADD34) (Marciniak et al. 2004), of which the pro-apoptotic function will be discussed later.

If the attenuation of translation imposed by p e lF2 α and the pro-survival activity of ATF4 are able to relieve the build-up of misfolded proteins, then the block on translation can be subsequently released. This function is performed by GADD34, which is induced by the transcription factor activity of CHOP and recruits protein phosphatase 1 (PP1) to dephosphorylate eIF2 α (Novoa et al. 2001). This action releases the repression of translation maintained by the phosphorylation of eIF2 α . However, as the block on translation is put in place to protect the ER from an excessive load of unfolded proteins, if the block is released in severely stressed cells then the resumption of translation and the import of nascent chains into an overloaded ER is fatal to the cell (Marciniak et al. 2004). This is used as a mechanism of apoptosis induction in the terminal stages of UPR signalling.

1.3.5 ATF6 branch

ATF6 has two Golgi-localisation sequences on its C terminal, ER lumen domain, which are exposed when BiP dissociates from ATF6 in the presence of misfolded proteins (Shen et al. 2002). With these sequences revealed, the entire 90kDa transmembrane protein is translocated from the ER membrane to the Golgi by COPII vesicle mediated ER-Golgi transport (Haze et al. 1999). After export, the N-terminus of ATF6 is cleaved by sequential activity of site-1 and site-2 proteases, and exported from the Golgi to the nucleus as a 50kDa transcription factor (Chen et al. 2002). The transcription factor ATF6 transcribes genes with either ATF/cAMP responsive elements (CRE) (Wang et al. 2000) or ER stress elements (ERSE) (Kokame et al. 2001). Genes upregulated by ATF6 include chaperones and folding factors, such as BiP and PDI, as well as a key component of the UPR, X-Box Binding Protein 1 (XBP1), a transcription factor which will be discussed in more detail later (Yamamoto et al. 2007).

Like PERK, ATF6 is also able to induce apoptosis in the event of prolonged UPR activation, and this is performed through the upregulation of regulator of calcineurin 1 (RCAN1) (Belmont et al. 2008). RCAN1 sequesters the calcium-activated phosphatase, calcineurin, which would otherwise be able to dephosphorylate Bcl2 antagonist of cell death (BAD). In its phosphorylated state, BAD sequesters the pro-survival protein Bcl2, leading to a pro-apoptotic environment (Wang et al. 1999).

1.3.6 IRE1 branch

Similar to the activation of PERK and ATF6, IRE1 activity is generally thought to be at least partially mediated by the chaperone BiP. During stress conditions, BiP dissociates from IRE1, leading to the formation of IRE1 homodimers and subsequent autophosphorylation (Bertolotti et al. 2000; Kimata et al. 2003). Once active, the IRE1 homodimer is then able to bind directly to misfolded proteins to mediate its own downstream signalling (Gardner and Walter 2011; Kimata et al. 2007). This model is controversial, however, and it has also been proposed that IRE1 is not capable of binding to misfolded proteins and BiP dissociation is sufficient to trigger IRE1 activity (Oikawa et al. 2009). An alternate model is that IRE1 can be activated either directly or through the dissociation of BiP, but these are two distinct mechanisms that respond to different stress stimuli (Promlek et al. 2011).

Once activated, IRE1 has two distinct modes of activity. It has an endoribonuclease domain that mediates the cleavage of certain RNA molecules, and a serine/threonine kinase domain. The most well characterised substrate of the IRE1 endoribonuclease domain is XBP1. The gene expression of XBP1 is constitutive under normal conditions and, as previously mentioned, it is upregulated by ATF6 during the UPR (Yamamoto et al. 2007). However, transcripts of XBP1 must be spliced by IRE1 to be converted into an active form that can be translated into the transcription factor XBP1S (Lee et al. 2002). The removal of a 26bp intron from the transcript causes a shift in the open reading frame, which leads to the translation of a 370 amino acid protein, as opposed to the 266 amino acid chain that is translated from the unspliced transcript. The splicing of XBP1 by IRE1 is considered unconventional as occurs only in the cytoplasm and it does not utilise the usual spliceosome machinery. It is instead performed entirely by IRE1, which performs the cleavage of the intron, and the tRNA ligase complex component RTCB, which ligates the molecule back together after the intron is excised (Jurkin et al. 2014). A small degree of XBP1 splicing occurs under normal physiological conditions (Wang et al. 2015), but it is far more prolific under conditions of ER stress where IRE1 is activated.

The XBP1S transcription factor generated from spliced XBP1 transcripts upregulates a range of chaperone genes and physically expands the contents of the ER, thereby increasing its capacity to fold proteins (Lee et al. 2003). XBP1S has also been shown to upregulate secretory pathways and increase ribosome numbers, giving it a wide range of adaptive functions (Travers et al. 2000). Another gene upregulated by XBP1S is p58^{IPK}, an inhibitor of PKR and PERK, which represents one degree of cross-regulation between the UPR branches. High levels of p58^{IPK} were shown to cause a reduction in eIF2 α

phosphorylation, a major function of PERK (van Huizen et al. 2003). As the upregulation of p58^{IPK} occurs many hours after the activation of PERK, it is thought that p58^{IPK} signalling represents the shift from the adaptation strategy of the UPR to the cell death phase (Szegezdi et al. 2006), and therefore XBP1, like many aspects of the UPR, has downstream effects that can be both pro-apoptotic and pro-survival.

In yeast, translation of the unspliced form of XBP1 is blocked by a mechanism that is poorly understood, and only the orthologue of XBP1s, hac1, can be translated (Hetz and Glimcher 2009). However, in mammalian cells XBP1u is translated into XBP1U, a protein with a rapid rate of degradation (Chen et al. 2014) that functions by sequestering bound proteins to the 26S proteasome for degradation (Yoshida et al. 2006). Two known substrates of XBP1U are XBP1S (Yoshida et al. 2006) and the active form of ATF6 (Yoshida et al. 2009), and XBP1U therefore functions as a regulator of the activity of these two proteins by downregulating these potent signalling molecules when the UPR stress response has ended.

IRE1 can also mediate other adaptive functions through its endoribonuclease domain beside those that are related to XBP1. Substrate transcripts that display the same stem-loop structure as XBP1u are degraded by cleavage (Moore and Hollien 2015) as part of a process named IRE1-mediated RNA degradation (RIDD) (Hollien and Weissman 2006). This degradation occurs predominantly in transcripts for transmembrane proteins, and it is thought that these proteins are especially challenging for the ER to fold and export. The degradation of these transcripts, therefore, provides a protective effect to a stressed ER, similar to the principle behind the attenuation of protein translation by PERK (Han et al. 2009; Hollien et al. 2009).

The IRE1 cytosolic kinase domain mediates pathways that are largely triggered late in the UPR and are pro-apoptotic (Yamamoto et al. 1999). For instance, IRE1 binds a mediator protein, tumour necrosis factor receptor associated factor 2 (TRAF2), to interact with Jun kinase and p38MAP kinase (Urano et al. 2000b), which promote cell death by downregulation of the pro-survival factor Bcl2 (Yamamoto et al. 1999). Phosphorylation of Bim by these kinases also promotes Bax-mediated apoptosis (Lei and Davis 2003).

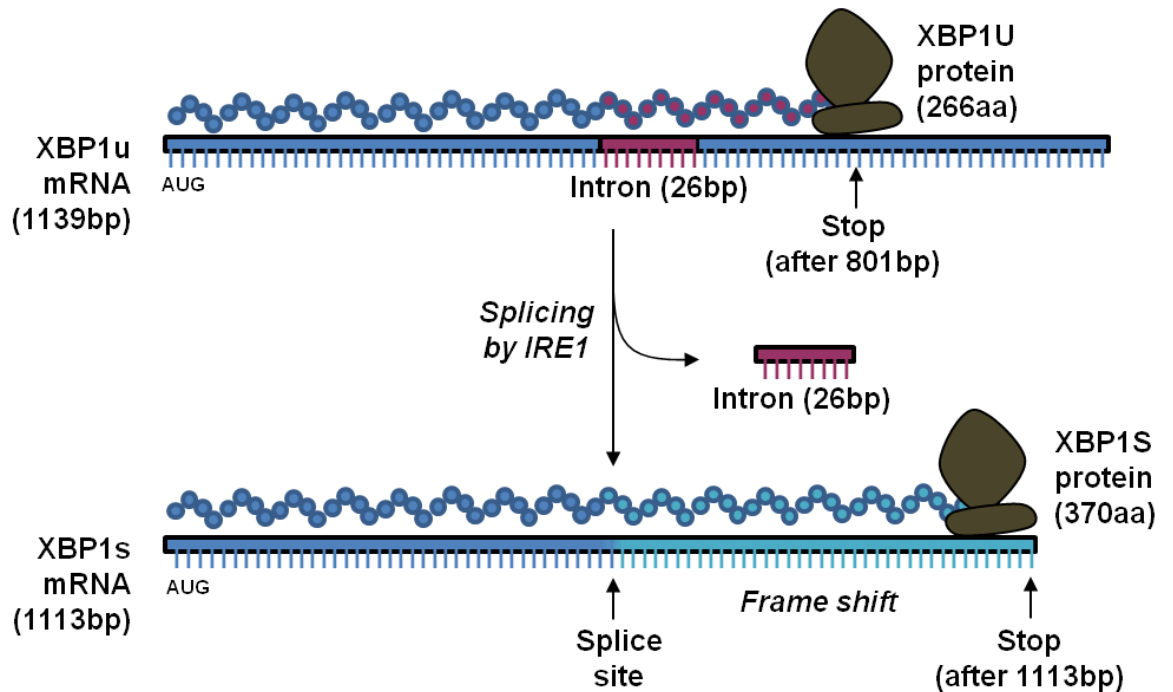


Figure 1-8 - Generation of the transcription factor XBP1S by splicing of XBP1 transcripts.

The reading frame of unspliced XBP1u transcripts has a stop codon after 801 nucleotides, which translates to a polypeptide chain of 266 amino acids and a protein of approximately 35kDa. Removal of the 26bp intron from XBP1u transcripts by IRE1 creates a frameshift in the open reading frame. This new reading frame has a stop codon after 1113 nucleotides, which translates to a polypeptide chain of 370 amino acids and a protein of approximately 60kDa that functions as a transcription factor.

1.4 Optimisation of protein production

1.4.1 Increasing productivity via genetic manipulation of folding factors

In addition to the previously described optimisation of host cell lines described in section 1.1, protein production can also be improved through genetic manipulation. The overexpression of an individual gene in a host cell line can often achieve the effect of amplifying its activity, although it should be noted that the effect of gene overexpression is not always predictable or beneficial. A number of gene manipulation strategies have been published with the aim of increasing the productivity of an exogenous protein from a host cell line. One such strategy is to optimise protein folding by amplification of folding factors, including PDI family members and chaperones.

The rationale behind this strategy is that it has been observed that recombinant gene transcript levels (Schroder and Friedl 1997) and gene copy number (Schroder et al. 1999) do not directly correlate with the amount of secreted antibody, suggesting that there is a bottleneck in protein production in post-translational steps such as protein folding (Mohan and Lee 2010). Due to this observation, it was hypothesised that overexpressing PDI or chaperones such as BiP may result in a faster rate of protein production and higher yields due to an increase in the rate of disulphide bond formation. This result was achieved in yeast (Xu et al. 2005); however, no such result has been obtained in mammalian cells. PDI family members were overexpressed in LBO-1 cells, a CHO derivative cell line, and no increase was observed in IgG4 formation (Hayes et al. 2010). The discrepancy between these two results highlights the differences between experiments performed in higher eukaryotes, where there is known overlap between the functions of folding factors, compared to lower eukaryotes, where these proteins are essential. It is also an example of the unpredictable nature of the ultimate effects of gene overexpression.

It has also been predicted that the recycling of PDI could be a rate limiting step in protein production (Lyles and Gilbert 1991). As this recycling reaction is now known to be catalysed by Ero1, the effect of the overexpression of Ero1 in host cell lines has been investigated. Ero1p was overexpressed in yeast and an increase in protein production was observed (Shusta et al. 1998). However, when mouse Ero1B was stably overexpressed in NS0 myeloma cells, no increase in monoclonal antibody production was observable (Hayes et al. 2010). A small increase in yield was seen with transient Ero1 α overexpression in CHO cells (Mohan and Lee 2010) and a greater increase when Ero1 α and PDI were co-overexpressed. However, this effect was only seen in transiently transfected cells, and stable cell lines showed a reduction in productivity. Western

blotting and immunostaining showed higher levels of intracellular antibody than normal, suggesting that Ero1 α overexpression promotes antibody retention in the ER and a reduction in secretion.

As calnexin and calreticulin have an essential role in glycoprotein folding and quality control, the manipulation of these proteins in host cell lines has also been investigated. Calnexin was overexpressed alongside subunits of nicotinic acetylcholine receptor (AChR)₂, a transmembrane channel protein, and it was reported that the folding rate of AChR had increased by twofold and the rate of degradation had decreased in COS and HEK293 cells (Chang et al. 1997). A similar effect was observed in CHO cells, where the inducible overexpression of either calnexin or calreticulin increased the yield of recombinant thrombopoietin (Chung et al. 2004).

1.4.2 Increasing productivity via manipulation of the Unfolded Protein Response

As the UPR has such a wide impact on the ability of cells to produce and fold proteins, and in cell survival, a number of elements of the UPR have been studied with the aim of exploiting in the industrial production of recombinant proteins. For instance, the yeast homologue of XBP1, *hac1*, was overexpressed in *Saccharomyces cerevisiae* to achieve an improvement in the production of two recombinant proteins, α -amylase and endoglucanase. In a mammalian equivalent to this approach, XBP1S was overexpressed in Chinese Hamster Ovary (CHO) cells, which resulted in an increase in the capacity of the ER and Golgi and a four-fold increase in the production of recombinant Vascular Endothelial Growth Factor (VEGF) (Tigges and Fussenegger 2006). A similar study found that overexpression of XBP1S increased the production of antibody, interferon and erythropoietin in both CHO cells and NS0 myeloma cells (Ku et al. 2008). This effect was observed when the cells' secretory pathways were saturated, and XBP1S was hypothesised to be able to overcome secretory bottlenecks, but was not hypothesised to have an effect when the pathways were not saturated. The inducible overexpression of XBP1s was also found to trigger a three-fold increase in yield of stably expressed antibody from CHO-K1 cells (Gulis et al. 2014). Interestingly, this increase was improved further by dropping the temperature of growth from 37°C to 30°C.

The UPR induced genes ATF4 (Ohya et al. 2008) and CHOP (Nishimiya et al. 2013) were overexpressed in CHO cells to achieve an increase in antithrombin III and IgG production respectively. The active form of ATF6 was overexpressed by Pybus and colleagues in CHO cells to achieve an increase in yield of a range of different 'difficult to express' antibodies. A similar improvement in yield was observed by this group with overexpression of BiP, PDI or XBP1s, and another noteworthy result was the observation

that reducing the extent of ATF6 or XBP1s overexpression improved the viability of the cell as well as the productivity of antibody, leading to an overall improvement in yield (Pybus et al. 2014). Together, these studies highlight the complexity of the balance between protein folding, degradation and secretion in mammalian cells, and also the unpredictability of engineering cells to possess the optimum properties for heterologous protein production.

1.5 Project aims and objectives

The first aim of the project was to identify potential genes or signalling pathways which could be manipulated in order to engineer CHO-derived host cell lines with increased capacity for producing high yields of recombinant protein. The initial approach to achieving this aim was to investigate protein folding pathways and the unfolded protein response, based on successes described in the literature achieved in this area. The project began with an investigation into the characteristics of an existing CHO-derived host cell line with a known high antibody yield, with the ambition that if the contributing factors towards this yield were known then further improvements could be made when developing future host cell lines. The cell line investigated was called CHO-S XE and was engineered by researchers at the pharmaceutical company UCB to stably overexpress the active form of XBP1, XBP1s, and the oxidoreductase Ero1 α (Cain et al. 2013). It was hypothesised that the high yield of CHO-S XE was a direct consequence of the activity of these two overexpressed genes, and the characterisation experiments performed in this cell line aimed to find to what extent this was the case.

A second aim of the project was to obtain a greater understanding of the stress responses of the cell; in particular, the activity and regulation of XBP1 during the UPR. This aspect of the project was investigated in the CHO-S XE cell line, and also in two other CHO-derived cell lines with inducible overexpression of XBP1s. By further elucidating the role of XBP1 in the UPR, and the attributes of cells that overexpress this key UPR component, it was thought that this information could contribute towards further improvements in the productivity and viability of antibody producing host cell line. As the activity of XBP1 is known to be tightly and complexly regulated, any potentially novel aspects of this regulatory process were sought in order to increase the overall understanding of this intricate signalling process.

These two project aims were approached with the following objectives:

- To characterise the high yield host cell line CHO-S XE.
- To generate a series of CHO-derived cell lines with inducible overexpression of the genes XBP1s, Ero1 α or GADD34.
- To find if the overexpression of these genes individually leads to an increase in antibody yield.
- To investigate the effect of co-overexpressing these genes on antibody yield.
- To find if a chemical inhibitor of IRE1 is able to improve viability and overall productivity of the XBP1s inducible cell line.
- To investigate the effect of exogenous XBP1s expression on endogenous XBP1 expression and the regulation of IRE1 activity.

Chapter 2 Materials and methods

2.1 Materials

2.1.1 Sources of chemicals, reagents and equipment

Unless otherwise stated, plasticware was sourced from Falcon, general reagents were sourced from Fisher and tissue culture plasticware was from Corning.

2.1.2 Solutions

Unless otherwise stated, solutions were made up in deionised water and stored at room temperature.

2.2 Cell culture methods

2.2.1 Maintenance of cell lines

Chinese Hamster Ovary suspension cells (CHO-S; *Life Technologies*) and CHO-S-derived cell lines were grown in a 25 mL culture volume of CD CHO medium (*Gibco*) supplemented with 4 mM glutamine (*Gibco*) in 125 mL vented Erlenmeyer flasks (*Fisher*). They were grown at 37°C with 95% humidity and 5% CO₂ on a SeaStar shaking platform (*Heathrow Scientific*) at 120 rpm with an orbital throw of 19 mm. They were diluted every 3-4 days to a density of 2-3 x 10⁵ cells/mL.

When CHO-S cells were grown in adherent culture, the medium used was DMEM supplemented with 10% foetal bovine serum (FBS), 2mM glutamine, and non-essential amino acids at a working concentration of 10 µM for each amino acid (*all Gibco*). Cells were grown on a stationary platform at 37°C with 95% humidity and 5% CO₂, and split every 3-4 days using a standard trypsin protocol. Briefly, confluent cells in a T75 flask were washed once with approximately 8 mL of Phosphate Buffered Saline (PBS) (*Gibco*) and then treated with 1.5 mL 0.05% Trypsin-EDTA (*Gibco*). The cells were incubated at 37°C for around 5 min, and then visualised under a light microscope to confirm that the cells had dissociated. Medium was added to the dissociated cells to a final volume of 10 mL, and 1 mL of this cell suspension was added to a fresh T75 flask to achieve a 1/10 split. An additional 11 mL of fresh medium was added to the split cells, including any appropriate selection: CHO-S XE cells were grown in medium supplemented with 1 mg/mL G418 (*Sigma*) and 200 µg/mL zeocin (*Invitrogen*); cells containing the pTetOne vector were grown in medium containing 5 µg/mL puromycin (*Sigma*); and the ER-BFP vector was maintained with 1mg/mL G418.

2.2.2 Cell count and viability

Cells were counted and the viable cell density was calculated using a Countess II FL cell counter (*Life Technologies*) by adding 10 μL of cell suspension to 0.4% (w/v) trypan blue in PBS and mixing thoroughly. The mixture was loaded onto a cell counting slide with 10 μL into each side and inserted into the cell counter for analysis. A Vi-CELL cell viability analyser (*Beckman Coulter*) was also used to count cells for some experiments.

2.2.3 Cryopreservation of cells

Suspension cell lines were counted and pelleted by low speed centrifugation, and then resuspended in CD CHO containing 10% (v/v) DMSO to achieve a cell density of approximately 1×10^7 cells/mL. Of this suspension, 1 mL was added to a 1.5 mL cryovial (*Alpha Laboratories*) and the vial was quickly chilled to -80°C . If long term storage was required, the cryovials were later transferred to a liquid nitrogen tank. Adherent cell lines were frozen by a similar method, but using FBS with 10% (v/v) DMSO instead of CD CHO.

2.2.4 Thawing cells from frozen stocks

Frozen cryovials were thawed carefully in a 37°C water bath and added to 9 mL pre-warmed cell culture medium. The cells were pelleted and resuspended in fresh medium and added to an appropriate cell culture flask.

2.2.5 Generation of stable cell lines

pTetOne stable cells were made by transfecting 4 μg of pTetOne vector (*Clontech*) containing cDNA for either GADD34, Ero1 α or XBP1s into CHO-S cells, co-transfected with 200 ng of a linear selectable marker for puromycin (a vector:marker ratio of 20:1) with 4.2 μL of the transfection reagent NovaCHOice (*Novagen*). Transfected cells and untransfected control cells were grown in a 6 cm diameter dish in adherent culture, and after 24 h of growth were trypsinised and 1/10 of the cells were transferred to a 15 cm dish and grown in 20 mL medium containing 12.5 $\mu\text{g}/\text{mL}$ puromycin. The transfected cells were grown for approximately 10 days, refreshing the selection medium every 3-4 days, until single cell derived colonies started to form in the dish. Colonies were identified and removed from the dish using trypsin-soaked colony discs and transferred into the wells of a 12 well plate, with one colony per well. The clones were grown under selection for another 3-5 days until the well was confluent, then the surviving clones were transferred into T25 flasks and later T75 flasks.

To generate a cell line containing ER-localised blue fluorescent protein, XBP1-pTetOne cells were transfected with BFP construct (a gift from Dr Erik Snapp (Costantini et al. 2015)) using the same method as described above. The vector for this construct contained a G418 resistance gene, and therefore the linear selectable marker was not required. Transfected cells were maintained under the dual selection of both 12.5 µg/mL puromycin, to maintain the XBP1-pTetOne construct, and 2 mg/mL G418 (*Promega*) to maintain the BFP construct. Successful integration of the gene of interest was confirmed using western blotting.

2.2.6 Doxycycline treatment

Doxycycline was prepared as a 1 mg/mL solution in water. This was shielded from light and stored at -20°C. Doxycycline was diluted to 1 µg/mL in fresh medium and added to the cells.

2.2.7 Tunicamycin treatment

Tunicamycin was prepared as a 10 mg/mL stock in DMSO and stored at -20°C. It was generally used at a working concentration of 10 µg/mL, unless otherwise stated.

2.2.8 4µ8C treatment

The IRE1 inhibitor 8-formyl-7-hydroxy-4-methylcoumarin (4µ8C) (Cross et al. 2012) was prepared as a 100 mM stock in DMSO. The stock was shielded from light and stored at -20°C. It was used at a working concentration of 32 µM.

2.2.9 Transient transfection

20 µg plasmid DNA was mixed with 20 µL of the chemical transfection reagent NovaCHOice (*Novagen*) in 2 mL warm CD CHO medium. The reagents were mixed thoroughly and incubated at room temperature for 10 min. After this period the transfection mixture was added to cells growing at a density of 1 x 10⁶ cells/mL, for a total culture volume of 25 mL. For determining antibody yield, pTetOne inducible cells were transfected with γ heavy chain and κ light chain of an IgG1 antibody targeting A33, a protein marker of colorectal cancer (Heath et al. 1997). Transfected cells were split 24 h post-transfection into six flasks. Three of these flasks were induced with doxycycline and three were left uninduced, and an anti-clumping agent (*Gibco*) was added at a 1:1000 dilution to all flasks. pTetOne cell lines were grown without puromycin when transfected. The cells were grown for a further three days in a culture volume of 12 mL, and then counted, pelleted by low speed centrifugation and the

medium was extracted for analysis using an antibody capture ELISA. Medium samples were stored at 4°C until required.

2.2.10 ER Tracker treatment

ER Tracker Green BODIPY FL Glibenclamide (*Molecular Probes*) was dissolved in DMSO to a 1 mM stock concentration. Experimentally treated cells were stained with 250 nM ER Tracker in Hank's Balanced Salt Solution (HBSS) for 30 min, then trypsinised and resuspended in DMEM.

2.2.11 Flow cytometry

Cells were washed once in HBSS then run on either a FACSCalibur or FACSCanto II flow cytometer (*BD Biosciences*) in HBSS. Dead cells were not generally excluded from the analysis, and 10000 events were counted for each sample. If dead cells were required to be identified then the cells were stained with 5 µg/mL propidium iodide before analysis, and detected using the FL3 filter on the FACSCalibur flow cytometer. ER Tracker Green has an excitation at 504 nm and emission at 511 nm, which can be detected using the FITC filter on the FACSCanto flow cytometer. Blue fluorescent protein has an excitation of 385 nm and emits at 448 nm, which is detectable using the Pacific Blue filter. The data obtained was analysed using Flowing Software (*Turku Bioimaging*).

2.3 DNA methods

2.3.1 Subcloning of pTetOne vector

Primers were designed to amplify cDNA for GADD34, Ero1 α or XBP1 using CLC Genomics Workbench (*CLC Bio*). Primer sequences are shown in Appendix 1. The forward primer sequence for each of these three genes contained a Not1 site, and the reverse primer contained an Age1 site. The cDNAs of interest were amplified by PCR, and the PCR products and pTetOne vector (*Clontech*) were treated with 20 units Not1 and Age1 (*NEB*) for 2 h at 37°C sequentially. The insert was ligated into the cut pTetOne vector using 1 unit DNA ligase (*Promega*), and the resulting vector was incorporated into XL1 Blue competent cells. These cells were grown overnight and the following day the pTetOne plasmid was purified out by alkaline lysis. To confirm the presence of the gene of interest in the pTetOne vector, a portion of the purified vector was treated with Not1 and Age1 and analysed by agarose gel electrophoresis. The presence of a DNA band at the appropriate size for the gene of interest confirmed that it had been successfully subcloned into pTetOne.

2.3.2 Plasmid prep

Plasmids were diluted 1:10 and added to XL1 Blue competent cells, and incubated on ice for 30 min. The cells were then heat shocked at 42°C for 90 s, briefly chilled on ice, and 800 μ L LB, made from 1% (w/v) bacto-tryptone, 0.5% (w/v) yeast extract and 1% (w/v) NaCl was added and the cells were shaken for 1 h at 37°C at 220 rpm in an Innova 4400 shaking incubator (*New Brunswick Scientific*). After shaking, 100 μ L of this culture was streaked onto agar plates, which were made with LB containing 1.5% (w/v) bacto-agar and a selection antibiotic (either 100 μ g/mL ampicillin (*Sigma*) or 50 μ g/mL kanamycin (*Roche*) depending on vector) and grown overnight at 37°C. Colonies were picked the next day and grown in 2 mL LB with antibiotic selection for 6 h, then added to 100 mL LB with antibiotic selection and grown overnight. The culture was pelleted at 1400 x g for 15 min and then the protocol for a MidiPrep (*Qiagen*) was followed. The resulting DNA was resuspended in 100 μ L DEPC-treated dH₂O and its concentration and purity (absorbance at 260 nm/280 nm) were measured on a Nanodrop 2000 spectrophotometer (*Thermo*), or a Spectrostar Nano LVis plate reader (*BMG Labtech*).

2.3.3 Agarose gel electrophoresis

Agarose gels were prepared by adding agarose (*Biorad*) to 40 mM Tris containing 20 mM acetic acid and 1 mM EDTA (TAE buffer), and heated until completely melted. Generally, 1% (w/v) agarose gels were used. The mixture was cooled to 50-60°C and

SYBR Safe (*Invitrogen*) was added at a 1:10000 dilution, and the gels were poured and set at room temperature. DNA was mixed with 6x purple loading dye (*NEB*) and added to the wells along with an appropriate DNA ladder (*NEB*). Gels were typically run at 100 V for 1 h, and then developed on a Uvidoc gel reader (*Uvitec*). Any DNA fragments requiring purification were cut from the gel with a scalpel and purified using a gel extraction kit (*Qiagen*), following the manufacturer's protocol.

2.3.4 XBP1 splice assay

RNA was extracted from stress treated cells using Trizol Reagent (*Ambion*) following the manufacturer's recommended protocol. First strand cDNA was synthesised using Superscript II Reverse Transcriptase (*Invitrogen*) with oligo dTs (*Invitrogen*) according to the manufacturer's specifications. cDNA for endogenous XBP1 was amplified using primers specific to the Chinese hamster XBP1 sequence, and the PCR yielded a 247 bp fragment for XBP1u and a 215 bp fragment for XBP1s, plus a hybrid band of approximately 280 bp. Both endogenous and exogenous XBP1 were amplified simultaneously with a second, less specific set of primers which can anneal to either the Chinese hamster or the human XBP1 sequence. PCR using these primers yielded the same fragments as the previous primer set but with the addition of a fragment of 221 bp for exogenous XBP1s. PCR was performed with Accuzyme DNA polymerase (*Bioline*) with an initial melting step of 95°C for 5 min, then 35 cycles of: 95°C for 45 s, an annealing step for 45 s, and 72°C for 45 s, followed by a final elongation step of 72°C for 10 min. The endogenous-only primers used an annealing temperature of 60°C and the exogenous/endogenous primers used 62°C. PCR products were run on a 2% (w/v) agarose gel in TAE buffer at 80 V for 1 h 40 min and then developed on a Uvidoc gel reader (*Uvitec*). If required, densitometric analysis was performed using ImageJ (*National Institute of Health*).

2.4 Molecular methods

2.4.1 Cell lysis

Suspension cells were counted using either a hemacytometer or a Countess II cell counter (*Life Technologies*), using 0.4% (w/v) trypan blue to exclude dead cells, then isolated by low speed centrifugation and resuspended in 5 mL PBS containing 20 mM N-ethylmaleimide (NEM). After 5 min the cells were isolated by centrifugation and resuspended in 1 mL of 50 mM Tris-HCl buffer containing 150 mM NaCl, 5 mM EDTA, 1% Triton X-100 (lysis buffer) and left on ice for 10 min. The lysates were centrifuged at 21000 x g for 10 min at 4°C, and the supernatant was extracted. If the lysate was not required immediately then it was frozen at -20°C.

Adherent cells were lysed by a similar method. After removing culture medium from the 6 cm diameter dish, the cells were washed with 20 mM NEM in PBS for 10 min. This was removed and 120 μ L lysis buffer was added to the monolayer and the cells were scraped into the buffer. This suspension was left on ice for 10 min, centrifuged at maximum speed for 10 min and the supernatant was extracted.

2.4.2 Preparation of polyacrylamide gels

Polyacrylamide gels were generally prepared on the day they were required. The resolving layer was usually 7.5%, 10% or 12% (v/v) acrylamide (*National Diagnostics*), depending on the protein of interest and the degree of separation required. The desired percentage of acrylamide was mixed with 5 mL 1.5 M Tris-HCl buffer (pH 8.8), 200 μ L of 10% (w/v) ammonium persulfate (APS), 200 μ L of 10% (w/v) sodium dodecyl sulphate (SDS) and the appropriate volume of water to achieve a final volume of 20 mL. After mixing, 25 μ L tetramethylethylenediamine (TEMED) was added and the mixture was poured into a mould and allowed to set. A thin layer of isopropanol was poured on top of the setting resolving layer to ensure an even surface. The stacking layer was prepared in a similar method as the resolving layer, except using 4% (v/v) acrylamide and 2.5 mL 0.5 M Tris-HCl buffer (pH 6.8), in a final volume of 10 mL. The isopropanol was removed from the mould and stacking mixture was added to the top of the resolving layer, and a 10 well or 15 well comb was set into the top. If the gel was not used immediately then it was wrapped in wet paper and cling film and stored at 4°C until required.

2.4.3 SDS PAGE

Crude lysates were mixed with 0.2 M Tris-HCl (pH 6.8) containing 10% (w/v) SDS, 20% (v/v) glycerol and 0.05% (w/v) bromophenol blue (sample buffer) in a 4:1 ratio of lysate to sample buffer. Dithiothreitol (DTT) was generally added as a reducing agent at a working concentration of 20 mM, unless the samples were required to be run under non-reduced conditions. Polyacrylamide gels were loaded with 20 μ L - 30 μ L of this sample mixture and run at 300 V and 20 mA per gel for approximately 2 h in a 25 mM Tris solution containing 200 mM glycine and 2.8 mM SDS.

2.4.4 Western blot

After separation, the samples were transferred to a nitrocellulose membrane (*GE Healthcare*) by wet transfer for 1 h at 300 V and 250 mA using 25 mM Tris containing 200 mM glycine, 3.5 mM SDS and 20% (v/v) methanol. The blots were blocked in 5% (w/v) non-fat milk powder (*Marvel*) in 50 mM Tris buffer (pH 7.5) containing 150 mM NaCl and

0.1% (v/v) Tween (TBST) for 1 h. Primary antibodies were diluted in TBST and generally incubated overnight, unless known to produce a sufficient signal within 1 h. Washes were performed three times for 10 min in TBST. Secondary antibodies were diluted in TBST and incubated for 1 h, and the blots were shielded from light throughout the incubation. Blots were developed using the Odyssey SA scanner (*Licor*) and analysed using Photoshop (*Adobe*) and ImageJ (*National Institute of Health*).

The following primary antibodies were used: anti-FLAG, mouse, 1:250 (*Sigma*); anti-Ero1 α , mouse, 1:500 (a gift from Dr Roberto Sitia; (Ronconi et al. 2010)); anti-PDI, rabbit, 1:500 (Jessop et al. 2009); anti-XBP1S, rabbit, 1:500 (*Biologend*); anti-GFP, rabbit, 1:1000 (*Thermo Scientific*); anti-GAPDH, mouse, 1:10000 (*Ambion*); anti-V5, mouse, 1:10000 (*Novex*); anti-tPA, goat, 1:250 (*Cambio*); anti-tubulin, mouse, 1:40 (*Santa Cruz*); anti-actin, rabbit, 1:500 (*Abcam*); anti-calnexin, rabbit, 1:2000 (*Stressgen*); anti-calreticulin, rabbit, 1:1000 (*Stressgen*); anti-BiP, rabbit, 1:500 (a gift from Dr Richard Zimmerman (Schäuble et al. 2012))

The following secondary antibodies were used: anti-mouse, 1:10000 (*Licor*); anti-rabbit, 1:10000 (*Licor*); anti-goat, 1:10000 (*Licor*). These antibodies are conjugated with a fluorescent molecule which emits at 800 nm. Fluorescently tagged Protein A was generated by Donna McGow using a method described in (Schellenberger et al. 2004). This targets the Fc region of antibodies and was used as a secondary probe at a 1:10000 dilution.

2.4.5 Protein A affinity purification

Medium from transfected cells was extracted and treated with 50 μ L 10% (w/v) Sepharose beads for 30 min to pre-clear the medium. The samples were centrifuged at 5500 x g for 5 min and the supernatant was kept. This was treated with 50 μ L 10% (w/v) Protein A Sepharose beads overnight. The samples were spun again at 5500 x g for 5 min to pellet the beads, these were kept and the supernatant discarded. The beads were resuspended with 1 mL of 50 mM Tris-HCl (pH 7.5) containing 1% (v/v) Triton X-100, 150 mM NaCl, 2 mM EDTA and 0.5 mM PMSF (immunoisolation buffer) and briefly centrifuged. The supernatant was removed and another 1 mL of immunoisolation buffer added. This washing was repeated two more times and then the beads were resuspended in 40 μ L of 100 mM Tris-HCl (pH 6.8) containing 4% (w/v) SDS, 0.2% (w/v) bromophenol blue and 20% (v/v) glycerol (sample buffer). The samples were frozen at -20°C.

2.4.6 TCA precipitation

Medium was removed from cell cultures and centrifuged at maximum speed to remove any floating cells, and then 1.2 mL of this medium was added to 300 μ L ice cold 100% (v/v) trichloroacetic acid and incubated on ice for 30 min. The samples were centrifuged at 21000 x g for 15 min at 4°C to generate a protein pellet. This was washed in 300 μ L of -20°C acetone, left on ice for 5 min then centrifuged for 5 min at 21000 x g. The acetone was removed and 100 μ L of sample buffer was added to the pellet and neutralised with 1M Tris solution. The samples were frozen at -20°C.

2.4.7 Antibody capture ELISA

Immulon 96 well flat-bottom plates (*Dynatech Laboratories*) were coated with 100 μ L/well anti-human CH1 antibody (*UCB*) in PBS and incubated at 4°C overnight. The plate was washed three times with PBS containing 0.1% (v/v) Tween (*Sigma*) and then blocked with 200 μ L/well of PBS containing 3% (w/v) BSA and 1% (v/v) Tween for 1 h. The plate was washed three times and then antibody-containing medium samples were added to the plate, diluted 1:20 in conjugate buffer (a 1/5 dilution of the blocking buffer in PBS). A standard IgG1 antibody (*UCB*) was added at 0.5 μ g/mL, and this was serially diluted in conjugate buffer across the plate with a 1/2 dilution each time. Antibody samples and standards were incubated for 1 h and then the plate was washed. The reveal antibody was a polyclonal mouse anti-human peroxidase-conjugate (*Southern Biotech*) used at a 1:5000 dilution in conjugate buffer; 100 μ L/well was added and incubated for 1 h at room temp. O-phenylenediamine dihydrochloride (OPD) substrate was made up by dissolving one urea buffer tablet and one OPD tablet (*Sigma*) in 20 mL dH₂O, and this was added to the washed wells at 100 μ L/well. After incubating for 20 min, the OD at 450 nm was read on a Pherastar plate reader (*BMG Labtech*) and adjusted for path length. The standard concentrations were calculated on a parabolic curve using Mars software (*BMG Labtech*) and these were used to calculate the concentrations of the medium samples.

2.5 Statistical methods

Densitometric analysis was performed using ImageJ (Schneider et al. 2012). Experimental variation was calculated using a Student's T test (two tailed, two sample equal variance) using Microsoft Excel. Variation was determined to be statistically significant when $p < 0.05$. Unless otherwise stated, error bars on graphs represent standard deviation across triplicate samples.

Chapter 3 Characterisation of the high yield cell line CHO-S XE

3.1 Introduction

3.1.1 Generation of a high yield host cell line

Chinese Hamster Ovary (CHO) cells are the most commonly used mammalian cell line for the industrial scale production of recombinant proteins. Due to the long history of the use of CHO cells, it is relatively easier to be granted licenser approval for products derived from CHO cells than for products made from a less commonly used cell type (Kim et al. 2012). Consequently, if a pharmaceutical company was seeking to increase the yield of therapeutic protein by engineering a novel host cell line with more advantageous characteristics over wild type CHO, it would be less risky for this company to use an engineered host cell line derived from a CHO lineage, than to invest significant time and resources in developing an entirely novel host cell line that may be rejected by regulatory bodies. Therefore, new methods of improving the yield of protein from CHO cells are being continuously sought by pharmaceutical companies. These methods, which are discussed in detail in Chapter 1, could involve changes to cell culture strategy, or genetic manipulation of the cells.

One aspect of the secretory process that has received relatively less attention as a strategy for the optimisation of yield is protein folding and the biochemistry of the ER. It was hypothesised that the folding of recombinant IgG antibodies - large, multi-domain proteins with 16-25 disulphide bonds, depending on the isotype (Frangione et al. 1968; Pink and Milstein 1967) - could be rate limiting (Mohan and Lee 2010). Disulphide bond formation was, therefore, identified as an area of potential improvement by the pharmaceutical company UCB, and a novel CHO cell line was developed by researchers that contained two stably overexpressed genes thought to be capable of improving the efficiency of protein folding (Cain et al. 2013). These two genes were XBP1s - a component of the UPR encoding a transcription factor that upregulates genes for chaperones and ER expansion (Lee et al. 2003; Shaffer et al. 2004) - and Ero1 α - a protein involved in the reoxidation and recycling of PDI (Cabibbo et al. 2000).

This novel cell line was named CHO-S XE and the first stage of its generation was to stably integrate an XBP1s overexpressing construct into CHO-S cells. The resulting intermediate cell line, named CHO-S X, was shown to have a higher yield of antibody than wild type CHO-S cells (Cain et al. 2013). CHO-S X was subsequently transfected with an Ero1 α overexpressing construct and put through another round of limiting dilution and clonal selection. Clones of CHO-S XE were selected based on antibody yield, and subsequent studies confirmed that three clones: XE1, XE2 and XE3, had

higher yield than both CHO-S and CHO-S X for a number of different antibody constructs, including difficult to express antibodies.

3.1.2 Preliminary characterisation of CHO-S XE

After engineering of the CHO-S XE clones XE1, XE2 and XE3, preliminary characterisation of these clones was performed by researchers at UCB and the PhD student Cathy Page at the University of Manchester. The XE clones were studied and compared to both wild type CHO-S and the intermediate cell line CHO-S X in a number of characteristics (Cain et al. 2013; Page 2012). Firstly, western blots of lysates from these five cell lines confirmed that the XE clones had higher Ero1 α protein levels than the endogenous levels found in CHO-S and CHO-S X, showing that these clones had successfully integrated the Ero1 α construct. The nomenclature of the XE clones reflects the extent of exogenous Ero1 α expression, in that XE1 had the highest expression of Ero1 α and XE3 had much lower expression, and not much higher than the endogenous protein levels found in CHO-S and CHO-S X. Western blots using an anti-XBP1S antibody showed that the three XE clones and CHO-S X had roughly equivalent XBP1S protein levels.

After confirming that the engineered cells contained the relevant genes of interest, the effect of the presence of these exogenous proteins on other signalling pathways in the cell was sought. It was found that XE1 and XE2 had upregulated levels of ERp57, a component of the calnexin/calreticulin quality control cycle; ERdj4, a chaperone and reductase upregulated as part of the UPR; and ATF4, a transcription factor involved in the UPR that operates downstream of PERK signalling. As these three proteins have a role in protein folding, they are possibly contributors to the increased rate of antibody production in CHO-S XE. While the upregulated ERp57 and ERdj4 are likely to be a direct result of XBP1s overexpression, ATF4 is not known to be upregulated by XBP1s. It is, therefore, likely that there is a low level of UPR activation present in CHO-S XE, with all three branches of the UPR active to some extent and not only the signalling downstream of exogenous XBP1s.

The growth rate and viability of the engineered cell lines was then investigated. All of the XBP1s overexpressing cell lines were found to grow faster than CHO-S and cultures reached a maximum viable cell density 1-2 days earlier. These traits are desirable in a good host cell line, as an increased cell count results in an increased amount of secreted protein from the culture. It is reported in the literature that there is often a trade-off between cell growth rate and protein secretion rate, and high producing cell lines often grow slower than their low producing counterparts (Stansfield et al. 2007). However, this did not appear to be the case for CHO-S XE. Additionally, glucose

consumption and lactate production were also lower for XE1 cultures than for CHO-S, and these are both traits associated with high producing cell lines (Zagari et al. 2013).

CHO-S and CHO-S XE1 were later stably transfected with two antibody constructs in order to carry out experiments involving the rate and reproducibility of recombinant protein production. One of these constructs was known to be relatively easy to express (Ab1), and the other was a difficult to express antibody (Ab2). For cells stably transfected with Ab1, the majority of the transfected CHO-S XE1 clones recovered showed expression of Ab1 to some extent: low expressing clones and high expressing clones were recovered, and very few clones were non-expressing. The maximum titre observed was 95 µg/mL. For CHO-S, there were far fewer clones that expressed Ab1 and the majority were non-expressing, but of the few clones that did express, the maximum titre recorded was also around 95 µg/mL. This data suggests that CHO-S XE1 is more amenable to stable transfection and construct integration than wild type CHO-S; however, the potential maximum yield of antibody is the same for both cell lines. A similar result was observed for Ab2, in that the majority of XE1 clones showed expression of Ab2 after stable transfection, although the titres were much lower with a maximum of 15 µg/mL. None of the CHO-S clones recovered showed any expression of Ab2.

The conclusion drawn from these experiments implies that the difference between the phenotypes of CHO-S and CHO-S XE is one of DNA uptake and retention, rather than of an increased efficiency of protein folding as originally intended. In order to test this hypothesis, DNA uptake from a transient transfection by electroporation was measured using a fluorescein labelled DNA probe. The fluorescence of the cells after transfection was measured by flow cytometry; however, it was found to be not significantly different between CHO-S and CHO-S XE1 at either 3 hours or 6 hours post-transfection.

As DNA uptake appeared to be the same for both cell lines, protein folding and secretory characteristics of the cell were studied instead. The size of the ER and Golgi were compared between the cell lines by transferring the cells from suspension to adherent culture in the presence of FBS, staining with organelle specific stains and mounting on coverslips for microscopy analysis. The CHO-S XE clones were seen to have a more dispersed and fragmented ER and Golgi than CHO-S, and the total staining of each organelle, as measured by pixel intensity, was significantly lower for the XBP1s overexpressing cell lines. This result was unexpected and counterintuitive, considering the well documented role of XBP1s in lipid biogenesis and ER expansion (Sriburi et al. 2004), and so researchers at UCB followed up on this experiment by using flow cytometry to measure the fluorescence of cells treated with an ER specific fluorescent

stain. This experiment showed an increase in ER size in CHO-S XE compared to CHO-S, which correlates more with what is known about the function of XBP1s.

In addition to ER size, the ability of the cells to cope with ER stress was also investigated. CHO-S XE1 showed a significantly faster rate of recovery from reductive stress, in the form of exposure to a strong dose of the reducing agent DTT, than CHO-S. It is possible that this increased rate of the restoration of redox balance is related to the larger ER size observed by flow cytometry. The extent of endogenous XBP1u splicing after tunicamycin treatment was also determined using PCR. Unexpectedly, the cell lines with exogenous XBP1s expression were found to have increased endogenous XBP1 splicing, and the counterintuitive nature of this result will be discussed in more detail in Chapter 5.

Although the specific contribution of XBP1s and Ero1 α to the high yield phenotype of CHO-S XE could not be clarified in more detail, it was still hypothesised that any differences observed between CHO-S and CHO-S XE were due to the function of exogenous XBP1s, Ero1 α or a combination of the two. In order to identify any effect on antibody yield caused by a depletion of one of the exogenously overexpressed genes in this cell line, Ero1 α expression in CHO-S XE1 was knocked down using siRNA. There was found to be a small reduction in stably expressed antibody with Ero1 α siRNA knockdown, but this reduction was not determined to be statistically significant when using a Student's T test. A similar experiment involving the knockdown of XBP1s was attempted, but XBP1s transcript levels could not be successfully lowered by siRNA and actually resulted in an increase in XBP1S protein, possibly through activation of the UPR. As both exogenous genes could not be knocked down simultaneously, it could not be determined if the loss of the exogenous genes would compromise the high yield phenotype of CHO-S XE1.

3.1.3 Objectives

The overall aim of this project was to identify methods of increasing the yield of secreted antibody in mammalian host cells through improving the efficiency of protein folding. The initial approach to achieving this aim was to expand on the promising results observed in CHO-S XE (Cain et al. 2013) and further characterise this cell line to determine the specific contribution of the co-overexpressed genes XBP1s and Ero1 α towards the high yield phenotype. It was thought that this information could then be used in the generation of novel host cell lines with greater yield than CHO-S XE.

The characterisation of CHO-S XE was continued in this project by comparing it to CHO-S, aiming to repeat some of the work performed by Cathy Page and Cain et al., and expand on any unanswered questions or other notable observations. For these experiments CHO-S cells were obtained from Life Technologies, and the CHO-S XE1 clone was received from UCB. It should be noted that for the remainder of this thesis the XE1 clone will be referred to as 'CHO-S XE-D', for CHO-S XE-derivative, as a number of differences were observed between the XE1 cells grown for this project and the cells described by Cain et al., and these differences will be discussed in detail throughout this chapter. No other clones of CHO-S XE were investigated during this project. CHO-S and CHO-S XE-D were compared in their viability and rates of growth, as well as in their yields of a number of different recombinant proteins in addition to antibodies. Another factor that was investigated was the relative abundance of endogenous proteins involved in protein folding and stress. These were compared between CHO-S and CHO-S XE-D as an indication of whether CHO-S XE-D has a larger ER than the parental cell line. ER size was also examined more directly using an ER specific stain which was detectable using flow cytometry, which was also used to determine overall cell size and mortality after transfection.

3.2 Results

3.2.1 CHO-S XE-D has a slower rate of growth than CHO-S

The first attribute that was investigated in CHO-S XE was a comparison of the rate of growth with that of CHO-S. Although this attribute was already documented by Cain et al, it was quickly observed after a few passages of culturing the cell lines that the CHO-S XE cells grown for this project (CHO-S XE-D) had a much slower rate of growth than previously reported for the CHO-S XE1 clone. In order to document this observation, CHO-S and CHO-S XE-D cells were cultured alongside CHO-S XE1 and an earlier passage of CHO-S, labelled EP in Figure 3-1. The cells were counted on a daily basis, as shown in Figure 3-1A, and the percentage of viable cells was calculated, shown in Figure 3-1B.

Both passages of CHO-S were shown to grow quickly in suspension culture, and reach a maximum cell count of 11-12 x 10⁶ cells/mL on the fourth day of culture. The viability of these cells remained constant across the time period and remained above 95% at all times. For CHO-S XE-D, not only was there a noticeably slower rate of growth than for CHO-S but there was also a discrepancy between the growth rate of XE-D and XE1, with XE-D having a cell count of 3.5 x 10⁶ cells/mL after four days compared to 8 x 10⁶ cells/mL for XE1. The viability of CHO-S XE-D was also low, and fluctuated between 65-75% during days 2-4 of culture and dropped as low as 55% on the first day of growth. The viability of XE1 was better, fluctuating between 80-95% across the time period. The data presented is representative of a consistent trend for the growth characteristics of CHO-S and CHO-S XE-D throughout the project.

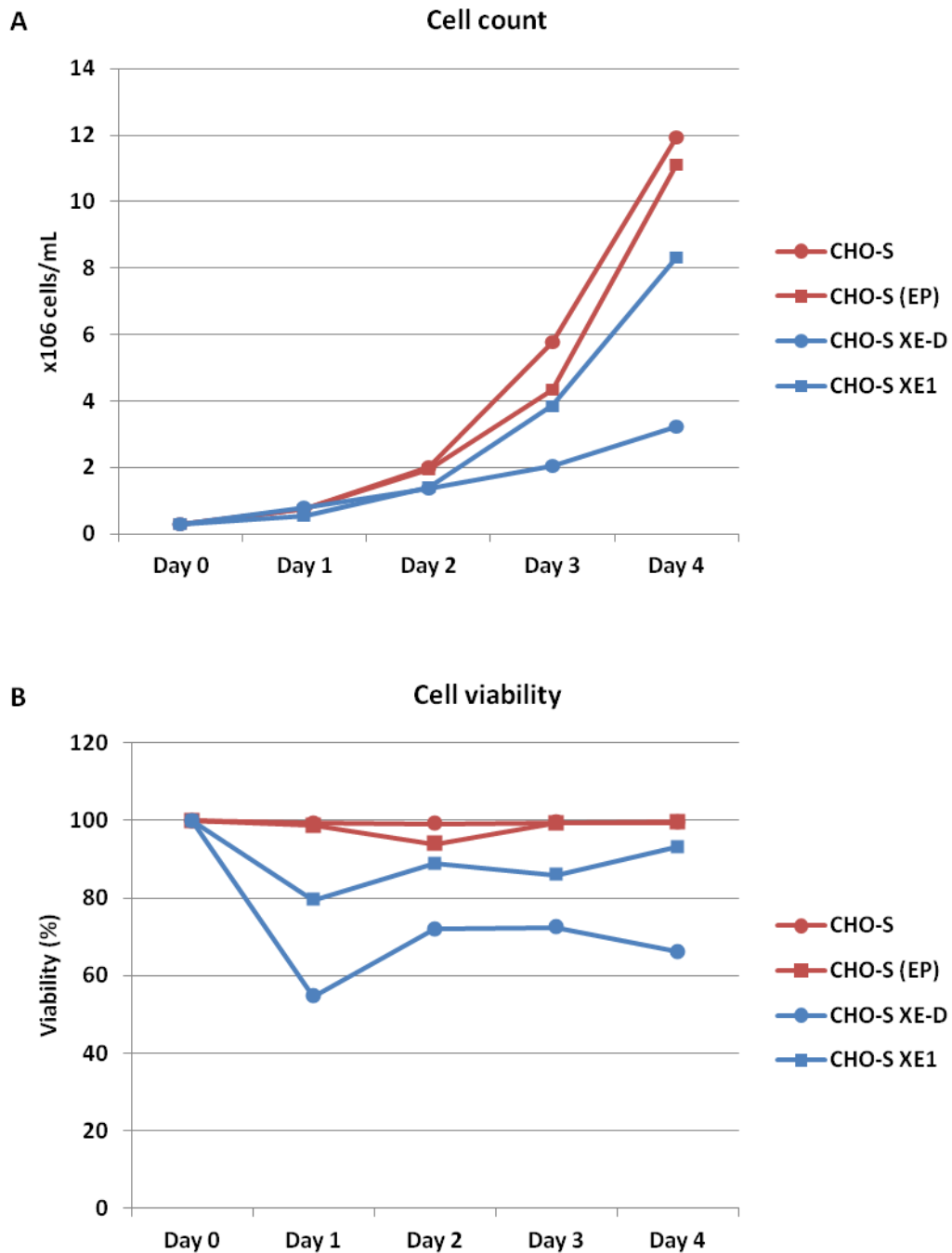


Figure 3-1 - CHO-S XE-D has a slower rate of growth than CHO-S

CHO-S and CHO-S XE-D cells were grown for four days and (A) cell counts (cells/mL) and (B) the percentage of viable cells were measured daily using a Vi-CELL cell counter. The growth characteristics of an earlier passage of CHO-S, labelled early passage (EP), and CHO-S XE1 were also investigated. A direct comparison of the growth and viability of these four cell types was performed only once, although the data represents a trend observed consistently throughout the project for CHO-S and CHO-S XE-D, as well as previously observed data for CHO-S XE1.

3.2.2 CHO-S XE-D has a high yield of secreted proteins

It was hypothesised that there may be a correlation between the number of disulphide bonds in a recombinant protein and the yield of that protein from CHO-S XE. The rationale behind the creation of the CHO-S XE lineage was that the overexpression of XBP1s in CHO-S XE would cause the ER of these cells to enlarge, and the overexpressed Ero1 α would increase the rate of recycling for PDI, which would in turn increase the rate by which disulphide bonds could be inserted into nascent proteins. By this rationale, CHO-S XE would be more efficient at producing a heavily disulphide bonded protein than CHO-S, and would, therefore, have a higher yield, but both cell lines should be equally capable of secreting proteins with no disulphide bonds. In order to test this hypothesis, CHO-S and CHO-S XE-D cells were transiently transfected with one of three recombinant proteins: IgG1 antibody heavy and light chains; alpha 1 anti-trypsin (α 1AT); or tissue plasminogen activator (tPA), and then grown for three days. Of these proteins tPA has the most disulphide bonds, 23, followed by IgG1 with 16 disulphide bonds, and α 1AT has no disulphide bonds.

After the three day growth period, the cells and medium were harvested. IgG1 was purified using protein A affinity isolation, and tPA and α 1AT were precipitated using TCA. The amount of exogenous protein in the medium or lysate was quantified using western blotting. Figure 3-2A shows the amount of IgG, α 1AT or tPA present in the medium, and Figure 3-2B shows levels of IgG and α 1AT in the lysate. The lysate blot of tPA is not shown as a sufficiently clear blot was not obtained. As previously mentioned, CHO-S has a faster growth rate than CHO-S XE-D and it was observed that the cell count for CHO-S was consistently 2-3 fold higher than for CHO-S XE-D after three days of growth. In order to take this into consideration, the protein bands were quantified using ImageJ software and normalised against the number of cells.

The relative increase in yield for CHO-S XE-D compared to CHO-S when normalised against the cell count is shown in Figure 3-2C for the medium samples and Figure 3-2D for lysates. The yield of IgG was 4.2 fold higher in CHO-S XE-D than CHO-S for secreted material, and 5.4 fold higher for intracellular material. For α 1AT the secreted material yield was 3.7 - 8.1 fold higher in CHO-S XE-D and the intracellular yield was 2.8 - 11.2 fold higher. The yield of tPA was quantified as being 15.2 fold higher in CHO-S XE-D in the blot shown, but this result cannot be directly compared to the others as it is derived from a single blot and not triplicate blots. The tPA produced from CHO-S was often too low to accurately quantify, and too few clear and quantifiable repetitions were obtained to perform accurate statistical analysis. Overall, the amount of transfected protein can be seen to be much higher for CHO-S XE-D than for CHO-S, even when its

lower cell count is not taken into consideration. While the high yield of CHO-S XE-D was anticipated due to the previously published work on the productivity of CHO-S XE1 (Cain et al. 2013), the nature of this high yield, in that it appears to be applicable to any secreted protein regardless of its structural complexity, is contrary to what was hypothesised. Despite this, a host cell line with an ability to potentially secrete any recombinant protein in high abundance is more desirable and industrially relevant than, for instance, a host cell line that can produce high titres of multi-domain proteins or single domain proteins would be.

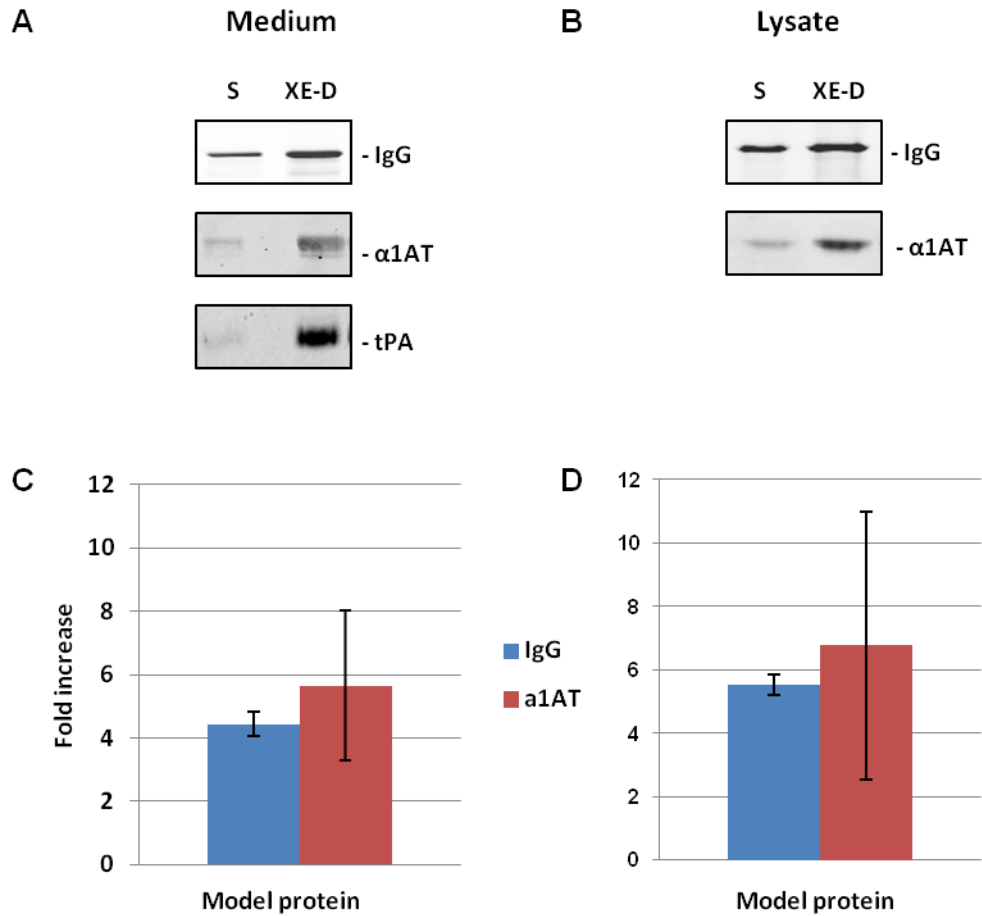


Figure 3-2 - CHO-S XE-D has a high yield of secreted proteins

(A) Western blots showing levels of recombinant protein present in the medium of CHO-S and CHO-S XE-D cells transiently transfected with one of the following proteins: IgG antibody; alpha 1 anti-trypsin (α 1AT), a protein with no disulphide bonds in its structure; or tPA, a protein with many disulphide bonds. (B) Western blots of intracellular material from transiently transfected CHO-S and CHO-S XE-D. (C) Quantification of the fold increase in yield for CHO-S XE-D for secreted material and (D) intracellular material. Error bars represent the standard deviation across triplicate flasks. Experiment was performed at least three times for each model protein.

3.2.3 CHO-S XE-D has higher levels of transiently transfected GFP

The high yield of CHO-S XE-D was further investigated by comparing the fluorescence from transiently transfected GFP between CHO-S and CHO-S XE-D using flow cytometry. Cells were transfected with either eGFP or empty vector, or were left untreated, and then grown for three days. At the end of the transfection period the cells were lysed and a western blot of transfected cell lysates probed with an anti-GFP antibody is shown in Figure 3-3A. More eGFP protein can be seen in CHO-S XE-D lysates than CHO-S from an equivalent number of cells. This result is similar in some aspects to the results shown in Figure 3-2, in that CHO-S XE-D displays higher productivity of a transfected, exogenous protein than CHO-S. However, one key difference between the experiments is that eGFP is not a secreted protein, and is localised to the cytosol of transfected cells. This result, therefore, suggests that the basis of the high yield phenotype of CHO-S XE-D is not related to the secretory pathway, and is instead due to an increase in efficiency in an earlier stage of protein production such as gene transcription, protein translation, or aspects of protein folding and maturation other than disulphide bond formation.

In order to further explore this finding, green fluorescence from the transfected cells was analysed by flow cytometry. This experimental approach would reveal the abundance of correctly folded, functional eGFP as only protein in this state has the ability to emit fluorescence, whereas a western blot would be capable of detecting misfolded or aggregated proteins in addition to correctly folded GFP. The amount of folded and functional eGFP present in the cells was estimated by comparing the fluorescence of the untreated and mock transfected controls (autofluorescence) with that of the eGFP transfected cells. Figure 3-3A shows histograms of green fluorescence intensity emitted by each cell plotted against cell count. The intensity of emitted fluorescence was categorised arbitrarily into regions of 'low', 'medium' or 'high' intensity on the histograms, and the percentage of cells found in each of these regions is indicated in the tables below the histograms. The number of cells found in the 'low' and 'medium' intensity regions in untreated cells is similar between CHO-S and CHO-S XE-D, and these values can be considered to be autofluorescence. The intensity of fluorescence from mock transfected cells is higher than that of untreated samples, possibly due to a small degree of cell stress resulting from exposure to the transfection reagent, but this increase in autofluorescence does not vary between CHO-S and CHO-S XE-D. Fluorescence intensity from GFP transfected CHO-S cells is found predominantly in the 'low' and 'medium' regions, which could represent autofluorescence or cells with a low transfection efficiency, and only the 23.49% of cells have emission higher than autofluorescence, found in the 'high' region. For the population of CHO-S XE-D cells

transfected with GFP, only 1.84% of cells emit 'low' fluorescence, whereas 52.24% of cells have 'medium' emission and 45.93% have 'high' emission. This indicates that the average intensity is higher for CHO-S XE-D cells than for CHO-S. The overlaid histograms in Figure 3-3B further highlight the increase in fluorescence intensity emitted from the CHO-S XE-D population compared to the CHO-S population. This experiment was performed three times and the results from a representative experiment are shown. The western blot and flow cytometry data together suggest that CHO-S XE-D is able to produce more correctly folded eGFP protein than CHO-S under the same transfection conditions, although the exact mechanism for this increase is not clear.

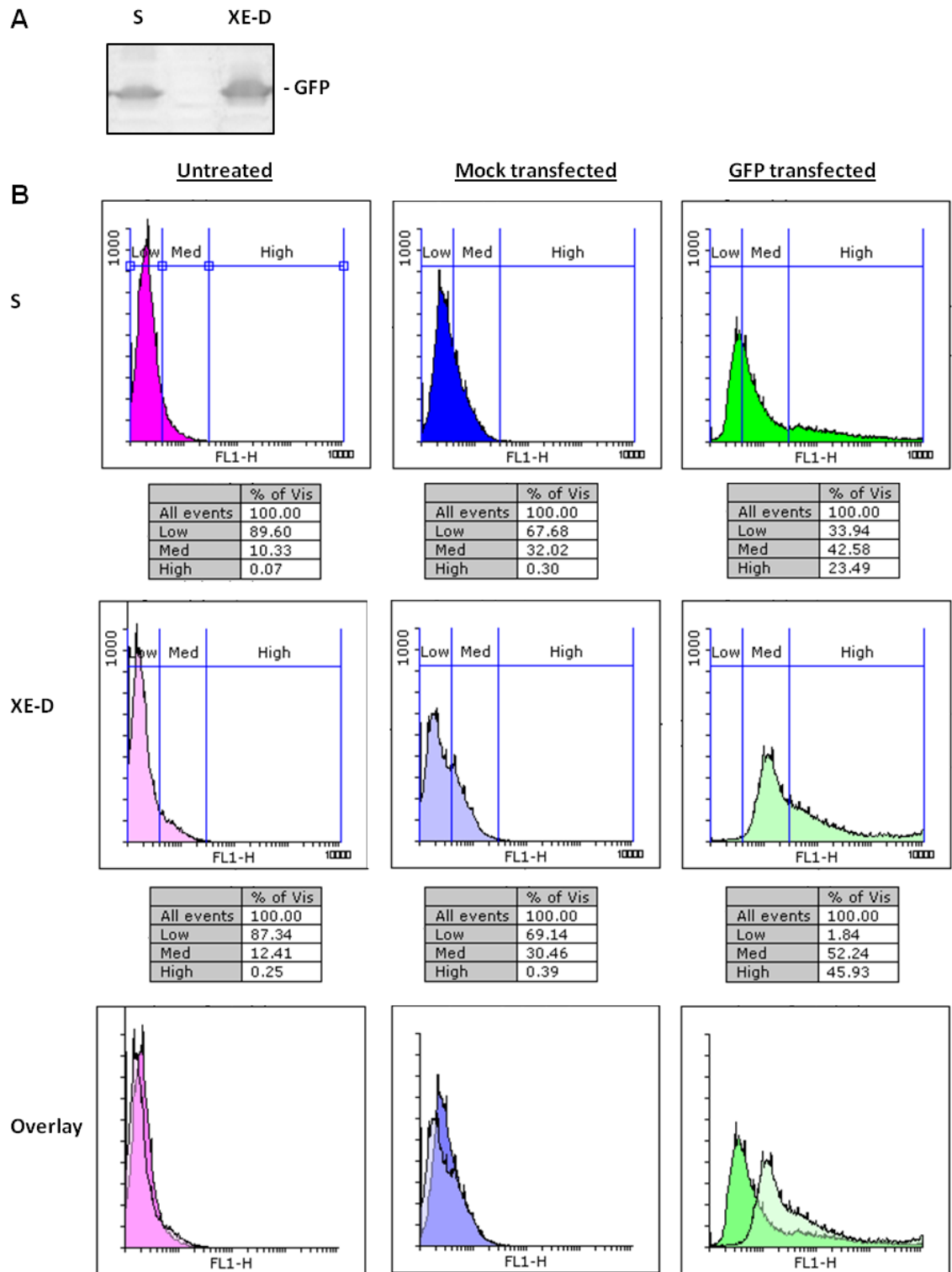


Figure 3-3 - CHO-S XE-D has higher levels of fluorescence from transiently transfected eGFP.

(A) Anti-GFP western blot of equivalent numbers of CHO-S and CHO-S XE-D lysates. (B) Flow cytometry analysis of fluorescence from CHO-S and CHO-S XE-D cells transiently transfected with eGFP or mock transfected. Fluorescence emitted from cells is categorised into regions of low, medium or high intensity. The percentage of cells found in each category of intensity is indicated in the table below each histogram. Experiment was performed three times, data from a representative experiment is shown.

3.2.4 CHO-S XE-D has high levels of endogenous proteins

In order to confirm that the genes XBP1s and Ero1 α were overexpressed in CHO-S and CHO-S XE-D, lysates from equivalent numbers of cells were separated by SDS-PAGE under non-reducing conditions and probed with antibodies targeting XBP1S or Ero1 α protein by western blot. Figure 3-4 shows that both proteins can be seen in CHO-S XE-D, whereas in CHO-S XBP1S can be seen only faintly and Ero1 α not at all. Ero1 α appears as a doublet on a non-reduced gel because the protein is present in two forms: the top band represents the active form and the lower band represents the inactive form. The regulation of the activity of Ero1 α by the rearrangement of active site disulphide bonds is explained in more detail in Section 1.2.3. The western blot indicates that these proteins are more abundant in CHO-S XE-D than CHO-S because they are exogenously overexpressed.

The relative abundance of a range of proteins involved in disulphide bond formation, protein folding and the UPR was then compared between the two cell lines, with the aim of determining whether these genes were being upregulated by either of the exogenous genes in CHO-S XE-D. Lysates from an equivalent number of CHO-S and CHO-S XE-D cells were separated by SDS-PAGE under reducing conditions and probed with a range of antibodies against proteins which are known to be involved either with XBP1s or with Ero1 α . The proteins investigated were: BiP, involved in identifying and stabilising unfolded proteins; calnexin, a lectin localised to the ER membrane that has a role in the quality control of protein folding; calreticulin, a homologue of calnexin localised to the ER lumen; CHOP, involved in apoptotic UPR signalling; PDI, which inserts, rearranges and reduces disulphide bonds and is a client protein of Ero1 α ; and PRX4, a member of the peroxiredoxin family. The protein folding/UPR related proteins shown in Figure 3-4 were analysed using ImageJ to measure the pixel intensity of the bands, and each of these proteins was found to be expressed between 1.41 - 3.28 fold higher levels in CHO-S XE-D when normalised against the number of cells.

As an alternative method of normalising the data, a range of commonly used 'housekeeping' proteins were also probed for in a western blot. These proteins were expected to remain relatively constant between the cell lines; however, the levels of both actin and tubulin are found to be 1.60 fold and 1.32 fold higher, respectively, in CHO-S XE-D than CHO-S. If it had been found that every identified endogenous protein was expressed at higher levels in CHO-S XE-D than CHO-S, then these results could perhaps be attributed to a flaw in the method for counting the cells, and it could be concluded that the lysates had not been taken from equivalent cell numbers. However, this appeared to not be the case as it was also found that GAPDH, a very commonly used

housekeeping protein, was found at approximately 50% lower abundance in CHO-S XE-D as in CHO-S. In fact, the images shown in Figure 3-4C for actin and GAPDH are cropped images taken from the same original blot, and therefore from the same samples of CHO-S and CHO-S XE-D. It was, therefore, unclear which housekeeping protein was the best to normalise the other data to in order to accurately measure endogenous protein levels in the two cell lines.

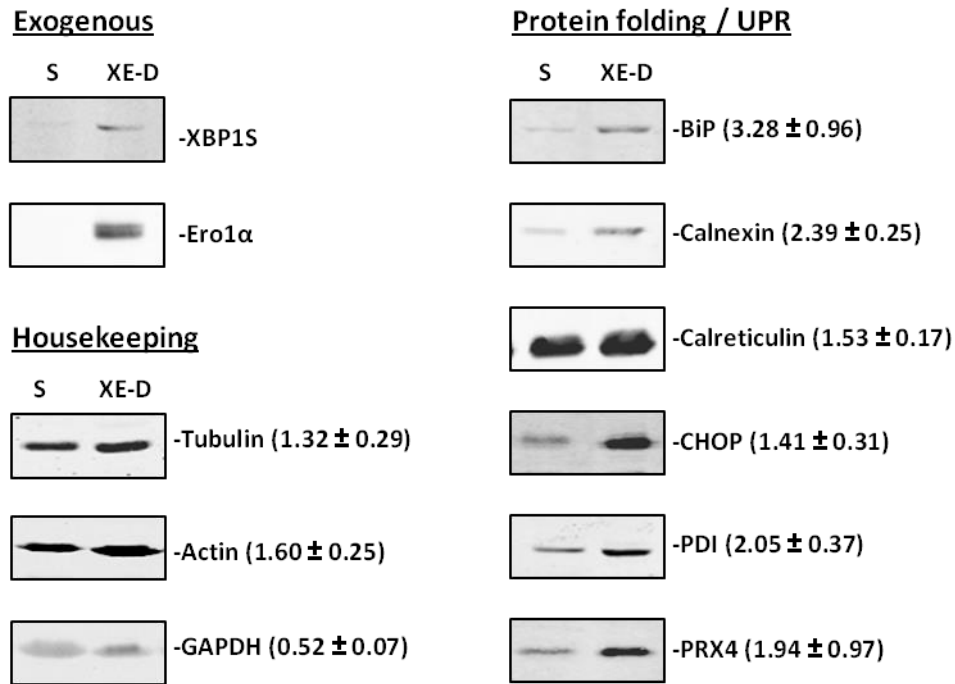


Figure 3-4 - CHO-S XE-D has high levels of endogenous proteins

Lysates from an equivalent number of CHO-S and CHO-S XE-D cells were probed with antibodies targeting XBP1S and Ero1α, the genes that are overexpressed in CHO-S XE-D. Lysates were also probed for a range of endogenous proteins involved in either protein folding and the UPR, or general housekeeping. Values represent the number of folds higher of protein in CHO-S XE-D than CHO-S \pm standard deviation across triplicate samples. Quantification is not shown for XBP1S and Ero1α due to the unquantifiable levels present in CHO-S.

3.2.5 CHO-S XE-D cells are larger than CHO-S

While culturing both CHO-S and CHO-S XE-D, it was observed that CHO-S XE-D cells appear noticeably larger than their wild type counterparts under a microscope. This observation, together with the western blot data showing that both ER and cytoskeletal proteins are found at higher abundance in CHO-S XE-D, suggesting that these cells may have a larger size than CHO-S, was further investigated using flow cytometry. Untransfected cells were analysed by the flow cytometer to measure forward scattering, an indication of cell size, and the forward scattering histograms are shown in Figure 3-5. CHO-S XE-D is shown to have a larger average cell size than CHO-S, which supports the previous observations from microscopy, and the western blot data on the levels of ER and cytoskeletal proteins. Dead cells and debris were not excluded from the analysis, and the CHO-S XE-D data appears to show more debris present than for CHO-S, as shown in the left hand of the histogram representing the smallest measurements for forward scattering.

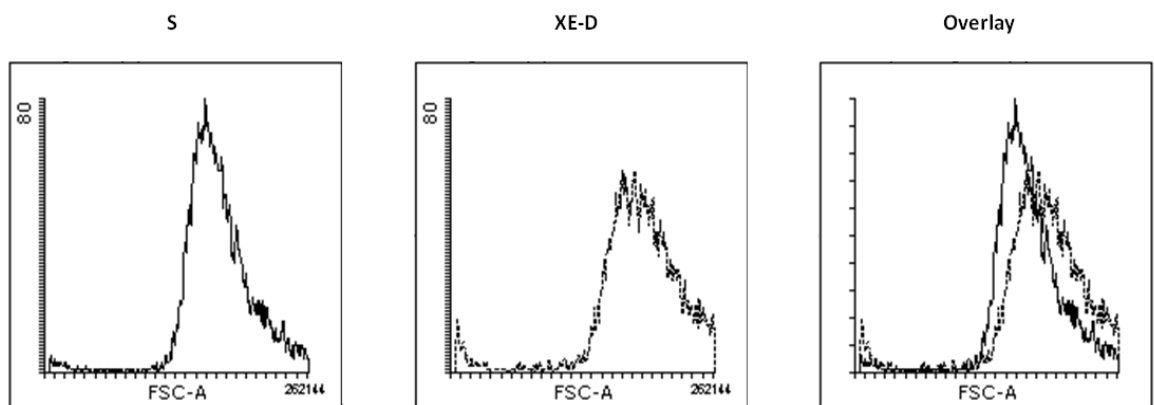


Figure 3-5 - CHO-S XE-D cells are larger than CHO-S.

Flow cytometry analysis of untransfected living CHO-S cells (solid line) and CHO-S XE-D cells (dashed line) showing forward scattering, an indication of cell size. Experiment was performed in triplicate, representative histograms are shown.

3.2.6 CHO-S and CHO-S XE-D have the same amount of ER membrane

In order to determine the effect of constitutively overexpressed XBP1s on the amount of ER membrane, CHO-S and CHO-S XE-D cells were stained with ER Tracker, a glibenclamide based fluorescent green dye which binds specifically to potassium channels prominent in the ER membrane. After staining, the cells were quenched, washed and analysed by flow cytometry in order to measure the green fluorescence from the two populations of cells. The green fluorescence emitted from each cell should be proportional to the amount of ER membrane contained within that cell. Figure 3-6 shows histograms of data gathered using the FITC filter on the flow cytometer, which detects green fluorescence.

The FITC histograms of CHO-S and CHO-S XE-D overlap closely, showing that the green fluorescence produced by both populations of cells is the same. This suggests that both cell lines have the same amount of ER membrane, despite the presence of increased levels of XBP1s in CHO-S XE-D, and this is contradictory to what is known about the function of XBP1s (Shaffer et al. 2004).

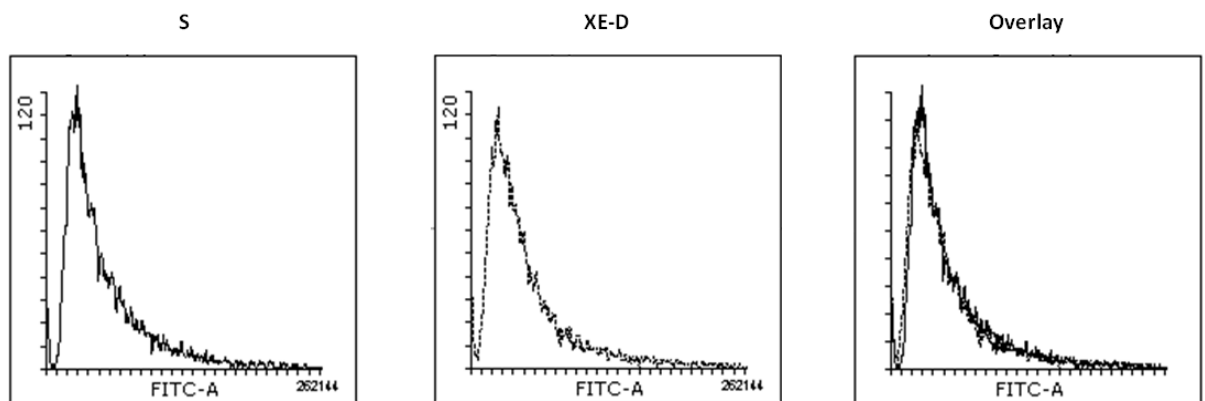


Figure 3-6 - CHO-S and CHO-S XE-D have the same size of ER membrane

Flow cytometry analysis of untransfected living CHO-S cells (solid line) and CHO-S XE-D cells (dashed line) showing data from the FITC channel, an indication of green fluorescence. Experiment was performed in triplicate, representative histograms are shown.

3.2.7 CHO-S XE-D shows higher cell mortality when transiently transfected

It was observed that CHO-S XE-D cells are more prone to clumping than CHO-S, particularly when transfected, and this may be another indication of the reduced viability seen in Figure 3-1. This observation was further investigated by using propidium iodide (PI) to stain dead cells, which allowed for any dead cells in a population to be identified using flow cytometry as the dye does not enter living cells. This staining was used to determine the viability of transiently transfected CHO-S and CHO-S XE-D when using the chemical transfection reagent NovaCHOice.

Cells with high PI fluorescence are shown in the blue regions of the histograms in Figure 3-7, and the percentage of cells found in this region is indicated. CHO-S showed 16.01% mortality when mock transfected and 13.01% mortality when transfected with GFP, whereas CHO-S XE-D showed 23.68% mortality when mock transfected and 19.97% mortality when transfected with GFP. This increase in post-transfection mortality may be an indication that CHO-S XE-D is under a higher level of stress than CHO-S under normal conditions, and the increased stress caused by transient transfection is fatal to more cells than in CHO-S.

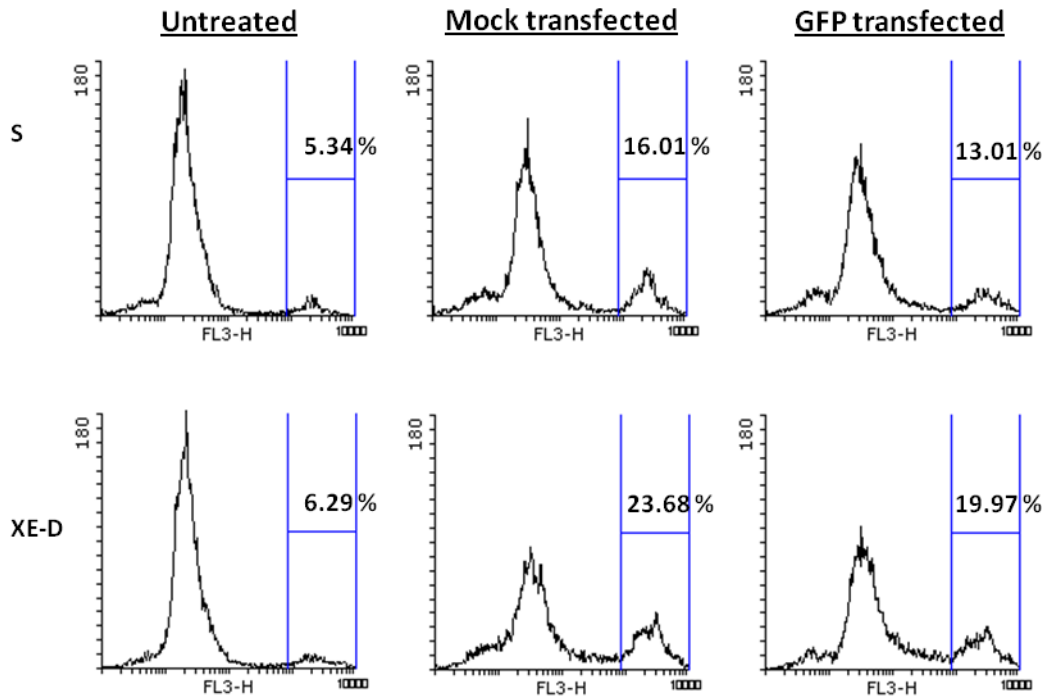


Figure 3-7 - CHO-S XE-D shows higher cell mortality when transiently transfected. Flow cytometry analysis of fluorescence from propidium iodide (PI) stained cells. Only dead cells are stained by PI as the dye does not permeate the plasma membrane of living cells, and therefore cells with high PI fluorescence (indicated in the blue region) can be identified as dead. The percentage of dead cells in each sample is indicated. Experiment was performed in triplicate, representative histograms are shown.

3.3 Discussion

CHO-S XE was originally engineered to be a host cell line capable of producing more recombinant protein than could be produced by wild type CHO-S. This criterion was confirmed during the preliminary characterisation experiments, and the high yield phenotype was seen to apply to a range of different antibody constructs (Cain et al, 2013). However, the ability of the cells to secrete other recombinant proteins had not been tested, and nor had the effect of varying disulphide bond complexity on the yield of secreted protein. In order to investigate this, the ability of CHO-S XE-D to secrete antibody was compared to its ability to secrete tPA, a heavily disulphide bonded protein, and α 1AT, which has no disulphide bonds in its native structure. As CHO-S XE-D was thought to be more capable of inserting disulphide bonds into nascent proteins than CHO-S due to the presence of exogenously expressed XBP1s and Ero1 α , it was expected that CHO-S XE-D would secrete more tPA than CHO-S, but both cell lines would produce a similar amount of α 1AT. Contrary to this expectation, CHO-S XE-D was seen to secrete more α 1AT, more tPA and more antibody than CHO-S. This suggests that the mechanism behind the high yield of CHO-S XE-D is not related to the complexity of the protein being secreted.

The data appears to show a greater increase in tPA secretion in CHO-S XE-D than the increase observed for α 1AT, which to some extent would support the original hypothesis that CHO-S XE-D has a greater capacity to secrete complex proteins than CHO-S. However, the lack of reproducibility in the results means that this cannot be reliably confirmed, and therefore the only conclusion that can be drawn is that CHO-S XE-D produces more of each of the three proteins tested, and the extent of this increase cannot be quantified from this data. The lack of reproducibility in the tPA experiments is attributed to the poor quality of primary antibody used in the western blot. Although alternative probes were tested and extensive optimisation carried out, western blots that showed clear and unambiguous bands for tPA produced by both CHO-S and CHO-S XE-D samples were rarely obtained. The increased variation in the results for α 1AT may be due to the different methods used for protein isolation, or it could be due to the differences in the probes used for western blotting. Overall, although CHO-S XE-D had a consistently lower cell count, the amount of recombinant protein secreted into the medium by those fewer cells was greater than that produced by a higher number of CHO-S cells.

The observation that CHO-S XE-D grows slower and has a lower viability than both CHO-S, and also the CHO-S XE1 lineage that XE-D is derived from, has two possible explanations. The first is that the cells were cultured in a different environment for

this project than the method they had been grown at UCB. The main difference in culture method was that the cells at UCB were grown in a dry incubator on a shaking platform with a larger orbital throw, whereas the cells cultured at the University of Glasgow were grown in a humidified environment on a smaller shaking platform. All other factors were equivalent, such as the culture medium, the temperature, and the concentration of selection antibiotics and glutamine added to the medium. It is possible that CHO-S XE cells are more susceptible to subtle environmental changes than CHO-S, and being thawed and cultured in an environment that they had not been adapted to was sufficient to cause a drop in cell viability. One contradiction to this hypothesis is the data showing that CHO-S XE1 was able to recover from ER stress, caused by a strong dose of the reducing agent DTT, faster than CHO-S was able to (Cain et al. 2013). This implies a greater ability in CHO-S XE1 to cope with stress; however, this ability may be specific to restoring redox balance and is not a general ability to cope with other forms of stress.

CHO lineages are notorious for being prone to genomic mutations (Chasin and Urlaub 1975), so it is possible that CHO-S XE1 is a mixed population of genotypes where some cells are more susceptible to stress than others. The stress of environmental change may have caused a speciation event, where the more vulnerable, faster growing cells were killed and the sturdier, slow-growing cells survived. One potential cause for a speciation event was the method by which cryopreserved cells were thawed. At the beginning of the project, vials containing CHO-S and CHO-S XE1 cultures frozen in CD CHO medium and 10% (v/v) DMSO were warmed briefly in a water bath and then transferred to a flask of pre-warmed CD CHO. The disadvantage to this thawing method is that a residual trace of DMSO remained in the initial culture passage; however, the reason why this method was used was to avoid the additional stress of centrifugal force and prolonged exposure to DMSO during its removal. The trace of DMSO in the initial culture was 0.4% (v/v) in CD CHO medium. The concentration at which DMSO becomes cytotoxic is debated, but concentrations under 0.5% (v/v) are generally considered to cause no adverse effects to cells (Qi et al. 2008). However, the cytotoxicity of DMSO varies depending on the cell type or tissue type being treated, and as no data has been published that specifically examines the effect of DMSO toxicity on CHO cells, it cannot be discounted that genomic mutations or epigenetic changes may have been caused by the freeze-thaw process in CHO-S XE. Regardless of the origin of the differences between CHO-S XE1 and CHO-S XE-D, the extent of these differences was not explored beyond the variation in growth characteristics, and all further experiments were only performed in CHO-S XE-D.

The drop in the viability of CHO-S XE-D was also supported by flow cytometry data showing that CHO-S XE-D cells show a greater extent of cell mortality when transiently transfected. It may be the case that CHO-S XE-D cells have compromised viability even under normal cell culture conditions, for an unknown reason, and the additional stress caused by chemical transfection is too much for CHO-S XE-D to cope with, whereas CHO-S cells are more capable of adapting to changing in cell culture conditions and with the stress of transient gene expression. It is also possible that the protocol for NovaCHOice, the chemical transfection reagent used, was optimised specifically for use with CHO-S and the concentrations of reagent used are not suitable for CHO-S XE-D. With further optimisation the viability of CHO-S XE-D could perhaps be improved, but this may be at the expense of reduced post-transfection viability for CHO-S or reduced yield for CHO-S XE-D.

CHO-S XE-D cells were also seen to have higher green fluorescence per cell when transiently transfected with GFP than the green fluorescence produced by the equivalent CHO-S cells. This result was unexpected, as it was originally anticipated that any increases to protein production in CHO-S XE-D would be achieved through an altered ER biochemistry caused by XBP1s and Ero1 α overexpression. To see such a large increase in the levels of a protein synthesised in the cytosol that has no disulphide bonds in its native structure implies that the increase in transfected GFP protein seen in CHO-S XE-D is a result of a mechanism other than the rate of disulphide bond formation. It is not clear which stage in the process of GFP production is the cause of this large increase, in other words whether it is due to improved gene transcription, protein translation or another aspect of protein folding.

Previous work showed that the uptake of fluorescently labelled DNA is the same between CHO-S and CHO-S XE1, implying that the differences in protein production between these cell lines is not due to changes in DNA uptake (Page 2012). However, another experiment indicated that stably transfected CHO-S XE cells produce more positively transfected clones than CHO-S, which does suggest a difference in DNA uptake or integration. This data appears to be conflicting, but the experiments are in fact testing different aspects of transfection and are not directly comparable. The first experiment is a measure of DNA transferred across the plasma membrane into the cytosol, whereas the second is a measure of the efficiency of DNA uptake into the nucleus and integration with the genomic DNA. Therefore, the experiment measuring the presence of fluorescently labelled DNA inside the cell may not be an accurate representation of the DNA uptake required for successful integration of a transfected gene. It is reported in the literature that cell lines can have a similar rate of DNA uptake across the plasma membrane, but can differ in their extent of nuclear

integration. For instance, both human primary cells and HeLa cells were shown to take up an equivalent amount of transfected DNA into the cytosol, but the human primary cells were more efficient at expelling foreign DNA from the nucleus than HeLa cells were, resulting in the HeLa cells having a greater transfection efficiency (Coonrod et al. 1997). It is therefore possible that CHO-S XE-D has a more sluggish rate of nuclear expulsion of DNA than CHO-S does, giving it a greater transfection efficiency, although this is not known to be an effect of either XBP1s or Ero1 α . Further work will need to be performed to compare the other stages of protein production between the two cell lines.

In regards to the western blot data confirming the presence of both exogenous genes in CHO-S XE-D, and their relative absence in CHO-S, it should be noted that both antibodies used are only documented to target the human version of these proteins, and their capability to recognise Chinese hamster proteins is not known. CHO-S XE-D overexpresses the human version of the XBP1S and Ero1 α , but also expresses its own endogenous Chinese hamster proteins, whereas CHO-S only expresses the Chinese hamster versions of XBP1 and Ero1 α . The human and Chinese hamster sequences for XBP1S are known to be quite similar, and therefore the antibody used in the western blot should be able to detect both forms of the protein, and the band shown in the blot should represent a combination both exogenous human and endogenous Chinese hamster XBP1S. However, the sequences for Ero1 α show more variation between human and Chinese hamster, and therefore it is possible that only the human form is being detected on the blot, and this may be why no band can be seen for Ero1 α in CHO-S. This possibility could be tested by using an antibody raised specifically against the Chinese hamster form of Ero1 α .

It was also discovered that CHO-S XE-D lysates contain higher levels of a number of different ER-localised endogenous proteins compared to CHO-S. These results could suggest that the ER of CHO-S XE-D is more abundant; however, it was also found that the cytoskeletal proteins tubulin and actin are expressed at higher levels in CHO-S XE-D. This could suggest that CHO-S XE-D has a larger overall size than CHO-S and has both a larger ER and cytosol, or that cytoskeletal proteins are being upregulated in CHO-S XE-D by an unknown mechanism. This hypothesis is supported by the flow cytometry data showing that the size of CHO-S XE-D cells was greater than CHO-S.

The observation that GAPDH, a protein involved in glycolysis that is commonly considered a 'housekeeping' protein for the purposes of normalising data, was expressed at lower levels in CHO-S XE-D was unexpected. The reason why this is the case is unclear, but it could suggest that the basic metabolism and glycolysis of the two

cell lines are different. A point which may support this hypothesis is that the CHO-S XE1 cell line was shown to have a lower uptake of glucose from the medium than CHO-S (Cain et al. 2013), suggesting that the rate of glucose metabolism of XE cells is slower, and this could be related to the lower levels of GAPDH.

It was also shown by flow cytometry that CHO-S XE-D cells have the same amount of ER as CHO-S cells. This result contradicts what is previously published on CHO-S XE1 (Cain et al. 2013) and it is also counterintuitive to what is known about the role of XBP1s in ER expansion and lipid biogenesis during the UPR (Shaffer et al. 2004). However, the conclusion drawn was based on the assumption that the uptake of ER Tracker dye and emission of green fluorescence was proportional to the amount of ER and would remain proportional after any expansion to the ER has occurred. This may not necessarily be the case, and the possibility exists that the potassium channels that ER Tracker specifically binds to are not upregulated to the same extent as the lipid component of the membrane. This could result in an expansion in ER membrane not being accurately reflected by a corresponding increase in green fluorescence, and ER expansion would therefore be undetectable by this method. However, as the ER Tracker dye has been used to reveal ER expansion in previous publications (Gulis et al. 2014), it appears more likely that the dye is able to accurately represent ER expansion. This validates the result in CHO-S XE-D, and indicates that CHO-S and CHO-S XE-D have the same amount of ER. An alternative method of measuring the amount of ER in CHO-S XE-D would be to analyse the cells by electron microscopy. This technique would allow for high resolution, direct imaging of organelle size, and could also be used to examine ER morphology between CHO-S and CHO-S XE-D.

Overall, when the results of these characterisation experiments and those undertaken by Cain et al are considered and rationalised together, one common conclusion is that both CHO-S XE1 and CHO-S XE-D differ from CHO-S in more ways than they are similar. Almost every experiment performed was a comparison between CHO-S and CHO-S XE-D, but as there is very little common ground to normalise the cells to it is difficult to draw any conclusions on which attributes of CHO-S XE-D are caused directly by the two overexpressed genes, and which are incidental or a result of spontaneous genomic mutation. In order to more reliably find the specific effects of exogenous expression of XBP1s and Ero1 α , a more controlled environment was required where the expression or absence of each of these genes was the only variable. To this end, a number of CHO-S cell lines with inducible overexpression of exogenous genes were engineered in order to better study the function of these genes and their effect on the yield of recombinant protein.

Attribute of CHO-S XE-D	Difference to CHO-S
Cell size	Larger
ER size	Same
Growth rate	Slower
Productivity of IgG	Higher
Productivity of α 1AT	Higher
Productivity of tPA	Higher
Productivity of GFP	Higher
Chaperone levels	Higher
Actin levels	Higher
GAPDH levels	Lower
General viability	Lower
Viability after transfection	Lower

Table 1 - Summary of differences between CHO-S and CHO-S XE-D.

The results of the experiments described in Chapter 3, indicating whether a particular attribute can be considered greater in CHO-S XE-D than in CHO-S, lesser, or the same.

Chapter 4 Effect of inducible gene overexpression on antibody yield

4.1 Introduction

4.1.1 Rationale behind the use of an inducible gene system

As the results from the comparative experiments in CHO-S and CHO-S XE-D did not shed light on the specific role of overexpressed XBP1s and Ero1 α in the high yield phenotype of CHO-S XE-D, another experimental approach was taken where each gene of interest was overexpressed in an inducible system, in separate cell lines. The advantage to this approach was that cell samples could be compared where the only variable was the presence or absence of the gene of interest, and all other factors could be kept constant. The main factor that was compared between induced cells and uninduced was the ability of the cells to secrete transiently transfected antibody, calculated as pg of secreted antibody per cell. Other factors such as ER expansion and XBP1 splicing upon gene induction will be discussed in Chapter 5.

4.1.2 Inducible CHO-S derived cell lines

Initially, three cell lines were generated from CHO-S: one with inducible overexpression of XBP1s; one with inducible Ero1 α ; and a third with GADD34 overexpression. XBP1s and Ero1 α were chosen for investigation due to their presence in CHO-S XE (Cain et al. 2013), and GADD34 was chosen due to its role in the regulation of protein translation during the UPR (Novoa et al. 2001).

GADD34 functions downstream of the PERK branch of the UPR, and recruits a phosphatase to phosphorylated translation initiation factor (eIF2 α) (Brush et al. 2003). This reactivates eIF2 α by dephosphorylation, alleviating the attenuation of protein translation mediated by PERK during earlier UPR signalling (Novoa et al. 2001). It was hypothesised that the overexpression of GADD34 could reduce the extent of eIF2 α phosphorylation and ensure that the majority of eIF2 α remains in the active, non-phosphorylated form, and thereby improve the rate of protein translation in transiently transfected cells.

However, GADD34 signalling during the UPR is also known to be capable of triggering apoptosis (Hollander et al. 1997). The repression of translation by eIF2 α phosphorylation has a protective effect to the cell under severe stress conditions where an abundance of misfolded proteins has built up in the ER, and resuming a normal rate of protein translation under these circumstances causes the level of stress to worsen and the cell to enter apoptosis. Therefore, depending on the extent of eIF2 α phosphorylation during a standard transient transfection, it was possible that the induction of GADD34 overexpression could either improve the rate of translation, which

may contribute to a higher yield of protein, or it could reduce cell viability and increase mortality.

The inducible system chosen for controlled expression of XBP1s, Ero1 α and GADD34 is named pTetOne, and functions on a Tet-On basis (Gossen and Bujard 1992) where gene expression is active in the presence of doxycycline, a tetracycline derivative, and inactive in the absence of doxycycline (Zhou et al. 2006). Unlike other Tet-On based systems where the gene of interest and the Tet responsive element exist on separate vectors, and need to be incorporated into the cells in separate rounds of stable transfection, the TetOne system has the promoter for the subcloned gene of interest and the transactivator protein for this promoter situated on the same vector. The transactivator protein is constitutively expressed by the pTetOne vector in an inactive conformation, and is switched to its active conformation by the presence of doxycycline in the cell culture medium. The advantage to having these two components on the same vector was that only one period of transfection and clonal selection was required, which not only reduced the time taken to engineer the cell lines but also reduced the risk of a speciation event resulting from spontaneous genomic mutation occurring during the process of clonal selection. After subcloning the gene of interest into pTetOne, the construct was co-transfected into CHO-S cells along with a linear puromycin resistance marker. Positively transfected clones were initially identified by puromycin resistance, and later confirmed by western blotting of the protein of interest.

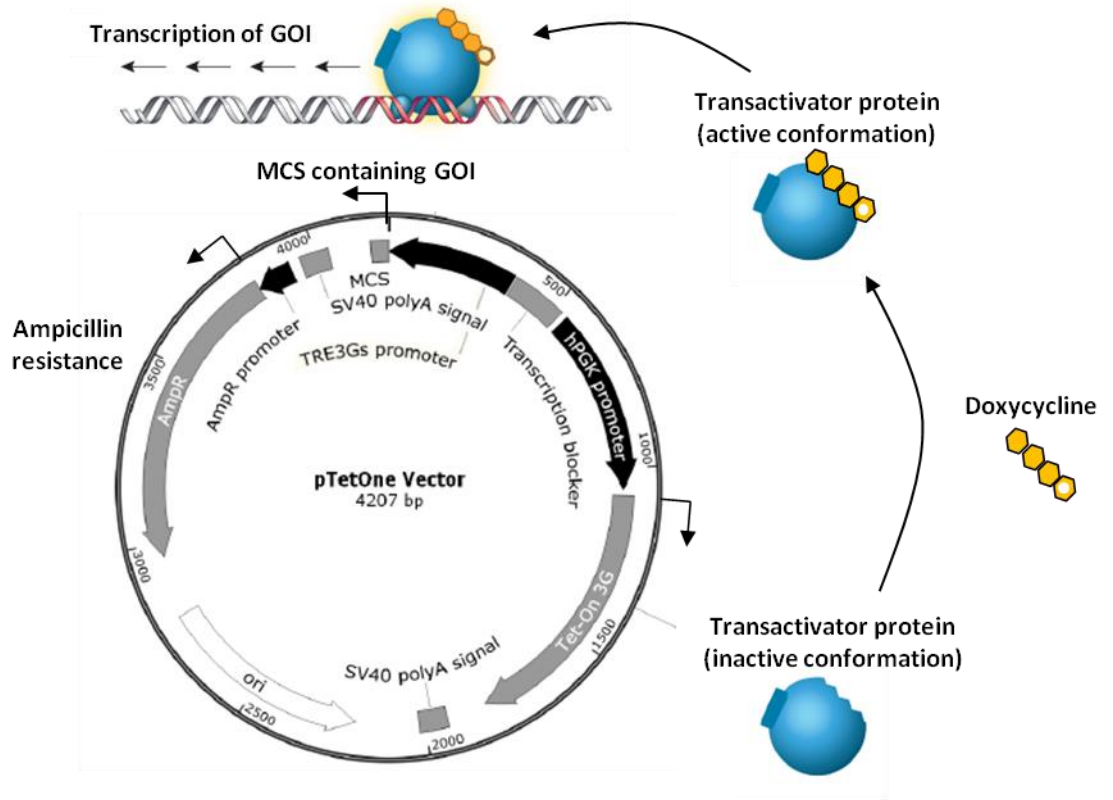


Figure 4-1 - Map of pTetOne vector showing activation by doxycycline.

The gene of interest (GOI) situated in the multiple cloning site (MCS) is transcribed by the Tet-On 3G transactivator protein. This protein is expressed constitutively in an inactive conformation from another location on the pTetOne vector. The binding of doxycycline changes the transactivator protein into its active conformation, allowing it to function as a promoter for the GOI. Adapted from Tet-One Inducible Expression System User Manual (Clontech), pages 3 and 14.

The cell lines generated were named CHO-S XBP1s-pTetOne (abbreviated to X1), Ero1 α -pTetOne (E1) and GADD34-pTetOne (G1). A derivative of X1 was later generated which constitutively overexpressed ER-localised blue fluorescent protein (BFP) (Costantini et al. 2015), and this cell line was named X1-B. It was intended that the presence of BFP in this cell line could be used to monitor any expansion of the ER caused by the overexpression of XBP1s in living cells. However, it was subsequently found that XBP1s overexpression actually caused a reduction in both BFP protein levels and the amount of blue fluorescence in the cell (data shown in Chapter 5), and therefore this cell line could not be used for its intended purpose. Despite this setback, it was found that X1-B had better growth characteristics and XBP1s induction than its parental cell line, X1, and therefore X1-B remained in use as an alternative example of an XBP1s overexpressing cell line.

It was also intended that a cell line be made with inducible overexpression of XBP1s and Ero1 α , to function as an inducible equivalent of CHO-S XE. To achieve this, the E1 cell line was stably co-transfected with XBP1s-pTetOne and a linear hygromycin resistance marker, resulting in a cell line with overexpression of both XBP1s and Ero1 α controlled by the addition of doxycycline. The selected clone from this transfection, named EX1, could grow in medium containing an otherwise lethal dose of puromycin and hygromycin, and initial western blot screening confirmed the presence of both Ero1 α and XBP1S. However, a later experiment to confirm GOI expression showed only endogenous levels of XBP1S, suggesting that expression of the second transgene had been lost over time. EX1 had retained expression of Ero1 α , however, and was therefore used as an alternative cell line to E1 with inducible Ero1 α overexpression.

In a similar principal to engineering EX1, an XBP1s co-overexpressing derivative of G1 was also made, where the presence of doxycycline could have potentially triggered the expression of both GADD34 and XBP1s. This would have been a novel combination of UPR genes which had not been previously investigated, but unfortunately, preliminary western blot screening of the selected GX1 cells showed no expression of XBP1S in any of the clones. The GX1 cell line was, therefore, abandoned and no subsequent experiments were performed in these cells.

Some success has been reported in the literature in increasing recombinant protein production by inducible overexpression of genes relevant to the secretory and stress response. These studies are discussed in detail in Chapter 1, but the work by Gulis and colleagues is of particular relevance to this work. In that study, XBP1s induction was controlled by a T-REx Tet-On inducible system in CHO-K1 cells that had constitutive expression of antibody (Gulis et al. 2014). The addition of doxycycline to these cells led

to a three-fold increase in antibody productivity after seven days of XBP1s induction, indicating that XBP1s overexpression can cause a demonstrable increase in antibody yield in cells with stable antibody expression. This project will expand on the work of Gulis and colleagues by investigating the effect of XBP1s overexpression, as well as that of Ero1 α and GADD34, in cells that have been transiently transfected with antibody. Although a transient gene expression system has some experimental disadvantages compared to a stable expression system, most notably the variation in transfection efficiency between experiments, it was chosen for use in this project as it more accurately reflects the production methods employed by UCB in the industrial scale manufacture of therapeutic proteins.

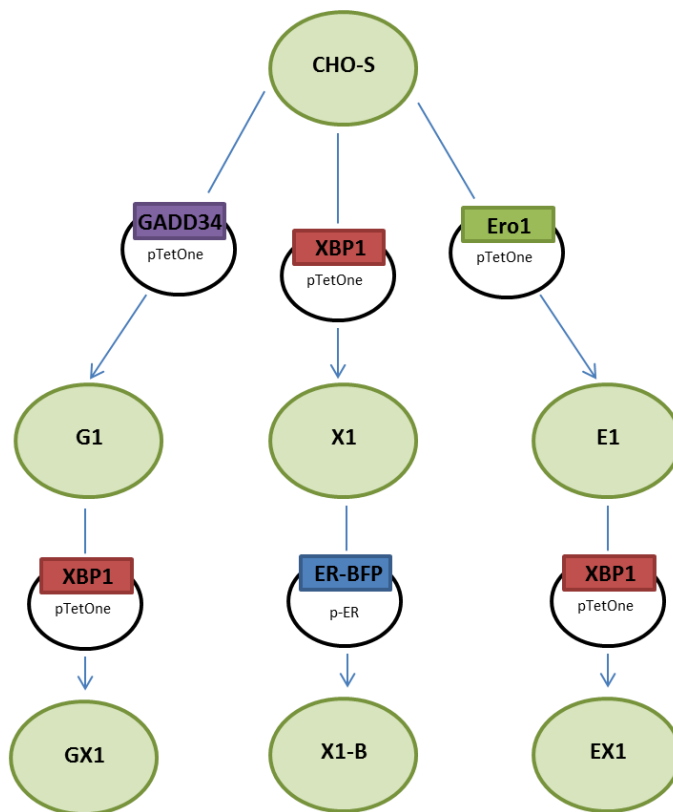


Figure 4-2 - Generation of CHO-S derived inducible cell lines.

Populations of CHO-S were transfected with GADD34-pTetOne, XBP1s-pTetOne or Ero1 α -pTetOne and puromycin resistant clones were selected and screened for GOI expression by western blotting. The resulting cell lines were then subsequently transfected: G1 and E1 with XBP1s-pTetOne, and X1 with an ER-localised blue fluorescent protein.

4.2 Results

4.2.1 Screening for GOI expression in X1 cells.

The engineered cell lines were first screened for GOI expression. In order to confirm expression of XBP1S in CHO-S X1, cells were either treated with doxycycline for the time periods indicated in Figures 4-3, or left uninduced. After this treatment period the cells were lysed, the lysates were separated by SDS PAGE and probed for the presence of XBP1S with an anti-XBP1S primary antibody by western blotting.

Figure 4-3A (i) displays an anti-XBP1S western blot performed with induced lysates of X1 cells. XBP1S is seen to be induced after 1 day of doxycycline treatment, and levels remain high on the second and third days of treatment. The protein bands of the anti-XBP1S blot, as well as that of an anti-GAPDH blot of the same samples, were quantified by densitometric analysis, and Figure 4-3B(ii) shows a graph of XBP1S intensities normalised against the GAPDH loading control. The y axis units of the graph are arbitrary, and reflect the relative abundance of XBP1S intensity when divided by the pixel intensity of GAPDH. These units have the potential to vary significantly between experiments, depending on the primary and secondary antibodies used and the development settings on the Licor Odyssey scanner. Therefore, the y axis units cannot be used to compare the expression of different proteins on different western blots, only for comparing the relative intensity of bands on the same blot. The quantification confirms the low levels of XBP1S in the uninduced control, and high protein levels in samples induced with doxycycline.

In order to find if the protein induced in X1 was capable of functional downstream signalling, the induced X1 lysates were later probed with anti-PDI, as this is a protein that is upregulated downstream of XBP1 signalling (Kaufman et al. 2002). The anti-PDI blot shown in Figure 4-3B(i) and the equivalent quantification in Figure 4-3B(ii) shows that PDI levels rise when X1 is treated with doxycycline, suggesting that this increase is due to upregulated XBP1S.

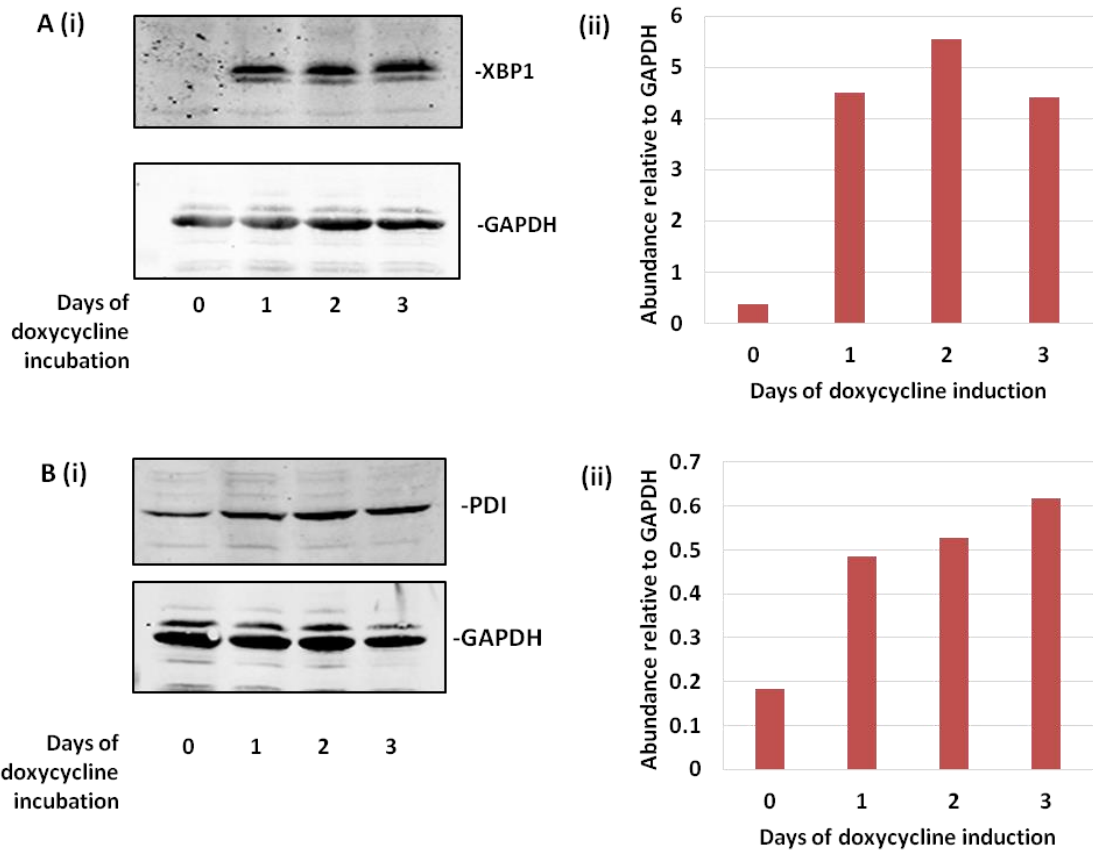


Figure 4-3 - Screening for XBP1S expression in X1 cells.

(A) (i) Western blot of lysates induced with doxycycline for the indicated number of days, probed with anti-XBP1S and anti-GAPDH, $n=3$, a blot a representative of the results obtained is shown (ii) Densitometric analysis of this blot, quantifying XBP1S normalised to GAPDH. (B) (i) Western blot of the same samples probed with anti-PDI, $n=1$. (ii) Quantification of this blot, showing PDI normalised to GAPDH expression.

4.2.2 Screening for GOI expression in E1 cells.

GOI induction in E1 cells was confirmed in a similar manner to X1 cells. The anti-Ero1 α blot in Figure 4-4A(i) and quantification in (ii) shows induction of Ero1 α after 16 hours of doxycycline treatment, and levels remain high at 20 hours, 24 hours and 40 hours post-induction. The concentration of doxycycline required for induction was also titrated, and the abundance of Ero1 α after 48 hours of treatment with the indicated concentrations shown in Figures 4-4B(i) and (ii). No induction is seen with either no doxycycline treatment or treatment with 1 ng/mL doxycycline, but a small degree of induction is seen at treatments with 10 ng/mL and 100 ng/mL doxycycline. The highest extent of induction is seen with 1000 ng/mL doxycycline. As doxycycline is known to have a relatively short half-life of 24 hours in cell culture medium (Gossen et al. 1995), this dose was determined to be optimal to allow a high degree of GOI induction without causing cell mortality, as it has been reported that concentrations of doxycycline above 1 μ g/mL can compromise cell viability (Gulis et al. 2014).

Ero1 α protein exists in both an active form and an inactive form, and these two forms are distinguished by the presence of an additional, regulatory disulphide bond in the inactive form which blocks the exchange of disulphide bonds between Ero1 α and its client proteins (Appenzeller-Herzog et al. 2008). The difference in disulphide bond configuration can be visualised by a band shift on an SDS PAGE gel when Ero1 α protein samples are separated under reducing and non-reducing conditions. In a reducing environment, Ero1 α exists entirely in a fully reduced form which appears on an SDS PAGE gel at around 58 kDa, whereas under non-reducing conditions Ero1 α appears as a doublet around 48 kDa - 52 kDa, where the upper band of this doublet is representative of the active form and lower band represents the inactive form. Figure 4-4C shows lysates of induced E1 cells separated in the presence or absence of the reducing agent DTT. The non-reducing sample shows a band for Ero1 α at 48 kDa, which appears to represent the inactive form, and only a faint smear can be seen above this to represent the active form. This suggests that the Ero1 α induced in E1 cells is found predominantly in the inactive form.

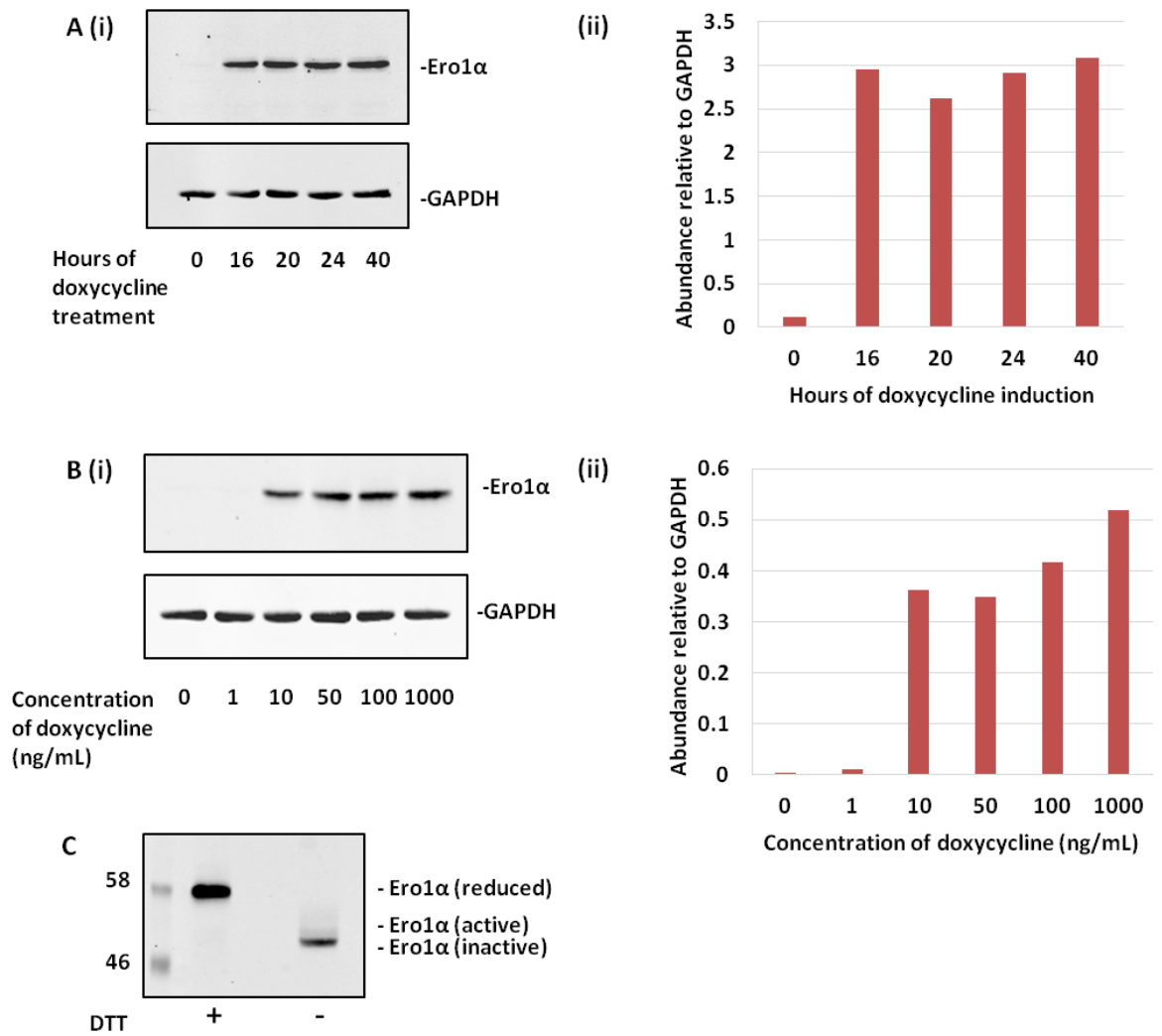


Figure 4-4 - Screening for Ero1α expression in E1 cells.

(A) (i) Western blot of lysates induced with doxycycline for the indicated number of hours, probed with anti-Ero1α and anti-GAPDH, n=1. (ii) Quantification of this blot, showing Ero1α normalised to GAPDH. (B) (i) Western blot of lysates from cells treated with the indicated concentrations of doxycycline for 48 hours, n=1. (ii) Quantification of Ero1α normalised to GAPDH expression. (C) Induced E1 lysates were separated by SDS PAGE in the presence or absence of the reducing agent DTT, to allow clearer identification of the active and inactive forms of the protein, n=1.

4.2.3 Screening for GOI expression in G1 cells.

The presence of GADD34 in induced G1 cells was probed for using an anti-FLAG antibody, as the sequence for GADD34 in the pTetOne vector was designed to incorporate a FLAG tag. G1 cells were treated with a range of doxycycline concentrations for 48 hours, and lysates of these cells were separated by SDS PAGE and probed with the anti-FLAG antibody. The western blot in Figure 4-5 (i) and quantification in Figure 4-5 (ii) indicates that G1 cells respond to lower concentrations of doxycycline in a similar manner to E1 cells, in that 1000 ng/mL doxycycline produces the strongest GOI induction, and lower concentrations produce lower levels of GADD34.

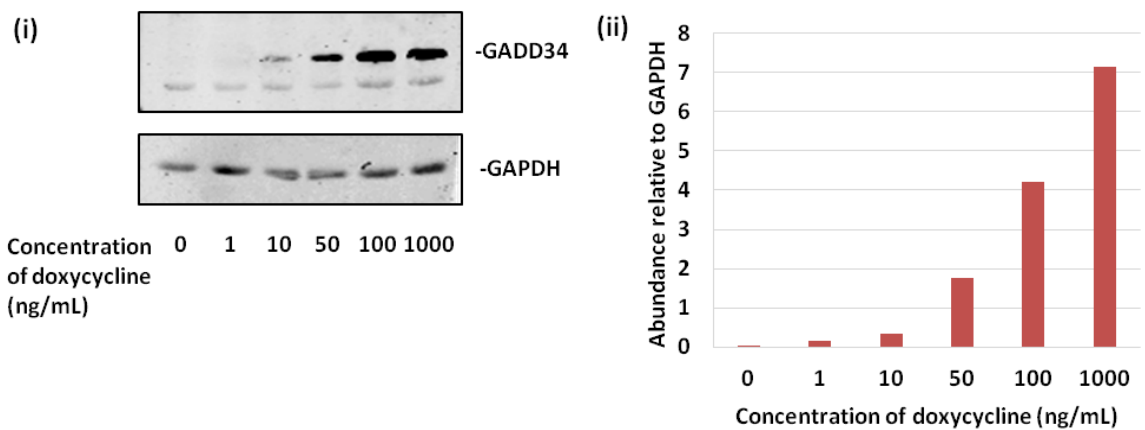


Figure 4-5 - Screening for GADD34 expression in G1 cells.

(i) Western blot of lysates from cells treated with the indicated concentrations of doxycycline for 48 hours, probed with anti-FLAG (to detect FLAG-tagged GADD34) and anti-GAPDH, n=1. (ii) Quantification of this blot showing GADD34 normalised to GAPDH expression.

4.2.4 Screening for GOI expression in X1-B cells.

The derivative cell line of X1, named X1-B, was engineered to stably express an ER-localised form of BFP in addition to the inducible overexpression of XBP1s. X1-B was characterised in terms of its retention of XBP1S expression and the presence of BFP protein. The western blot in Figure 4-6A (i) and the equivalent quantification in Figure 4-6A (ii) shows the induction of XBP1S with doxycycline, indicating that the clone of X1-B selected has retained the XBP1s-pTetOne vector.

In order to confirm the presence of stable BFP expression, CHO-S, X1 and X1-B cells were transiently transfected with the same BFP vector that was used to make X1-B, or left untransfected, to act as a positive control for the presence of BFP. Each of the cell lines was then either induced with doxycycline or left uninduced, and then lysed 48 hours later. Figure 4-6B(i) displays an anti-BFP western blot of these lysates, and Figure 4-6B(ii) shows the quantification of the BFP normalised to GAPDH. X1-B is seen to stably express BFP, whereas S and X1 do not, but the extent of stable BFP expression in X1-B is lower than the BFP protein levels observed after a transient transfection in any of the three cell lines. Although it may be expected that transiently transfected X1-B would have higher BFP levels than CHO-S or X1, as X1-B has two sources of BFP expression, it does not appear that the BFP derived from stable expression and transient expression in X1-B are cumulative. It can also be observed that there is a small decrease in BFP expression in untransfected X1-B cells that are induced, compared to uninduced samples, and this observation will be expanded on in Chapter 5.

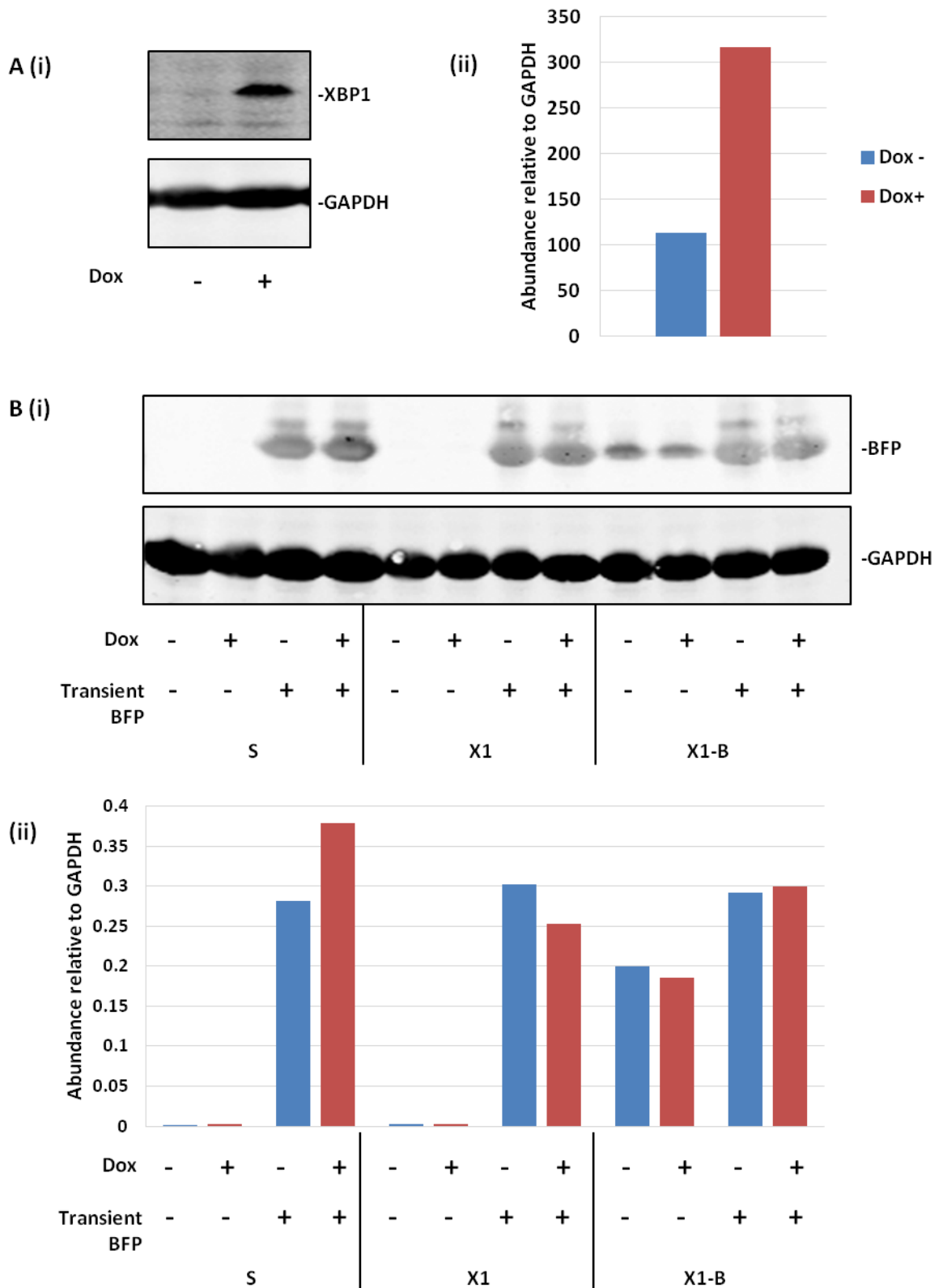


Figure 4-6 - Screening for XBP1s induction and BFP expression in X1-B cells.

(A) (i) Immunoblot of lysates from X1-B cells treated with or without doxycycline probed with anti-XBP1S, n=1. (ii) Quantification of XBP1S band intensity normalised against intensity of GAPDH. (B) (i) Anti-BFP western blot of induced and uninduced CHO-S, X1 and X1-B lysates that have been transiently transfected with BFP as a positive control, or left untransfected, n=1. (ii) Quantification of this blot.

4.2.5 Screening for GOI expression in EX1 cells.

The EX1 cell line is a derivative of E1, and was generated by stable transfection of E1 with XBP1s-pTetOne, the same inducible vector that was used to make the X1 cell line. It was intended that EX1 would have both XBP1s and Ero1 α expression controlled by the presence of doxycycline, and this was tested by western blots of induced EX1 lysates. Figure 4-7A (i) shows the initial anti-XBP1S blot of lysates from selected EX clones. The EX1 clone is seen to have higher XBP1s induction than that of another selected clone of EX, which for this experiment is named EX-null. Although XBP1s expression after doxycycline treatment is high in EX1, it is also fairly high in untreated cells which suggests that the expression is leaky. The anti-Ero1 α immunoblot of the same lysates, shown in Figure 4-7A(ii), displays very high induction of Ero1 α in doxycycline treated EX1, and little to no Ero1 α expression in untreated EX1 or the EX-null clone.

An additional screen for continued GOI expression was performed after the EX1 clone had been freeze-thawed once and cultured for around 10 passages. In this screen induced and uninduced lysates were compared to samples from X1-B, which has been shown previously in Figure 4-6 to have XBP1S induction and is included as a positive control for XBP1 expression. In the anti-XBP1S western blot in Figure 4-7B(i), EX1 is seen to have much lower expression of XBP1S than X1-B, and appears to not have induction of XBP1S at all. This disappointing result meant that EX1 could not be used as an example of a cell line with both XBP1S and Ero1 α overexpression, proteins that would have been interesting to investigate together due to their relevance to the CHO-S XE cell line. However, an anti-Ero1 α immunoblot showed the presence of Ero1 α in induced EX1 cells, shown in Figure 4-7B(ii), and EX1 was therefore retained in culture as an alternate sample of an Ero1 α overexpressing cell line.

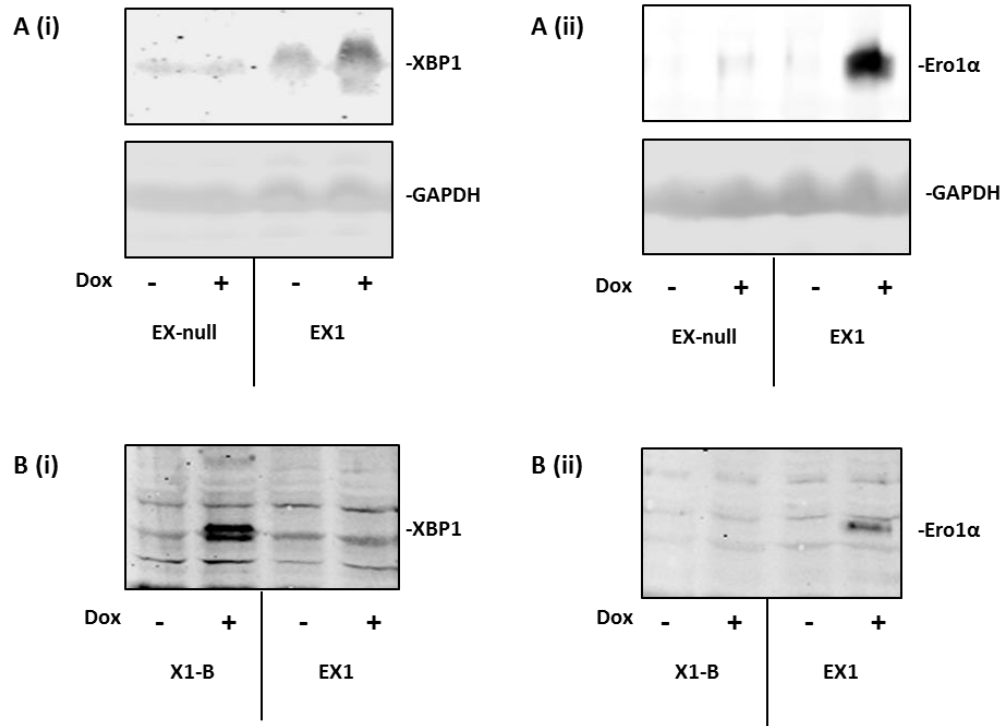


Figure 4-7 - Screening for XBP1S and Ero1 α induction in EX1 cells.

(A) Initial screening of clones of E1 stably transfected with XBP1s-pTetOne. Cells were treated with or without doxycycline and probed with (i) anti-XBP1S or (ii) anti-Ero1 α . The clone with the highest expression of XBP1S and Ero1 α was named EX1, and expression is shown in comparison to another selected EX clone with little to no expression of the two GOI, named EX-null. (B) (i) Anti-XBP1S and (ii) anti-Ero1 α western blots of lysates from cells that had been freeze-thawed once and grown for approximately 10 passages after thawing. EX1 lysates were examined with X1-B lysates as a positive control in the anti-XBP1S blot and a negative control in the anti-Ero1 α blot.

4.2.6 Comparison of induction in XBP1s expressing cell lines

In order to find if XBP1s was induced to a similar extent in X1-B as in X1, and how this compares to the stable overexpression of XBP1s in CHO-S XE-D, induced and uninduced samples of each of the XBP1s expressing cell lines were separated by SDS PAGE and probed with anti-XBP1S. Samples from CHO-S, X1 and X1-B are shown in Figure 4-8A(i) and XE-D and EX1 samples are shown in Figure 4-8A(ii). The quantification of XBP1s expression normalised to GAPDH is shown Figure 4-8B(i) for S, X1 and X1-B and Figure 4-8B(ii) for XE-D and EX1. As the different samples were loaded onto two different SDS PAGE gels, the relative quantification of XBP1 induction in B(i) and B(ii) cannot be directly compared.

X1-B is seen to have the highest induction of XBP1 with doxycycline treatment, higher than the equivalent expression in X1. This increase in expression in X1-B compared to X1 was observed on multiple occasions, and as the only known difference between X1 and X1-B is the presence of BFP in X1-B, it is not immediately apparent why X1-B would have higher XBP1 expression.

EX1 has previously been shown (Figure 4-7) to have no additional expression of XBP1 in the presence of doxycycline, implying that the inducible vector was lost with successive passages. EX1 is, therefore, functioning as a negative control for XBP1 expression for the purposes of this western blot, and XE-D is seen to have higher expression of XBP1 than EX1, as would be expected based on previous gene expression data for XE-D. Somewhat surprisingly, doxycycline treated XE-D samples appear to have higher expression than uninduced. This was unexpected as the promoter for XBP1 in XE-D is not doxycycline responsive. As previously mentioned, the expression of XBP1 cannot be quantitatively compared between X1, X1-B and XE-D, but visual comparison of the western blot data suggests that the stable expression of XBP1 in XE-D is lower than the inducible expression in X1 and X1-B.

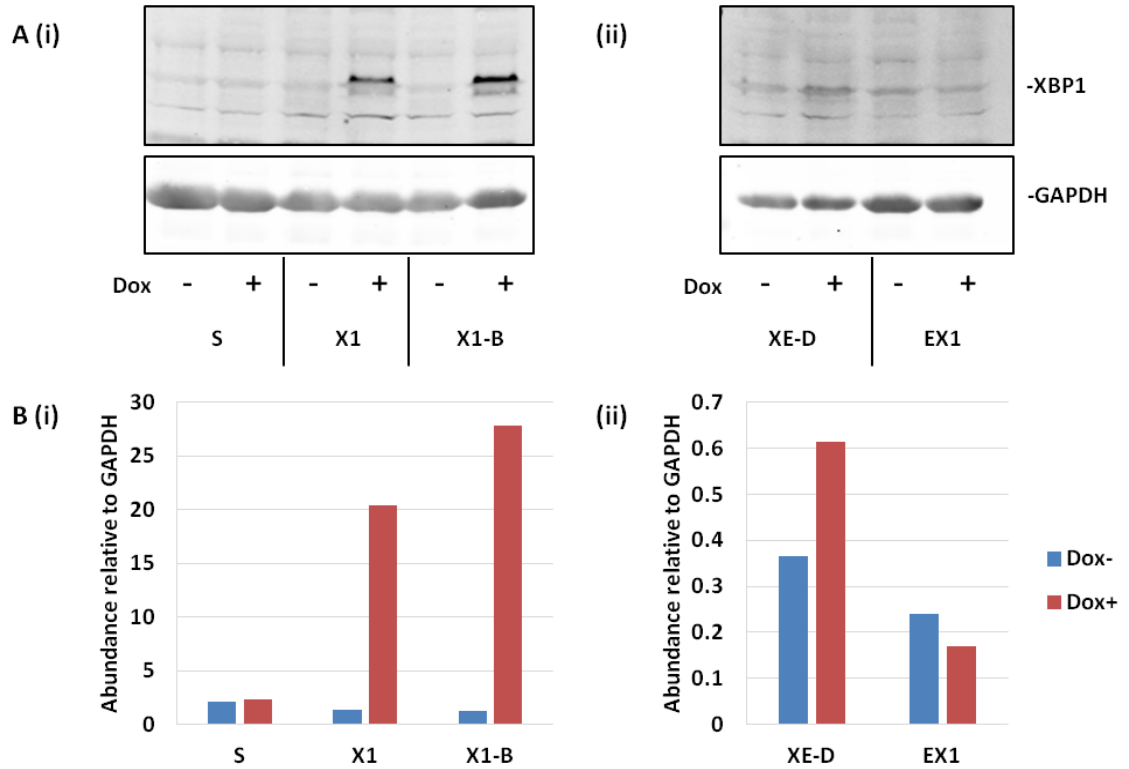


Figure 4-8 - Comparison of XBP1 induction in X1, X1-B, XE-D and EX1 cells.

(A) Anti-XBP1 immunoblots of induced and uninduced lysates from (i) CHO-S, X1, X1-B (ii) XE-D and EX1. Samples of doxycycline treated and untreated cells were obtained at least three times for CHO-S, X1 and X1-B, and once for XE-D and EX1. A side-by-side comparison of these samples was performed once. (B) Quantification of the above western blots, normalising XBP1 expression to GAPDH. The y axis units are arbitrary; quantifications derived from different western blots cannot be directly compared, and the only comparison that can be reliably made is the relative difference between samples on the same blot.

4.2.7 Determining altered antibody yield in induced cells.

After determining that each of the engineered cell lines had the ability to overexpress the intended GOI, other than the exceptions previously mentioned, the effect of inducible gene expression on antibody yield was then investigated. A population of one of the inducible cell lines was transiently transfected with IgG heavy and light chains using a chemical transfection method and grown in a small scale (25 mL) suspension culture overnight. The following day, this single transfected population was split evenly into six flasks: three of these flasks were induced with doxycycline and three were left uninduced. As it was observed that transfected CHO-S cells are prone to clumping, an anti-clumping agent was added to all six flasks. The cells were grown for a further three days, and on the final day the number of viable cells in each flask was counted using duplicate readings and a sample of medium containing secreted antibody was extracted.

The concentration of antibody in this sample was determined using an antibody capture ELISA against a standard curve of a known concentration of IgG1 antibody. Medium samples were loaded onto the ELISA plate in triplicate, and the triplicate readings for each of the three flasks of the same treatment were averaged together to calculate an overall average for doxycycline treated and untreated cells. Productivity was calculated by dividing the average final concentration of antibody in each flask by the average number of viable cells in that flask at the end of the three day period to obtain a value for productivity measured in pg/cell.

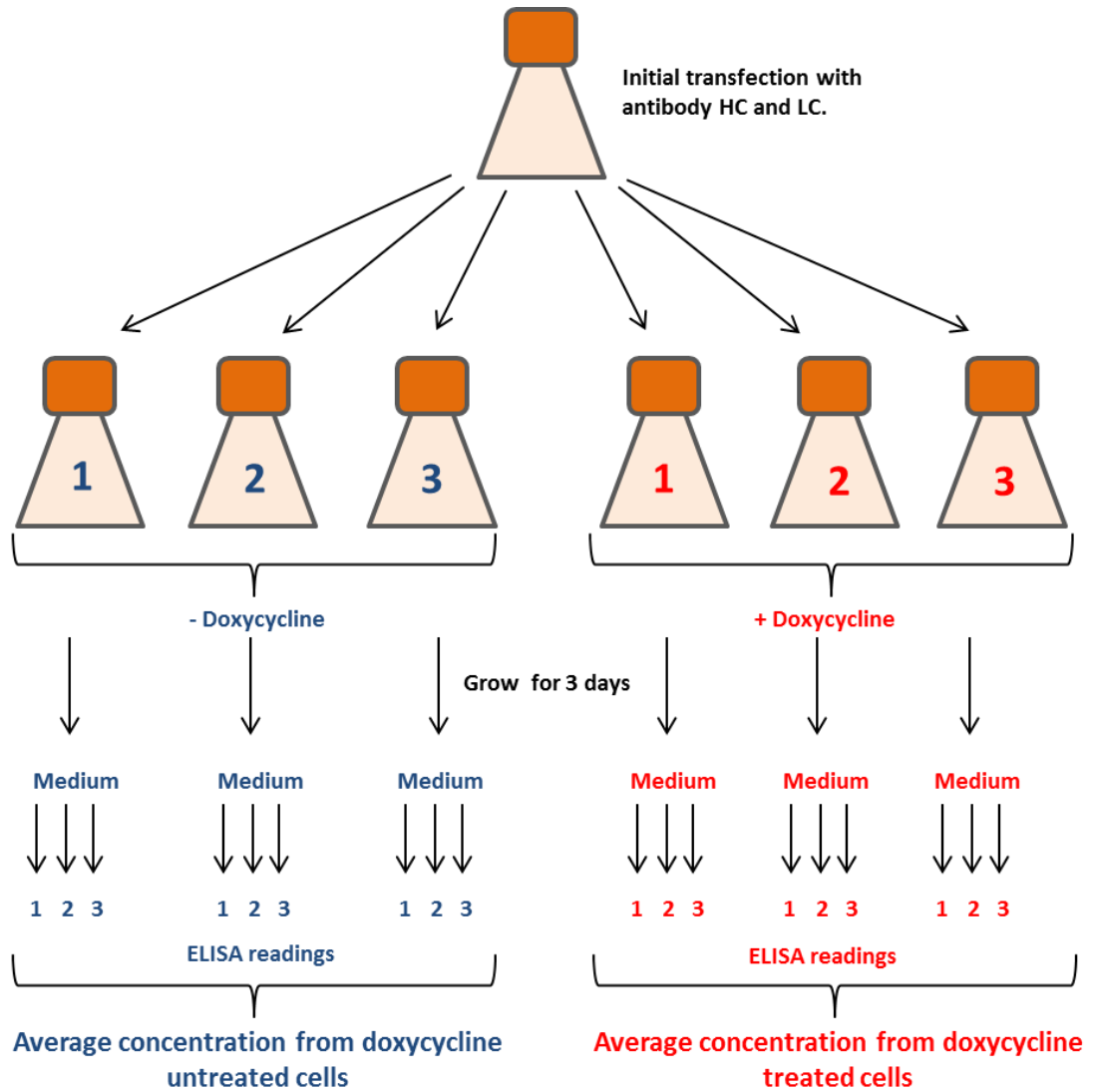


Figure 4-9 - Schematic of antibody yield experiments.

A single transfection was performed per experiment, and three separate experiments were performed for each cell line. In a single experiment: cells were transfected and split 24 hours post transfection into six identical flasks. Doxycycline was added at this point to three flasks. After three days of growth, medium samples were taken from each flask and the concentration of antibody was read in triplicate by antibody capture ELISA. An average was taken of the replicate readings and the triplicate flasks to obtain an overall average of antibody concentration calculated from nine readings. This value was normalised against the average final cell count of the three flasks to calculate the productivity of cells under each treatment. Productivity was represented by pg of antibody per cell (pg IgG/cell)

4.2.8 Antibody yield in wild-type CHO-S cells

As wild-type CHO-S cells do not contain any genes under the control of a doxycycline responsive promoter, this cell line was used as a control to ensure that the doxycycline treatment was not impairing the growth of the cells. Figure 4-10 shows the average concentration of transiently transfected antibody across the triplicate flasks at the end of the three day period; the average cell count of the transfected cells; and the average productivity of the flasks (pg/cell), calculated as the concentration of antibody (in ng/mL) divided by the cell count (cells/mL). The data for triplicate experiments are shown separately and labelled as experiments 1, 2 and 3, where each of these experiments represents a single initial transfection.

The concentration of antibody post-transfection does not vary significantly between untreated and doxycycline treated cells for each of the three experiments. Cell count is also not significantly altered by doxycycline treatment, suggesting that any changes observed in cell count for the inducible cells lines is due to the activity of the induced gene, and not caused by the presence of doxycycline in the medium. The cell count does appear to vary between the triplicate experiments, however, and the average cell count of experiment 3 is almost three times the cell count of experiment 1. It is not clear why this is the case, as the number of cells transfected in each experiment was the same. Productivity is shown to be significantly higher in doxycycline treated CHO-S for one of the three experiments, as determined by a Student's T Test ($p = <0.05$), significantly lower in doxycycline treated cells in another experiment, and the third experiment showed no significant difference between treated and untreated cells. Therefore, there does not appear to be a consistent effect of doxycycline on either the growth of CHO-S or the ability of the cell to secrete antibody.

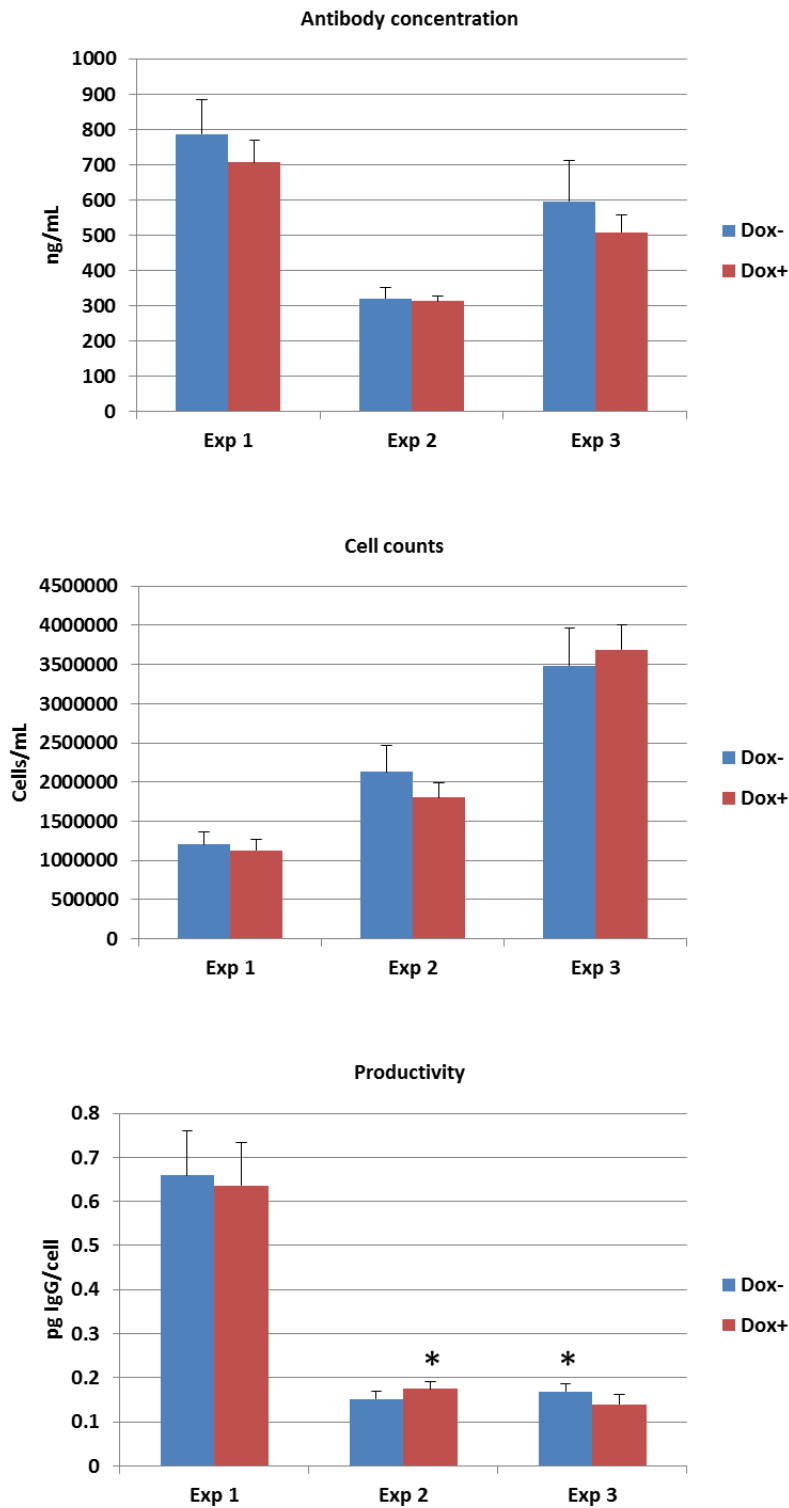


Figure 4-10 - Antibody yield from transiently transfected CHO-S cells.

The concentration of secreted antibody (ng/mL) present in the medium of cells treated with or without doxycycline for three days was measured by antibody capture ELISA. This was normalised against the final cell count (cells/mL) to calculate productivity (pg/cell). The experiment was performed three times; each experiment represents a single transfection. Samples marked with * are significantly different ($p = <0.05$ as determined by T test) to the differently treated sample for that experiment.

4.2.9 Antibody yield in X1 cells

X1 cells were transfected with antibody using the same experimental protocol as described for CHO-S. The final concentration of antibody, cell counts and calculated productivity are shown in Figure 4-11. Antibody concentration does not vary significantly between XBP1s induced and uninduced cells, but the cell count is shown to be significantly lower in cells which overexpress XBP1s. Due to this lower cell count, when the productivity of each sample is calculated by dividing the antibody concentration by the number of cells, the productivity is significantly higher in doxycycline treated cells. This significant difference is consistent across the three experiments, and suggests that XBP1s overexpression is compromising the viability of the transfected cells. However, as antibody concentration remains the same between doxycycline treated and untreated cells, it is possible that there is a small increase in yield in XBP1s overexpressing cells that makes up for the lower number of cells in these flasks.

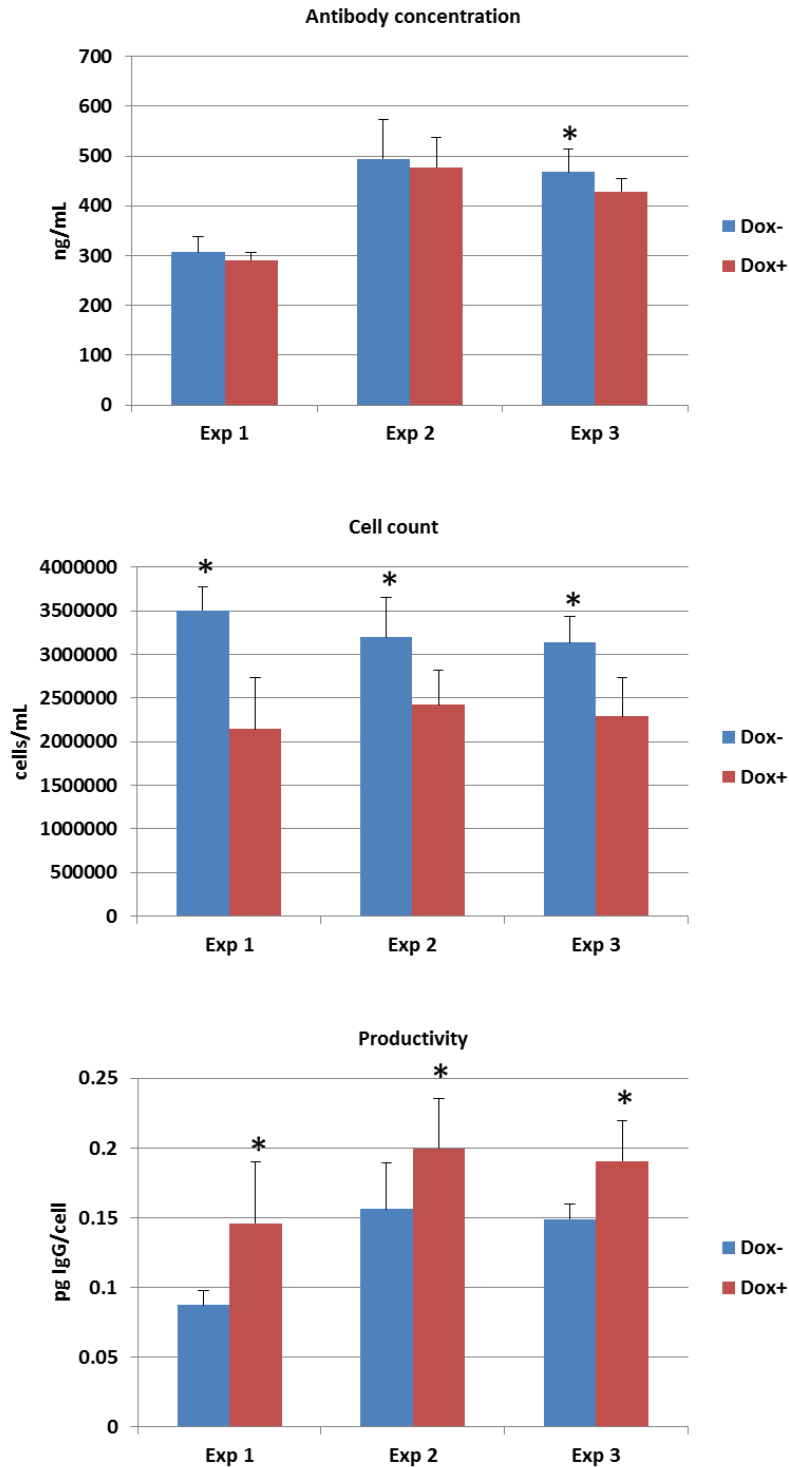


Figure 4-11 - Antibody yield from transiently transfected X1 cells.

The concentration of secreted antibody (ng/mL) present in the medium of cells treated with or without doxycycline for three days was measured by antibody capture ELISA. This was normalised against the final cell count (cells/mL) to calculate productivity (pg/cell). The experiment was performed three times; each experiment represents a single transfection. Samples marked with * are significantly different ($p = <0.05$ as determined by T test) to the differently treated sample for that experiment.

4.2.10 Antibody yield in E1 cells

The final concentration of antibody from transfected E1 cells is equivalent between cells with induced Ero1 α and uninduced cells, as shown in Figure 4-12. The cell count also remains equivalent, with the exception of the uninduced cells in experiment 3 which have a significantly higher number of viable cells. This variation in cell count leads to a significantly higher value for productivity for Ero1 α induced cells in experiment 3. However, as there is no observable difference in productivity in experiments 1 or 2, it is most likely that the overexpression of Ero1 α has no significant effect on cell viability or antibody yield.

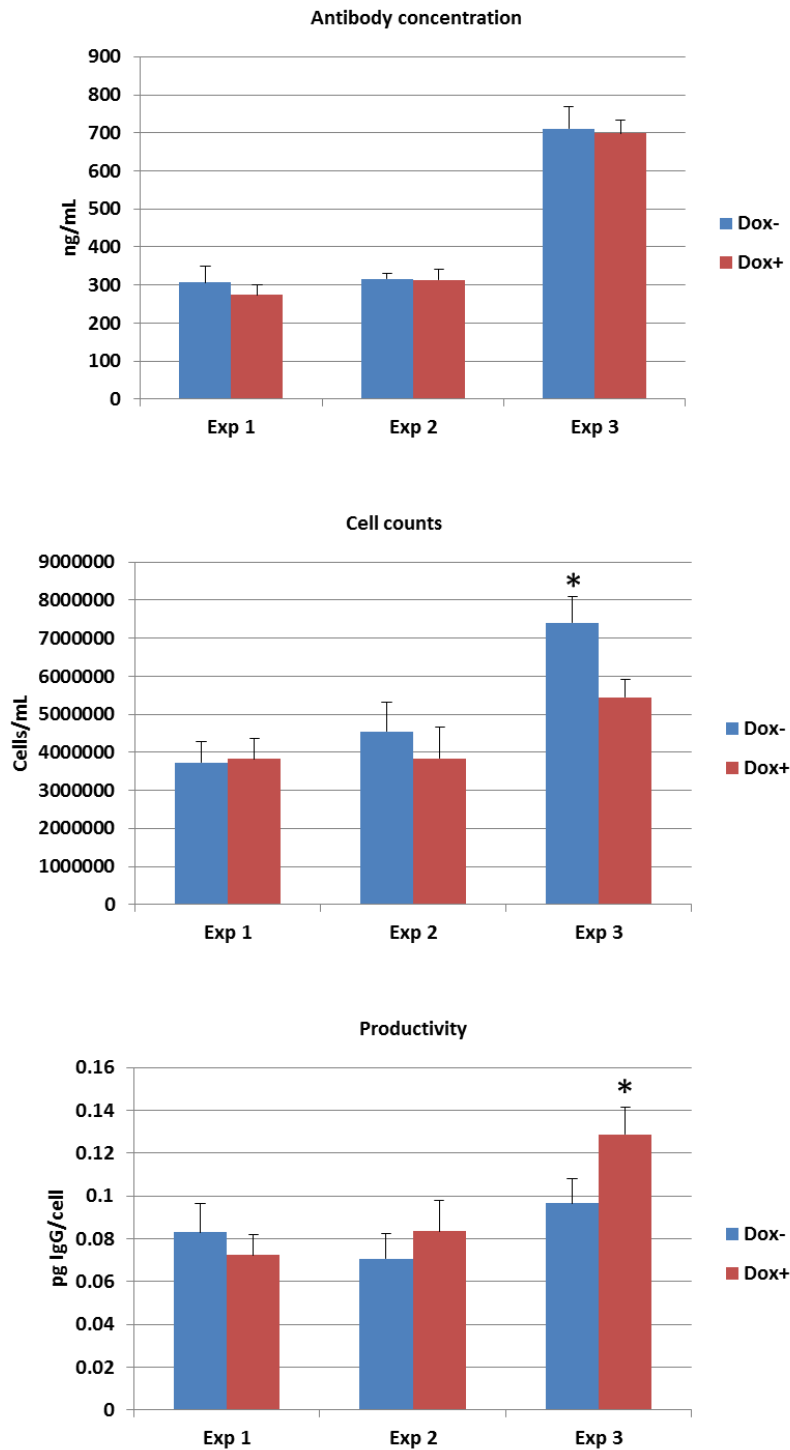


Figure 4-12 - Antibody yield from transiently transfected E1 cells.

The concentration of secreted antibody (ng/mL) present in the medium of cells treated with or without doxycycline for three days was measured by antibody capture ELISA. This was normalised against the final cell count (cells/mL) to calculate productivity (pg/cell). The experiment was performed three times; each experiment represents a single transfection. Samples marked with * are significantly different ($p < 0.05$ as determined by T test) to the differently treated sample for that experiment.

4.2.11 Antibody yield in G1 cells

The induction of GADD34 in G1 cells causes a significant drop in the concentration of transfected antibody in all three experiments. It appears that the transfection efficiency was fairly low in experiment 1 as the concentration of antibody and cell count is much lower for experiment 1 than for the other two experiments. The cell count does not vary significantly in induced cells in either experiment 2 or 3, which suggests that the drop in antibody productivity observed is not as a result of a drop in cell viability. This is surprising as GADD34 has a known role in apoptosis, and so the drop in antibody yield appears to be mediated by an unknown mechanism.

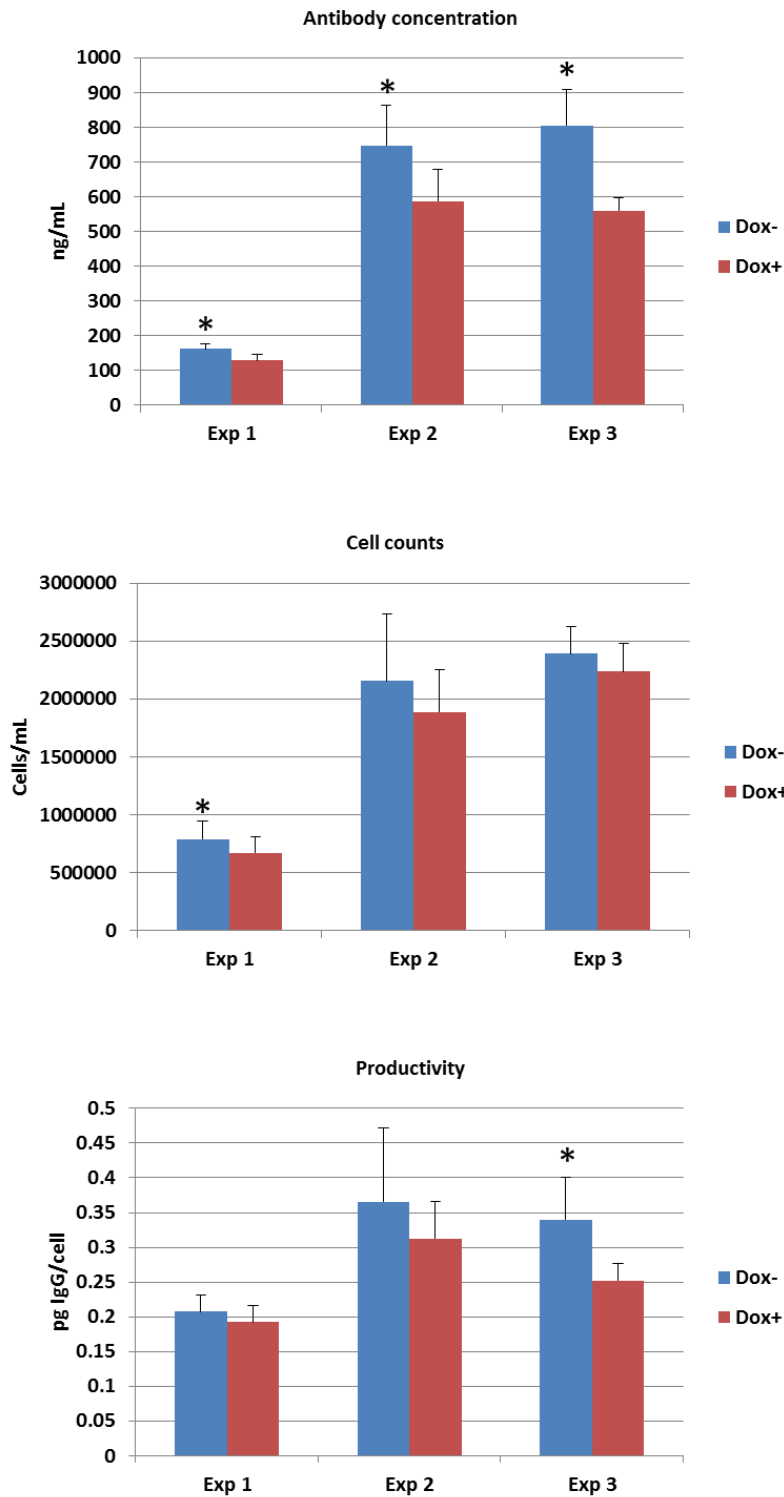


Figure 4-13 - Antibody yield from transiently transfected G1 cells.

The concentration of secreted antibody (ng/mL) present in the medium of cells treated with or without doxycycline for three days was measured by antibody capture ELISA. This was normalised against the final cell count (cells/mL) to calculate productivity (pg/cell). The experiment was performed three times; each experiment represents a single transfection. Samples marked with * are significantly different ($p = <0.05$ as determined by T test) to the differently treated sample for that experiment.

4.2.12 Antibody yield in X1-B cells

The X1-B cell line has inducible, doxycycline responsive expression of XBP1s and constitutive expression of ER-localised BFP. When the antibody yield of this cell line was measured by the same procedure as previously described, there is a significant rise in the final concentration of antibody for one of the three experiments, and no variation in yield for the other two, as shown in Figure 4-14. However, there does not appear to be the same drop in cell viability in induced X1-B as there was in X1, as only experiment 3 has a significantly lower cell count for induced cells. Productivity is calculated to be significantly higher in experiments 1 and 3, and it appears that this increase is representative of an increased capacity for X1-B to produce antibody, and not simply a reflection of lowered cell viability as was seen in X1.

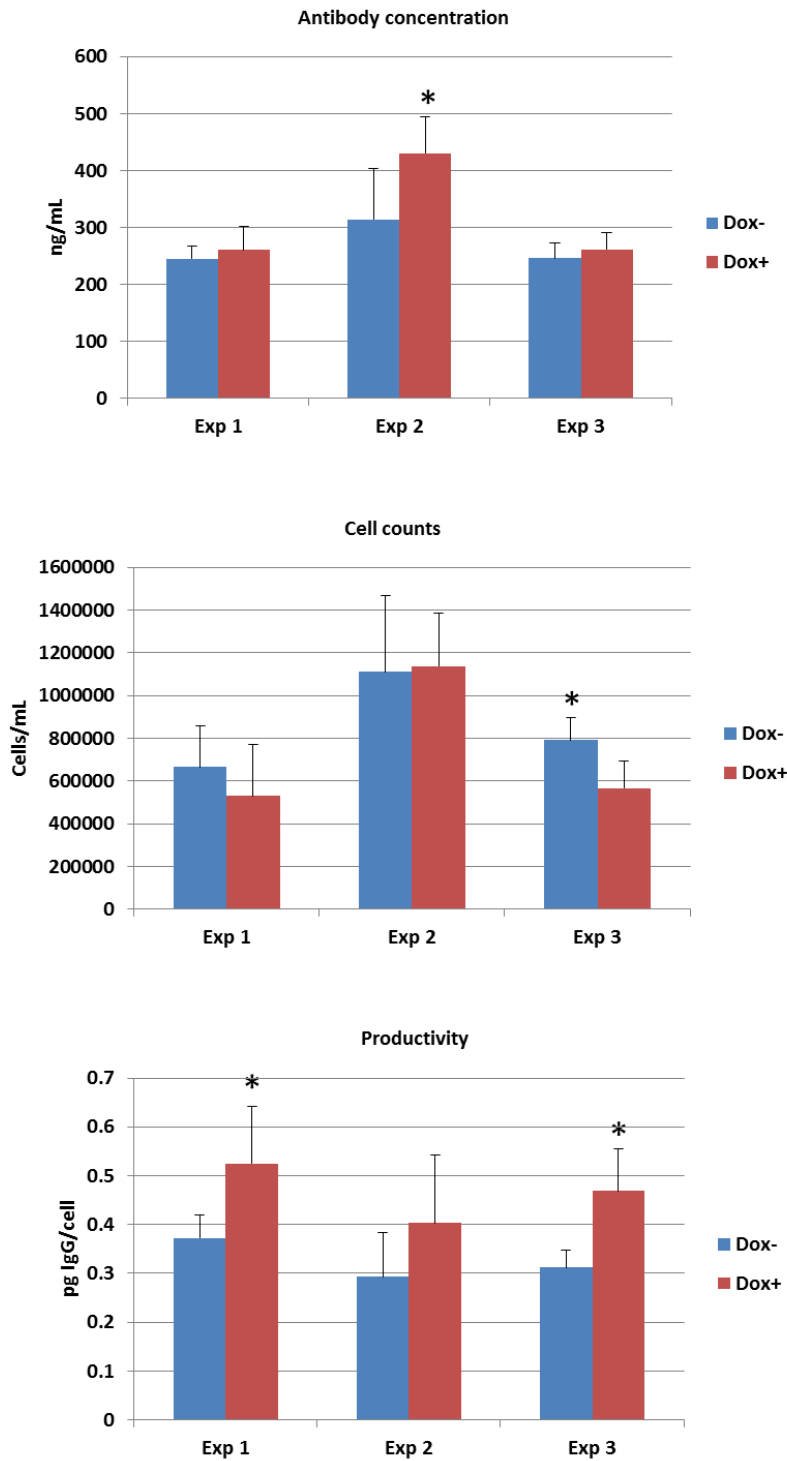


Figure 4-14 - Antibody yield from transiently transfected X1-B cells.

The concentration of secreted antibody (ng/mL) present in the medium of cells treated with or without doxycycline for three days was measured by antibody capture ELISA. This was normalised against the final cell count (cells/mL) to calculate productivity (pg/cell). The experiment was performed three times; each experiment represents a single transfection. Samples marked with * are significantly different ($p < 0.05$ as determined by T test) to the differently treated sample for that experiment.

4.2.13 Antibody yield in EX1 cells

The EX1 cell line is a derivative of E1 that was stably transfected with XBP1-pTetOne, the same inducible XBP1 vector used to generate X1. Despite the initial western blot screening of this cell line that showed both XBP1 and Ero1 α expression in the presence of doxycycline, a later screen showed that although Ero1 α induction had been retained, XBP1 expression had been lost. The experiments to measure antibody productivity in EX1 had been performed immediately prior to this screen, so it can be assumed that at the time of these experiments the addition of doxycycline to EX1 would only induce the expression of Ero1 α , and not XBP1.

The concentration of secreted antibody and viable cell density of induced and uninduced, transiently transfected EX1 cells were measured and the productivity calculated, as shown in Figure 4-15. Antibody concentration is not significantly higher in doxycycline treated EX1 cells, which is similar to the result observed in E1. The average cell count is also significantly lower in one of these experiments, but not in the other two, which is also similar to E1. Productivity is significantly higher in two out of three experiments for EX1, whereas only one experiment was higher for E1. Generally, there does not appear to be a consistent positive effect of doxycycline treatment on antibody productivity in EX1, but EX1 appears to have slightly better secretory properties than E1.

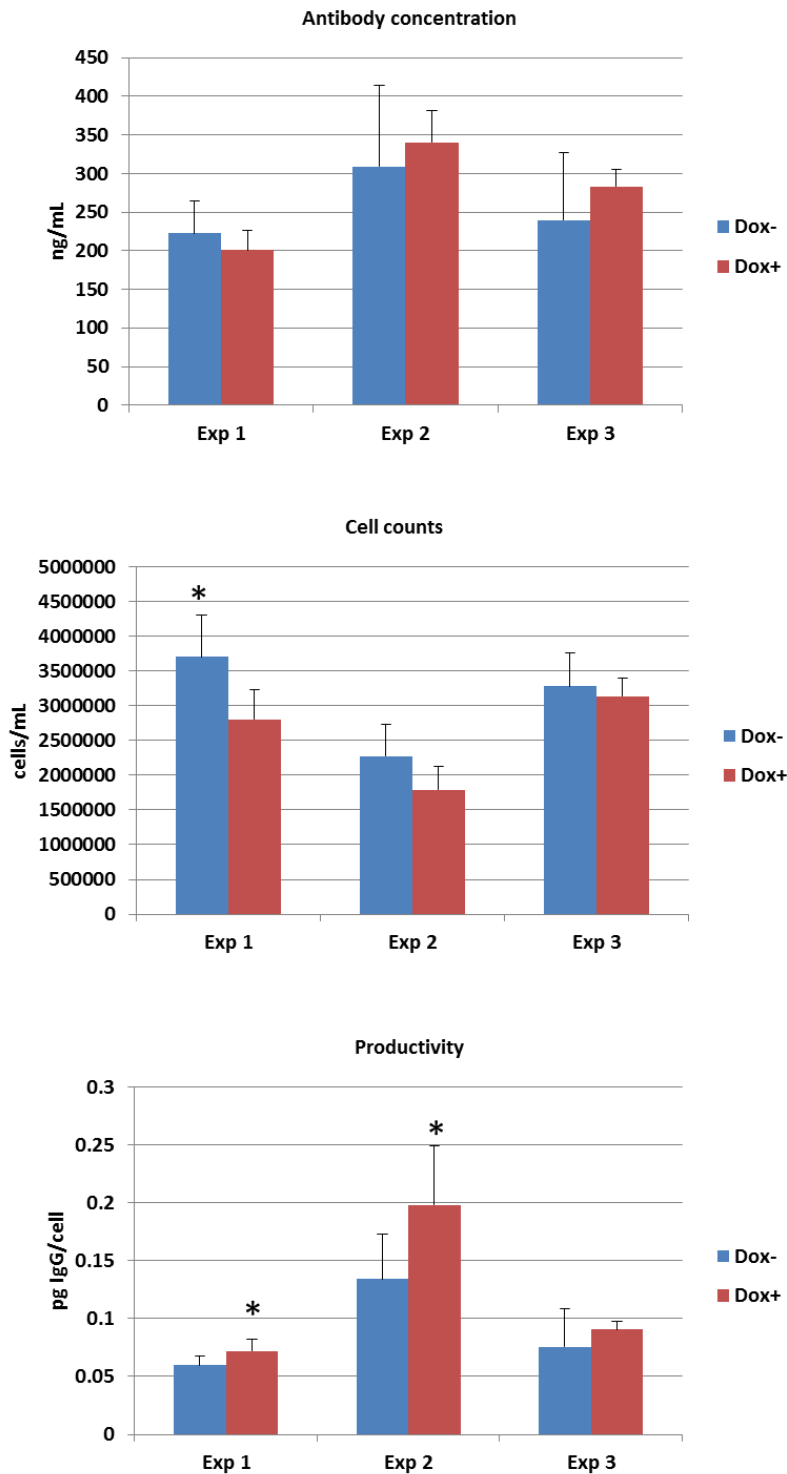


Figure 4-15 - Antibody yield from transiently transfected EX1 cells.

The concentration of secreted antibody (ng/mL) present in the medium of cells treated with or without doxycycline for three days was measured by antibody capture ELISA. This was normalised against the final cell count (cells/mL) to calculate productivity (pg/cell). The experiment was performed three times; each experiment represents a single transfection. Samples marked with * are significantly different ($p = <0.05$ as determined by T test) to the differently treated sample for that experiment.

4.3 Discussion

The purpose of engineering the inducible cell lines was to analyse the effect of the overexpression of a single gene on the ability of the cell to secrete antibody in a tightly controlled environment. It was first confirmed that each of the cell lines was capable of inducing the intended GOI, and then the concentration of secreted antibody from induced and uninduced cells was measured. X1 and X1-B were shown to strongly induce XBP1S after 24 hours of doxycycline treatment, and the levels of induced protein remained high for at least a further two days. Out of these two cell lines, X1-B was shown to have higher induction of XBP1S than its parent, X1.

X1 was calculated to have higher productivity in induced cells for all three of the experiments; however, a closer examination of the data revealed that this apparent increase could be mostly attributed to a significant drop in viable cell density. Therefore, it appears that doxycycline treatment in X1 did not cause any desirable improvement to the cells' secretory phenotype, and merely reduced the viability of the cell. Despite this finding, the derivative of X1, X1-B, did appear to show a genuine improvement in antibody productivity when induced. X1-B also did not display the same drop in viability upon doxycycline treatment as was observed in X1, although it should be noted that the cell counts were much lower for X1-B than X1 in the three antibody yield experiments whether they were induced or not. The discrepancy between the results observed in X1 and X1-B could be attributed to the increased extent of XBP1s induction in X1-B, resulting in there being a greater distinction between induced and uninduced X1-B than there was for X1.

Although the induction of XBP1s in X1-B causes around a 1.4 fold, statistically significant increase in productivity, it is smaller than the three fold increase observed by Gulis et al when using a similar XBP1s inducible system (Gulis et al. 2014). There are a number of notable differences in methodology between this work and the experiments performed in X1 and X1-B which could contribute to the differences in results. Gulis et al performed their experiments in CHO-K1 cells stably transfected with antibody, grown in adherent culture, and induced XBP1s using a T-REx system over seven days; whereas X1 and X1-B are CHO-S derived cell lines, transiently transfected with antibody, grown in suspension culture and induced XBP1s by a pTetOne system over three days. Of these factors, perhaps the most significant would be the use of a transient antibody transfection with a shorter period of induction. It is possible that the effect of XBP1s on the ability of the cell to secrete antibody is consistent between the experiments, but a longer period of induction would have allowed a greater degree of distinction between induced and uninduced cells.

E1 was shown to have strong induction of Ero1 α , but the induced Ero1 α also appears to mostly exist in an inactive form. This finding could perhaps explain the similarity of the antibody secretion and cell counts of induced and uninduced E1, as the induced Ero1 α protein is mostly not functional and is not able to recycle PDI. In the literature, it has been shown that CHO-K1 cells stably transfected with Ero1 α had increased antibody productivity than wild-type CHO-K1 (Cain et al. 2013). Ero1 α was also one of the overexpressed genes in CHO-S XE, alongside XBP1s, and was presumed to have an essential role in its high yield phenotype. Therefore, it would be expected that the inducible overexpression of Ero1 α would have a similar effect on antibody expression in E1, but this does not seem to be the case. One possible explanation for this discrepancy is that the exogenous Ero1 α in CHO-S XE1 was shown to exist in roughly equal abundance of the active and inactive forms (Cain et al. 2013), whereas the Ero1 α in E1 is almost entirely inactive. This suggests that the Ero1 α in CHO-S XE1 has a greater ability to recycle PDI than the Ero1 α in E1, which may explain why CHO-S XE1 has higher productivity than induced E1. In order to compensate for the low levels of active Ero1 α induced in E1, it is possible that sustained induction for a time period of longer than three days would allow accumulation of active Ero1 α , and this would show a more pronounced effect on the secretory properties of the cell.

G1 cells induced with doxycycline displayed a lower final concentration of secreted antibody in all three of the experiments performed. The cell count is significantly lower in one of the experiments, and lower in the other two but not to a significant degree. This reduction in the number of viable cells could explain the lower concentration of secreted antibody, and could be due to the activity of overexpressed GADD34 triggering apoptosis in the cells.

The observed results in G1 are contradictory to the findings published by Omasa and colleagues, who reported a two-fold increase in recombinant antithrombin III (AT-III) production in a clone with constitutive expression of both GADD34 and AT-III, compared to its parental cell line which only expressed AT-III (Omasa et al. 2008). In this study, the GADD34 overexpressing clone had a slower rate of growth and lower maximum viable cell density than its parent population, which is similar to the results seen in G1. However, no increase was observed in recombinant protein production in G1, and this could be due to a number of factors. The experiments by Omasa and colleagues were performed over six days, whereas the experiments in G1 were performed over three days, and therefore, as previously mentioned, a longer period of GADD34 induction and antibody secretion could have revealed a greater distinction between induced and uninduced G1. Another difference between the experiments is that a transient system was used in G1, for both GADD34 expression and recombinant protein expression, and

the cell line used by Omasa et al. utilised stable gene expression. It has been reported that stable and transient gene expression can generate different results involving the same recombinant proteins (Ku et al. 2008), and this discrepancy may depend on the function of the exogenous proteins, and the presence and extent of bottlenecks in the secretory pathways.

Although EX1 appeared to lose expression of XBP1s with subsequent passages, productivity was shown to be higher in induced EX1 than uninduced in two out of the three experiments. Therefore, it is possible that induction of XBP1s was not lost completely in EX1, but the extent of induction was reduced to levels that are slightly higher than endogenous, but still indistinguishable from uninduced by a western blot. This could perhaps explain why EX1 appears to have a different capacity to secrete antibody than E1, when the western blot suggests that E1 and EX1 induce the same proteins.

One hypothetical basis for the differences between EX1 and E1, and between X1-B and X1, is that EX1 and X1-B have both been subjected to two rounds of transfection and clonal selection, whereas E1 and X1 were only transfected once. During a stable transfection the vector containing the transgene is incorporated into the host genome at a random site, which can disrupt the host cell genome in unexpected ways and lead to gene silencing or enhancement. CHO cells are also notorious for genomic instability (Chasin and Urlaub 1975), therefore, it is possible that unexpected mutations arose in EX1 and X1-B during the second round of stable transfection that led to an improvement in XBP1s induction and viability in X1-B, and a small increase in antibody secretion in EX1.

For all of the cell lines tested, it could be proposed that lengthening the period of doxycycline induction from three days to between five and seven days could improve the reliability of the results obtained. In fact, a time period of five days was used initially for induction during the antibody productivity experiments; however, a number of technical problems were encountered when using this protocol. The most severe of these problems was that the cells were observed to reach a maximum cell density four days after the addition of doxycycline and a large proportion of cells on the final day of the experiment were shown to be dead. In order to rectify this, the number of transfected cells in each flask was reduced, but this only resulted in the cells taking longer to reach the exponential phase of growth. It is possible that the culture period could be extended even further to account for this, if the medium and doxycycline were to be refreshed at appropriate intervals, but this would reduce the throughput of experiments.

Additionally, as a transient transfection system was used it is possible that the expression of transgene would drop with a lengthened culture time, as gene expression from a transient transfection is known to be diluted by successive cell divisions (Wong et al. 2015). The experimental protocols described in (Gulis et al. 2014) and (Omasa et al. 2008) both employ stable expression of antibody, and therefore an increased experimental time period would not affect transgene expression. By this logic, the inducible CHO-S cells used could be stably transfected with antibody to allow longer periods of transgene expression and doxycycline induction. Experiments performed in these hypothetical cell lines would produce interesting results that could be contrasted with the results obtained using transient expression.

Another alternative experimental procedure that could be performed with the inducible cell lines would be to swap the order of transfection and induction treatments. If the cells were first induced with doxycycline over a period of two or three days and then subsequently transfected with antibody, the effect of inducible gene overexpression on antibody secretion could become more pronounced. In addition to the previously mentioned disadvantages of lengthening the experiment by a few days, another disadvantage of this method is that there would be an increased level of statistical variation between induced and uninduced cells as each population would have been transfected separately. As transfection efficiency is generally highly variable, and the results obtained when performing a single transfection were already seen to vary significantly between successive experiments in the same cell line, it was thought that performing two separate transfections in each experiment instead of one would increase statistical variation to unacceptable levels and reduce the reliability of the results obtained, and this is the primary reason why this experimental protocol was not used. With a sufficient degree of optimisation, this alternative protocol could perhaps be utilised, and it has the potential to generate very useful and relevant data.

As the greatest increase in antibody productivity was seen in cells overexpressing XBP1s: namely X1 and X1-B, as well as the previous findings from CHO-S XE-D, the focus of the project was refined onto the overall consequences of XBP1s overexpression on the phenotype of the cell. The results from this section of work will be discussed in the next chapter.

Chapter 5 Consequence of XBP1s overexpression

5.1 Introduction

5.1.1 Further investigation of CHO-S X1 and CHO-S X1-B

This chapter will expand on the characterisation experiments described in Chapter 4 of the stable cell line named CHO-S X1, which has inducible expression of XBP1s, and the derivative of this cell line named CHO-S X1-B, which contains stably expressed ER-localised blue fluorescent protein (ER-BFP) (Costantini et al. 2015). These cell lines were chosen for further analysis as the induction of XBP1s overexpression appeared to have the greatest impact on the phenotype of the cell, namely the significant increase in antibody yield observed in X1-B and the significant drop in viability seen in X1. This, together with the results described in Chapter 3 from the XBP1s overexpressing cell line CHO-S XE-D, pointed to XBP1s being a more compelling candidate for further study, as opposed to either GADD34 or Ero1 α . The consequence of XBP1s induction on the biochemistry of the ER was studied to find potential explanations for the previously observed improvements to antibody yield, which could lead to further areas of improvement in engineered host cell lines. It was also thought that experiments utilising the controlled overexpression of XBP1s could be used to gain a greater understanding of the regulation of ER stress response signalling, an intricate and incompletely understood area of biochemistry.

After determining the extent of XBP1s induction in X1 and X1-B in Chapter 4, and the effect of this induction on the yield of transiently transfected secreted antibody, the impact of XBP1s induction on other characteristics of the cell was investigated; in particular, the extent of ER expansion and endogenous XBP1 splicing after exogenous XBP1s induction. An additional line of investigation was into the observed depletion of BFP in induced X1-B cells. It was originally planned that the ER-localised BFP in X1-B could be used to monitor ER expansion in living cells, but unfortunately it was discovered that BFP was degraded during stress conditions and, therefore, was not fit for the purpose of the planned experiments. However, as the X1-B cell line was found to have slightly higher levels of induced XBP1S than X1, it was retained in culture and used as an alternate example of an XBP1s inducible cell line. In addition to the experiments quantifying the yield of antibody from these cells shown in Chapter 4, the mechanism behind the depletion of BFP was sought as it appeared to occur as a consequence of the upregulation of XBP1s in X1-B. Therefore, it may have been an indication of upregulated ERAD, which is a known effect of XBP1s signalling (Acosta-Alvear et al. 2007). This possibility was tested using a proteasome inhibitor alongside the upregulation of XBP1s by either doxycycline or tunicamycin treatment. Tunicamycin is an inhibitor of N-linked glycosylation which is able to induce the UPR through

disruption of the quality control procedures that would normally ensure the correct folding of proteins (Surani 1979).

5.1.2 Quantification of XBP1 splicing

The extent of XBP1 splicing was visualised and quantified using an RT-PCR based assay (Shang and Lehrman 2004). As mentioned in Chapter 1, the splicing of XBP1 is performed by the endoribonuclease IRE1 under stress conditions and forms part of the UPR. Spliced XBP1 transcripts are translated into XBP1S protein, a transcription factor which upregulates genes for chaperones, ERAD and lipid biogenesis as part of a concerted effort to expand the ER and increase the abundance of chaperones, in order to clear any misfolded proteins that may have triggered the UPR in the first place. It should be noted that, although considered to be a hallmark of ER stress, a basal level of XBP1 splicing does occur as part of normal cell physiology (Wang et al. 2015). Unspliced XBP1 transcripts are translated to XBP1U, which is not a transcription factor but can instead bind to XBP1S and target it to the proteasome as a method of regulating the abundance of XBP1S after a stress response has ended (Yoshida et al. 2006). This degradation occurs at a rate almost equivalent to synthesis, and continued activation of IRE1 is required for sustained downstream XBP1S signalling (Tirosh et al. 2006).

By designing primers that flank the XBP1 spliced intron, cDNA derived from XBP1s and XBP1u transcripts can be amplified by PCR and distinguished from each other by a subtle, 26bp difference in product size when run on an agarose gel. This assay is also known to generate a third PCR product, shown diagrammatically in Figure 5-1, which is thought to be a hybrid double-stranded cDNA product consisting of one strand XBP1s and one strand XBP1u. This hybrid product migrates above double-stranded XBP1u on an agarose gel due to its bulkier structure (Shang and Lehrman 2004).

Two sets of primers were designed for the assay. The first set was designed to only anneal to the endogenous Chinese Hamster sequence of XBP1, and these primers were used to quantify only endogenous XBP1s and XBP1u. A second set of primers was designed to bind to both forms of endogenous CHO XBP1, and also to the exogenous human XBP1s transcripts that are expressed only by the pTetOne vector in response to doxycycline, allowing visualisation of all forms of XBP1 present in the cell. These primer sets were utilised in the assay to determine the effect of exogenous induction of XBP1s on the regulation of endogenous XBP1 splicing.

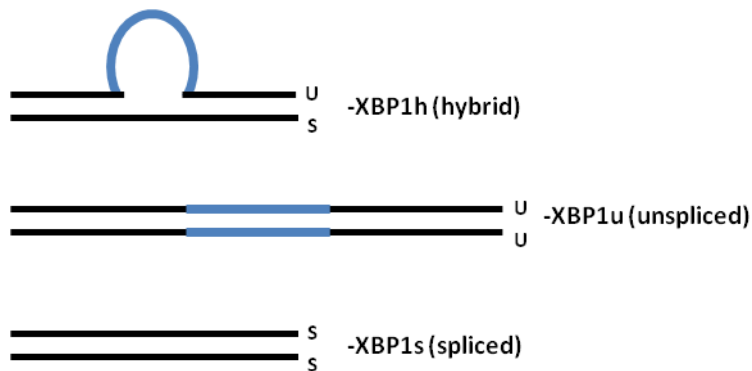


Figure 5-1 - cDNA products generated by RT-PCR XBP1 splicing assay.

Schematic of the three possible cDNA products generated by primers that flank the XBP1 spliced intron, which is indicated in blue. Single stranded cDNA, reverse transcribed from unspliced XBP1 or spliced XBP1, can anneal to either its complementary strand to generate double stranded XBP1u and XBP1s products, or to a non-complementary strand to generate a hybrid, XBP1h, formed from one strand XBP1u and one strand XBP1s. Of these three PCR products, XBP1s migrates the furthest on an agarose gel, followed by XBP1u and then by XBP1h, leading to the appearance of three distinct DNA bands. Adapted from Shang and Lehrman, 2004, Figure 1B.

5.2 Results

5.2.1 ER size in XBP1s overexpressing CHO cell lines.

As XBP1s has a known role in ER expansion and lipid biogenesis (Shaffer et al. 2004), it was hypothesised that CHO cells with upregulated XBP1s would display a greater amount of ER than cells with endogenous XBP1s levels. In order to determine the effect of high levels of XBP1s on the amount of ER, CHO-S, CHO-S X1, CHO-S X1-B and CHO-S XE-D cells were grown with or without doxycycline for three days, and then stained with ER Tracker. This green fluorescent dye binds specifically to potassium channels prominent on the ER membrane (Zünkler et al. 2004), and the extent of green fluorescence taken up by the cell should be proportional to the amount of ER membrane. Green fluorescence from stained cells was quantified using flow cytometry, as displayed in the histograms in Figure 5-2. The blue line on the histograms represents the fluorescence of the population of cells not treated with doxycycline, and the red line represents doxycycline treated cells.

CHO-S X1 and CHO-S X1-B show an increase in average green fluorescence per cell in response to doxycycline whereas CHO-S cells do not, implying that induced XBP1s is causing the ER to expand. This result confirms that the XBP1s expressed by the pTetOne vector is functional as a transcription factor, and also provides a potential explanation for the increase in antibody productivity observed in X1-B cells in Chapter 4. It could perhaps be expected that CHO-S XE-D cells would display a larger ER than parental CHO-S cells due to the constitutively upregulated levels of XBP1s present in this cell line. However, similar to the result observed in Chapter 3, CHO-S XE-D is seen to have the same amount of ER as both CHO-S, and uninduced X1 and X1-B.

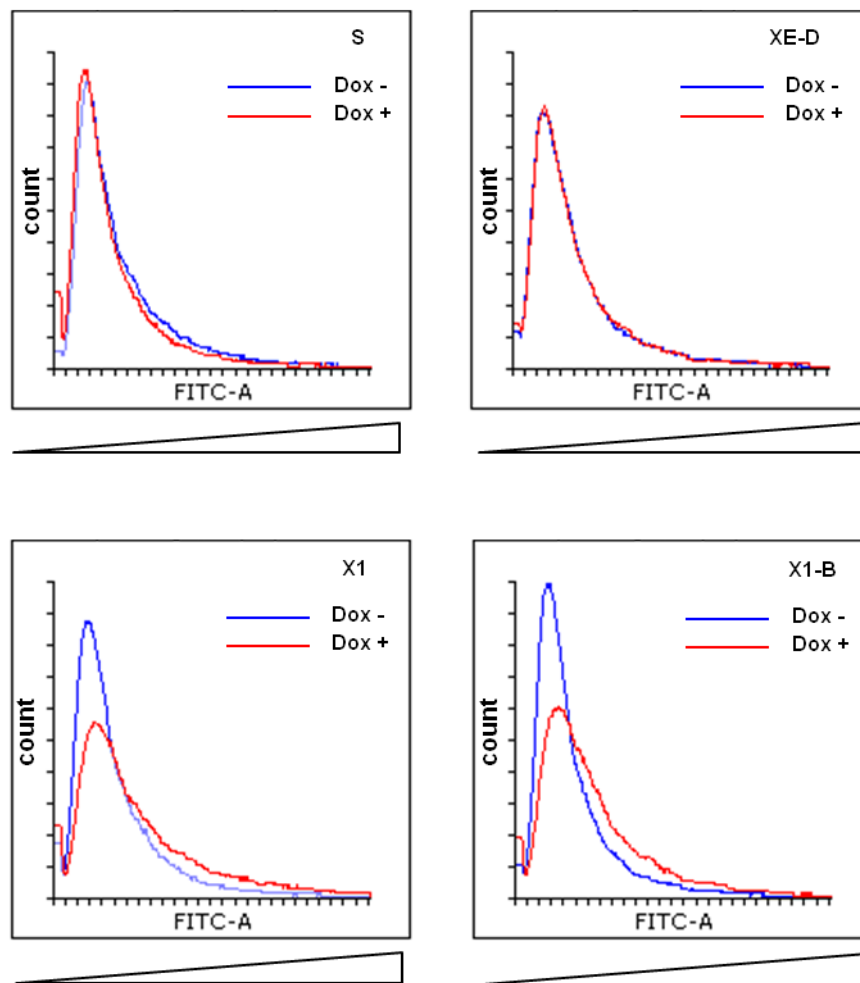


Figure 5-2 - ER expansion is triggered by doxycycline in XBP1s inducible cell lines. Cells treated with doxycycline (red line) or without doxycycline (blue line) for three days were analysed by flow cytometry to measure green fluorescence after staining with ER Tracker. Histograms of green fluorescence intensity against event count are shown for CHO-S, CHO-S XE-D, CHO-S X1 and CHO-S X1-B. Experiment was performed three times, data from a representative experiment is shown.

5.2.2 Investigation of the loss of BFP in induced X1-B cells

In the anti-BFP western blot shown in Figure 4-6, it was noted that a small decrease in BFP could be seen when X1-B was induced with doxycycline. This observation was expanded on: firstly to confirm that the observed drop was genuine and reproducible, and secondly to find the cause of this depletion of BFP. As a clarification of the differences between the two constructs in X1-B: only XBP1s expression should be altered by the presence of doxycycline, as the expression of BFP is controlled by a constitutive promoter.

X1-B cells were treated with doxycycline for three days, or left untreated, and subsequently lysed. Lysates were separated by SDS PAGE and probed with an anti-BFP antibody, and the resulting western blot is shown in Figure 5-3(i). The intensity of BFP protein was normalised to the expression of GAPDH in the same lysates, and this normalised quantification of BFP is shown in Figure 5-3(ii). The quantification confirms that BFP is found in lower abundance in doxycycline treated X1-B cells than untreated cells, and the logical implication of this is that the drop in BFP protein levels is caused directly by the upregulation of XBP1s. GAPDH is seen to drop in doxycycline treated X1-B cells, though this reduction is not equivalent to the drop seen for BFP. The reduction in GAPDH could be a reflection of reduced cell viability, which would be similar to the reduction in viable cell density observed for doxycycline treated X1 cells in Chapter 4. It is also possible that the reduction in GAPDH is a direct effect of XBP1s overexpression, as CHO-S XE-D was observed to have consistently lower levels of GAPDH than CHO-S in equivalent numbers of cells.

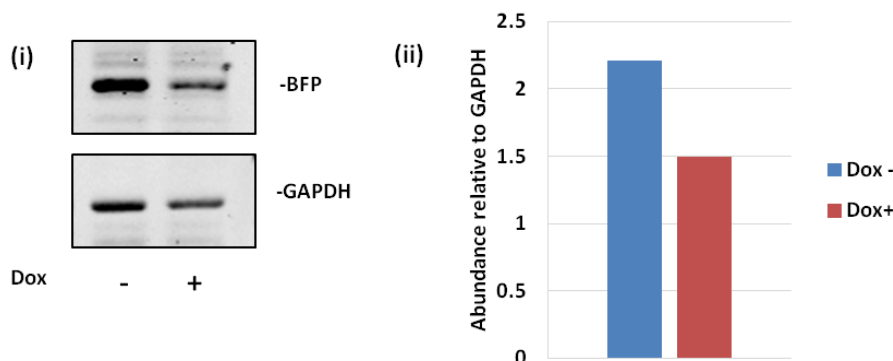


Figure 5-3 - BFP is depleted by XBP1s overexpression in X1-B cells.

(i) Anti-BFP western blot of lysates from X1-B cells induced with doxycycline for 48 hours, and anti-GAPDH blot of the same lysates, n=1. (ii) Quantification of this western blot showing BFP expression normalised to GAPDH expression.

5.2.3 The loss of BFP in induced X1-B corresponds to a reduction in blue fluorescence

In order to further explore the observed depletion of BFP, the effect of doxycycline treatment on the blue fluorescence from CHO-S X1-B cells was compared to the effect of tunicamycin treatment, which should upregulate endogenous XBP1s via triggering of the UPR. CHO-S X1 and CHO-S X1-B cells were treated with either doxycycline or 100ng/mL tunicamycin, or a combination of the two, for seven days. Treatments were refreshed once after three days of incubation, and at the end of the seven day treatment period the cells were trypsinised, washed once, and then analysed by flow cytometry. Figure 5-4 shows histograms of data captured using the Pacific Blue filter, which corresponds to the emission spectrum from BFP.

Samples of X1 cells display a single peak of low intensity blue fluorescence, which represents autofluorescence as X1 cells do not contain the BFP construct. Autofluorescence is not seen to alter with either doxycycline or tunicamycin treatment. X1-B samples display the same peak for autofluorescence as X1, but also display a second, smaller peak of higher intensity fluorescence which represents blue fluorescence emitted by BFP. It can be inferred from the large size of the autofluorescence peak in X1-B that the X1-B cell line is not clonal for BFP expression, and only a small subset of the population shows expression of BFP. For instance, in the histogram of untreated X1-B cells, only 37.9% of cells emit a higher intensity of blue fluorescence than the equivalent X1 population.

When the histograms for each cell line are overlaid, the right hand, higher intensity peak for fluorescence is seen to be largest in untreated X1-B cells, and smaller in cells treated with either doxycycline or tunicamycin. Cells incubated with both treatments are seen to have the lowest blue fluorescence of all, which suggests that the downstream effects of doxycycline and tunicamycin are cumulative. The reduction in blue fluorescence would appear to correlate with the previous result where levels of BFP protein were seen to decrease with doxycycline, and also expands on it with the observation that tunicamycin can cause a similar drop in the number of high fluorescing cells as that triggered by doxycycline. This suggests that the depletion of BFP is mediated by XBP1s, and that this XBP1s can be derived from either exogenous or endogenous sources.

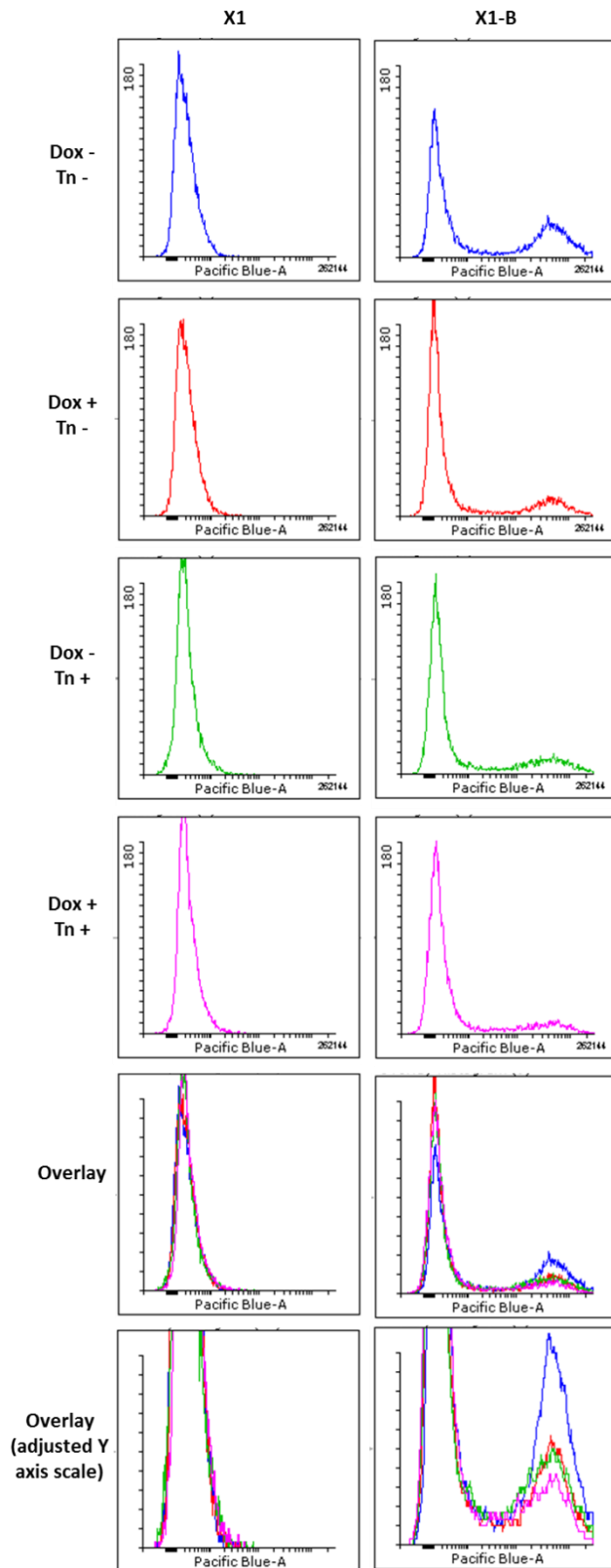


Figure 5-4 - BFP fluorescence in CHO-S X1-B cells is reduced by XBP1s induction or treatment with tunicamycin.

Histograms of blue fluorescence against cell count data from CHO-S X1 and CHO-S X1-B cells treated with doxycycline and/or tunicamycin. Two overlaid histograms are shown for each cell line below the histograms of single samples. These display the same data, but the bottom histogram has a shortened y axis scale to allow a clearer comparison of the data. Experiment was performed three times, data from a representative experiment is shown.

5.2.4 Proteasomal inhibition does not affect the loss of BFP in CHO-S X1-B

From the results obtained, it was hypothesised that the depletion of BFP was mediated by an upregulation of ERAD triggered by XBP1s overexpression, as this is a known downstream effect of XBP1s signalling (Acosta-Alvear et al. 2007). In order to test the validity of this hypothesis, the proteasome inhibitor MG132 was used to block ERAD in CHO-S X1-B cells to determine if any reduction in BFP depletion could be observed. CHO-S X1-B cells were incubated with following treatments: 1 µg/mL doxycycline or 100 ng/mL tunicamycin for three days; and/or 50 µM MG132 for six hours. Lysates from these cells were probed with anti-BFP, as shown in Figure 5-5, or anti-XBP1, as shown in Figure 5-6.

BFP is seen to decrease in abundance in cells treated with either doxycycline or tunicamycin, which correlates with the previous result from flow cytometry obtained for blue fluorescence. Contrary to what was hypothesised, the subsequent addition of MG132 to these treated cells does not inhibit the loss of BFP, and in fact makes the depletion more severe than in cells not treated with MG132. It can be seen that cells that were only treated with MG132 have a small increase in BFP, however, as each western blot was performed only once, no statistical analysis can be performed to determine if this increase is significant. Similar to the western blot in Figure 5-3, a drop in GAPDH expression can be seen in cells treated with either doxycycline or with tunicamycin when compared to untreated cells. As previously mentioned, this could be attributed to a drop in viable cell density caused by the added treatment, or could reflect a change in cell metabolism caused directly by XBP1s overexpression.

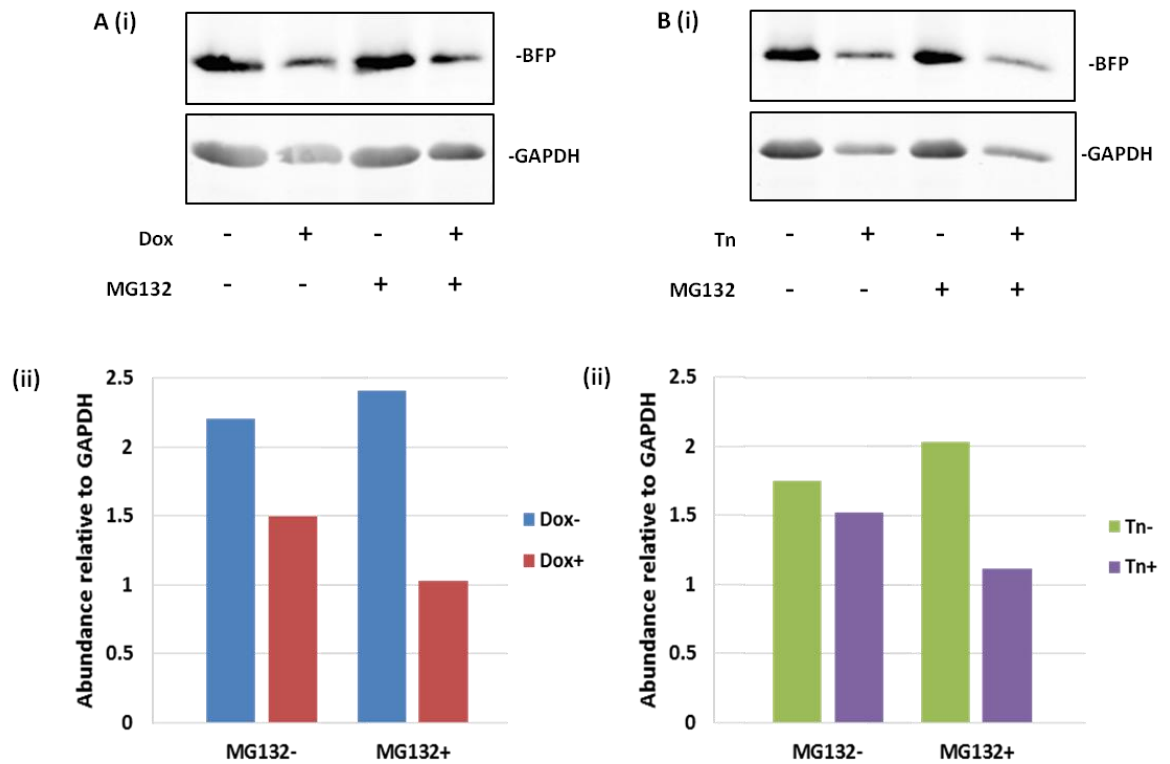


Figure 5-5 - Proteasome inhibition does not block the depletion of BFP in induced X1-B cells.

Anti-BFP western blot of lysates from X1-B cells treated with (A) doxycycline (B) tunicamycin, and/or the proteasome inhibitor MG132, n=1. (ii) Quantification of these western blots showing the relative abundance of BFP normalised against GAPDH expression.

The same lysates as shown in Figure 5-5 were probed with anti-XBP1S, and the resulting western blots are shown in Figure 5-6. XBP1S is seen to be induced by doxycycline, indicating that the inducible construct is functional and responds to doxycycline. There is a large increase in XBP1S abundance in cells treated with both doxycycline and MG132 when compared to cells only treated with doxycycline. As XBP1s protein is known to be turned-over rapidly by proteasomal degradation (Tirosh et al. 2006), the sharp increase in XBP1S in the presence of MG132 is likely to be due to the accumulation of protein that cannot be degraded, rather than any increase in gene expression. This result indicates that the dose and time period of MG132 treatment used is sufficient to inhibit the activity of the proteasome and, therefore, the loss of BFP observed in Figures 5-3, 5-4 and 5-5 appears to be mediated by a mechanism other than proteasomal degradation.

In Figure 5-6B(i), cells treated with tunicamycin for six hours are not seen to display any quantifiable upregulation of XBP1S. However, there does appear to be an increase in endogenous XBP1S in MG132 treated cells, which is likely to be due to the accumulation of protein which would otherwise be degraded by the proteasome, similar to the accumulation observed in Figure 5-6A.

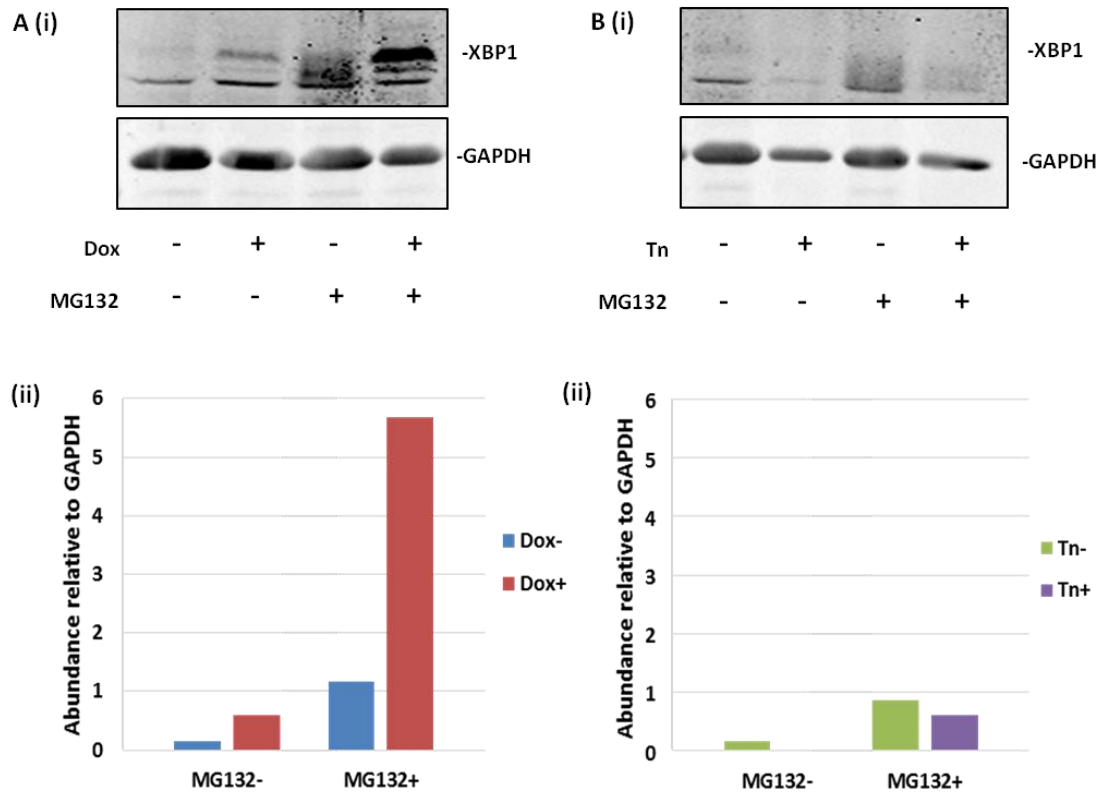


Figure 5-6 - XBP1S protein levels with proteasome inhibition.

Anti-XBP1S western blot of lysates from CHO-S X1-B cells treated with (A) doxycycline (B) tunicamycin, and/or the proteasome inhibitor MG132, n=1. (ii) Quantification of these western blots showing XBP1S protein levels normalised against GAPDH expression.

5.2.5 Quantification of XBP1 splicing in the presence of tunicamycin

The activity of XBP1 is known to be tightly controlled at both the transcriptional level (Lee et al. 2002; Shang and Lehrman 2004) and the protein level (Tirosh et al. 2006; Yoshida et al. 2006). The effect of induced overexpression of exogenous XBP1s on this intricately regulated system was examined: firstly, to investigate the possibility of exogenous XBP1s conferring resistance to ER stress, and secondly, to further elucidate the molecular mechanisms that regulate the activity of XBP1.

The splicing of XBP1 after the induction of exogenous XBP1s expression was analysed using an RT-PCR assay; the principle of this assay is described in Section 5.1.2. CHO-S and CHO-S X1-B cells were treated with doxycycline for 3 days, and/or tunicamycin for 3 hours, or left uninduced. RNA was extracted from the cells using Trizol reagent, and converted into cDNA by RT-PCR. Figure 5-7 shows the products amplified using primers that recognise only endogenous XBP1. Untreated CHO-S cells show a band for XBP1u and XBP1h. As XBP1h is formed from one spliced strand and one unspliced strand of XBP1, it may be surmised that untreated, unstressed cells contain a small amount of spliced XBP1. This result is consistent with a basal level of UPR signalling active under normal physiological conditions (Wang et al. 2015). The results were consistent across a number of experiments performed, and similar results were published by Shang and Lehrman. Therefore, the results seen in Figure 5-7 can be considered representative of unstressed cells.

The addition of doxycycline to CHO-S does not alter XBP1 splicing, but adding tunicamycin causes XBP1u to be spliced into XBP1s, represented by a band shift on the agarose gel. X1-B cells show the same band shift when treated with tunicamycin, however, when cells are pre-treated with doxycycline and then with tunicamycin, XBP1 splicing is shown to be remarkably reduced and the majority of XBP1 remains in the unspliced form. This reduction in splicing may indicate a resistance to ER stress, which could have implications for cell viability which will be explored more fully in future experiments. It could also be an indication of an additional level of regulation of XBP1, where IRE1 is able to detect the level of XBP1s present in the cell, and modulate its own endoribonuclease activity to downregulate the splicing of XBP1 in the presence of an abundance of XBP1s.

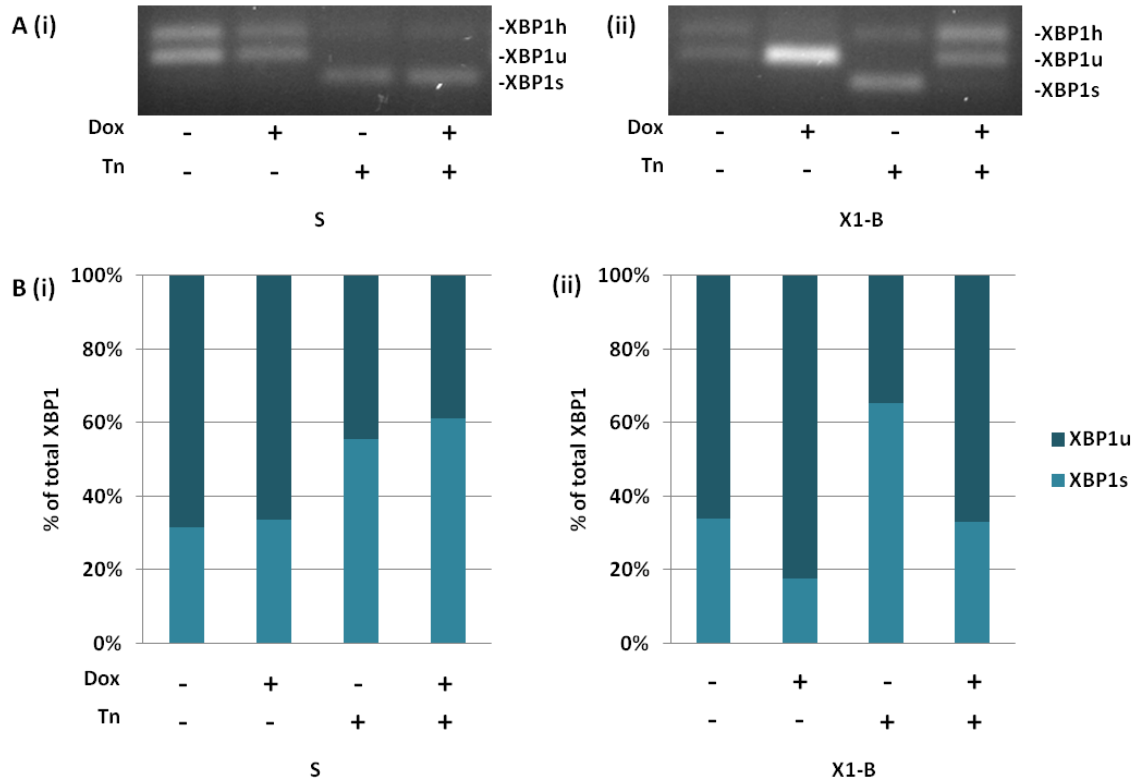


Figure 5-7 - Endogenous XBP1 splicing in tunicamycin treated cells.

(A) XBP1 splice assay of cDNA extracted from either (i) CHO-S or (ii) CHO-S X1-B cells treated with doxycycline and/or tunicamycin, using primers that anneal only to the endogenous CHO XBP1 sequence. Experiment was performed four times, data from a representative experiment is shown. (B) Densitometric quantification of the above agarose gels. For the purposes of quantification, XBP1h is considered to be 50% spliced and 50% unspliced.

When the same cDNA samples as in Figure 5-7 were amplified using the primer set that recognises both endogenous and exogenous XBP1, a different pattern of bands were observed for the X1-B samples, but not for CHO-S, as seen in Figure 5-8. This primer pair is able to detect the spliced human XBP1 expressed by the doxycycline-inducible vector, in addition to both forms of endogenous XBP1. The exogenous XBP1s band can be seen in X1-B samples treated with doxycycline, and runs at the same mobility as endogenous XBP1s. A band for XBP1s also can be seen to a lesser extent in uninduced X1-B, and this is likely to be caused by leaky expression from the pTetOne vector in the absence of doxycycline. Intriguingly, XBP1u is shown to be upregulated with doxycycline treatment, as seen in both Figure 5-7A(ii) and Figure 5-8A(ii). There is no exogenous source of XBP1u in X1-B. Therefore, the additional XBP1u observed must be endogenous. It is thought that XBP1S is able to induce the transcription of its own gene (Shang and Lehrman 2004; Yoshida et al. 2000), and the observed increase in XBP1u transcripts that occurs with a rise in XBP1S would appear to support this hypothesis.

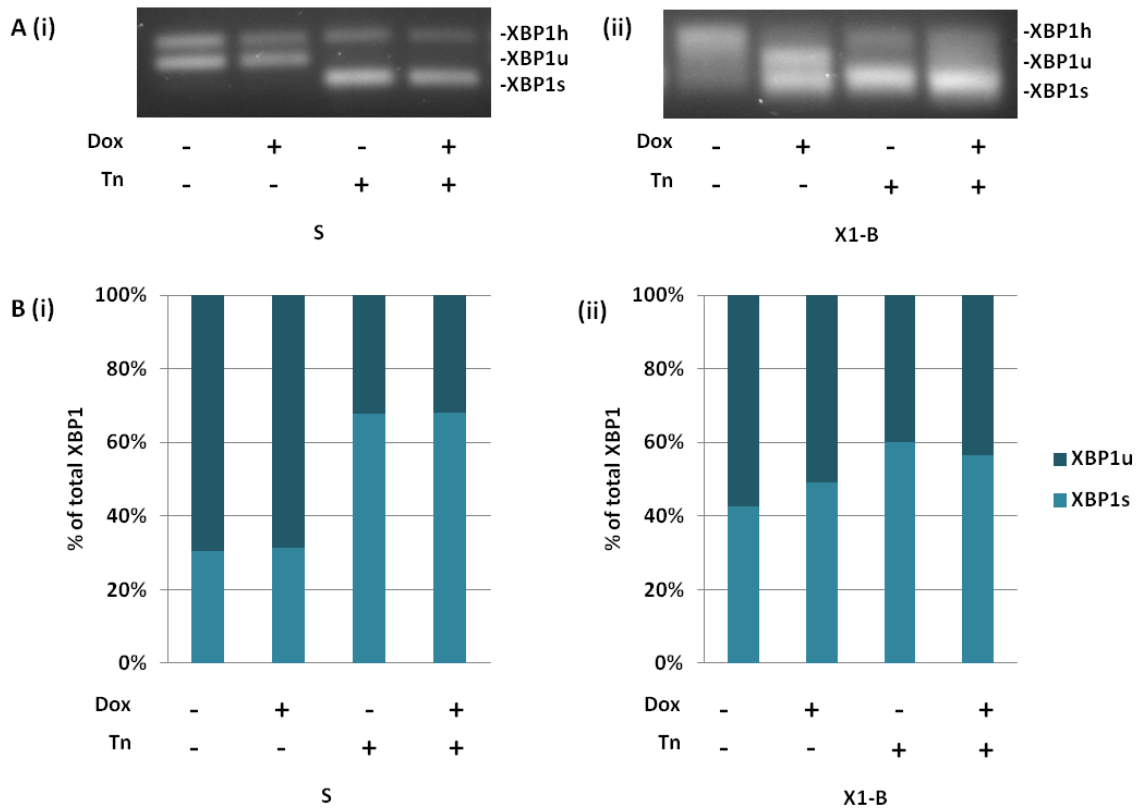


Figure 5-8 - Total XBP1 transcripts in tunicamycin treated cells.

(A) XBP1 splice assay of cDNA extracted from either (i) CHO-S or (ii) CHO-S X1-B cells treated with doxycycline and/or tunicamycin, using primers that anneal to both the endogenous sequence and the exogenous human XBP1s transcripts induced in the presence of doxycycline. Experiment was performed three times, data from a representative experiment is shown. (B) Densitometric quantification of the above agarose gels. For the purposes of quantification, XBP1h is considered to be 50% spliced and 50% unspliced.

In order to determine if the results observed in induced CHO-S X1-B, namely the upregulation of XBP1u and the downregulation of XBP1 splicing in the presence of exogenous XBP1s, are also seen in cells that stably overexpress XBP1s, a similar XBP1 splicing assay was performed in CHO-S XE-D cells. Figure 5-9 shows the PCR products generated from cDNA from CHO-S and CHO-S XE-D cells treated with or without tunicamycin, amplified using the endogenous-only primer set. Untreated CHO-S XE-D cells are seen to have more XBP1u and less XBP1h than untreated CHO-S cells. This indicates that XBP1S is able to upregulate XBP1u transcription, and also that XBP1 splicing is downregulated in XE-D when compared to CHO-S. These results in untreated XE-D cells are similar as previously observed in induced X1-B, and are likely to be due to the constitutive expression of XBP1s.

When treated with tunicamycin, the XBP1 in CHO-S cells is seen to be entirely in the spliced and hybrid forms, indicating that the UPR is strongly induced in these cells. Conversely, CHO-S XE-D cells do not display the same extent of splicing and the majority of XBP1 in these cells remains in the unspliced form. This is a similar result to what was observed in induced X1-B cells, and supports the hypothesis that an abundance of XBP1S is able to downregulate XBP1 splicing. It also indicates that the observed effects are not unique to X1-B, and is instead a general consequence of XBP1s overexpression.

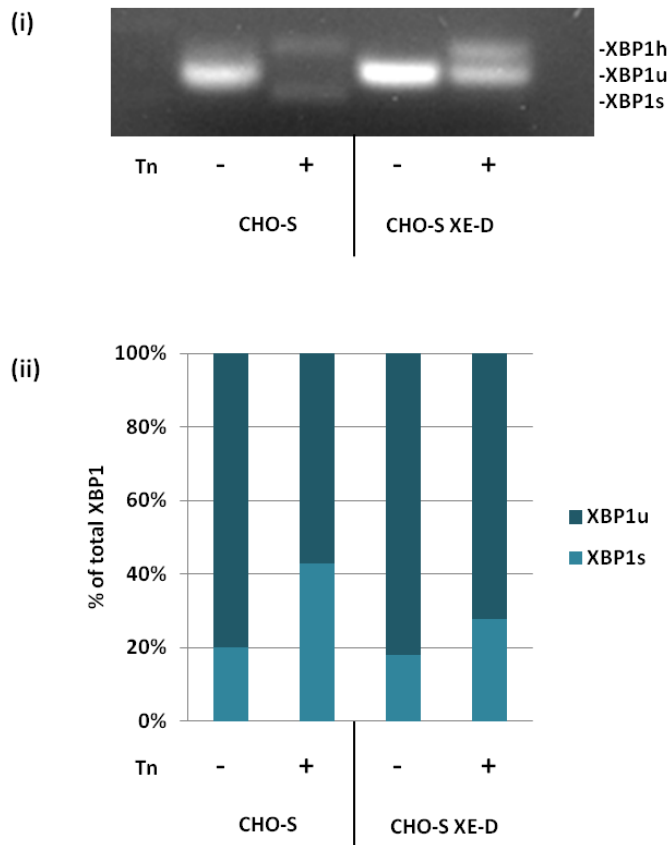


Figure 5-9 - Endogenous XBP1 splicing in CHO-S and CHO-S XE-D cells treated with tunicamycin.

(i) Agarose gel of PCR products from cDNA extracted from CHO-S and CHO-S XE-D cells treated with tunicamycin, amplified with primers that anneal to endogenous XBP1.
(ii) Quantification of the PCR products shown on the above gel.

5.2.6 Quantification of XBP1 splicing during a transient transfection

The assay was then used to determine the extent of XBP1 splicing caused by a standard transient transfection protocol, in order to find the severity of cell stress induced by transient transfection. CHO-S and CHO-S X1-B cells were either transfected with antibody heavy and light chains using the chemical transfection reagent NovaCHOice, or left untreated. The next day, each population of cells was divided into two and either induced with doxycycline or left uninduced. After an additional two days of growth, the cells were homogenised with Trizol Reagent, RNA was extracted and converted into cDNA by RT-PCR and used as a template for the XBP1 splice assay.

Figure 5-10 shows PCR products from a splice assay performed with the primers for endogenous XBP1, separated on an agarose gel. In CHO-S, very little difference in XBP1 splicing is seen when the cells are transfected or treated with doxycycline. This indicates that transient transfection does not trigger the UPR. However, when the pixel intensity of each band is quantified, as shown in Figure 5-10B(i), a subtle increase in spliced XBP1 can be seen in the transfected samples compared to the untransfected control.

A similarly subtle increase can be seen for uninduced, transfected X1-B cells in Figure 5-10B(ii). When X1-B cells are induced, however, this small increase in splicing is not seen and instead the ratio of spliced:unspliced XBP1 shifts in favour of XBP1u, similar to the result shown in Figures 5-7, 5-8 and 5-9. Generally, this experiment shows that a low level of stress is triggered by a transient transfection, but it is small compared to the ER stress caused by tunicamycin.

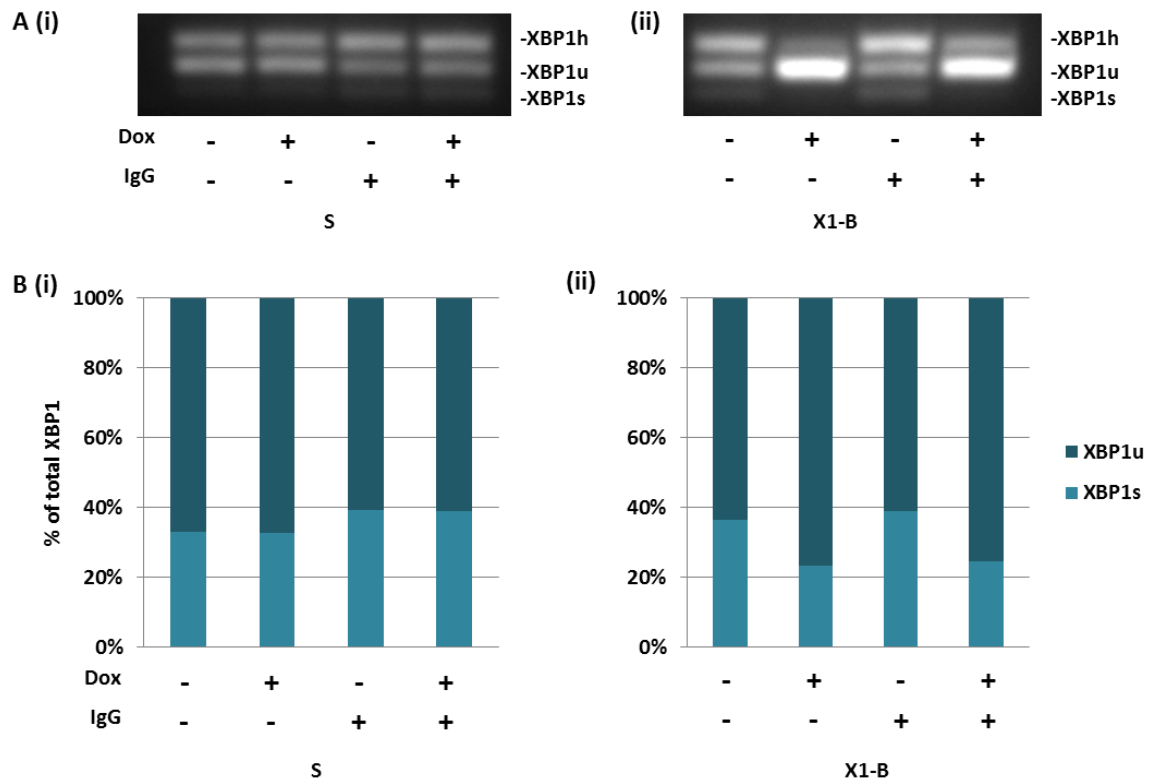


Figure 5-10 - Endogenous XBP1 splicing in transiently transfected cells.

(A) Agarose gels showing endogenous XBP1 splicing in the presence of doxycycline and/or a standard transient transfection with IgG antibody in (i) CHO-S cells and (ii) CHO-S X1-B cells, n=1. (B) Densitometric quantification of the total XBP1u and XBP1s present on the above gels. For the purposes of quantification, XBP1h is considered to be 50% spliced and 50% unspliced.

5.2.7 XBP1 splicing in cells treated with the IRE1 inhibitor 4 μ 8C

XBP1 splicing is performed by IRE1, a protein with endoribonuclease and kinase functions localised to the ER membrane which is activated during the UPR. IRE1 has other roles in the UPR besides XBP1 splicing, as it is also involved in pro-apoptotic processes through interaction with Jun Kinase and p38MAP Kinase (Urano et al. 2000b), and through a process named IRE1-mediated RNA degradation (RIDD) (Han et al. 2009; Hollien et al. 2009), both of which are active during sustained stress responses and can lead to cell death. It was hypothesised that having an exogenous source of XBP1s would selectively upregulate the functions of IRE1 that are beneficial to recombinant protein production (i.e. XBP1 signalling), while the negative aspects of IRE1 activation (i.e. apoptosis) might be downregulated.

4 μ 8C is a chemical inhibitor of IRE1 that binds to K907 of its endoribonuclease domain to block substrate binding. This inhibits two of the functions of IRE1: XBP1 splicing and RIDD, but does not inhibit its kinase activity (Cross et al. 2012). By inducing expression of XBP1s using doxycycline and subsequently blocking endogenous splicing and RIDD with 4 μ 8C, it was hypothesised that the viability of the cell could be improved by blocking the apoptotic functions of RIDD (Han et al. 2009; Hollien et al. 2009) while maintaining the larger, more efficient ER phenotype caused by XBP1S, allowing for greater production of antibody.

The effect of 4 μ 8C on the XBP1 splicing function of IRE1 was confirmed by treating CHO-S X1-B cells with varying combinations of: 1 μ g/mL doxycycline for 48 hours; 10 μ g/mL tunicamycin for three hours; and/or 32 μ M 4 μ 8C for 24 hours. cDNA was prepared from the treated cells as previously described and an XBP1 splicing assay was performed using the endogenous XBP1 primers. The PCR products generated under this range of treatments are shown in Figure 5-11. The ratio of XBP1s:XBP1u is the same under tunicamycin and doxycycline treatment as was previously observed in Figure 5-7. The addition of 4 μ 8C causes all XBP1 to exist in only the unspliced form, which implies that IRE1-mediated splicing is blocked. This effect is the same regardless of the presence of either doxycycline or tunicamycin alongside 4 μ 8C.

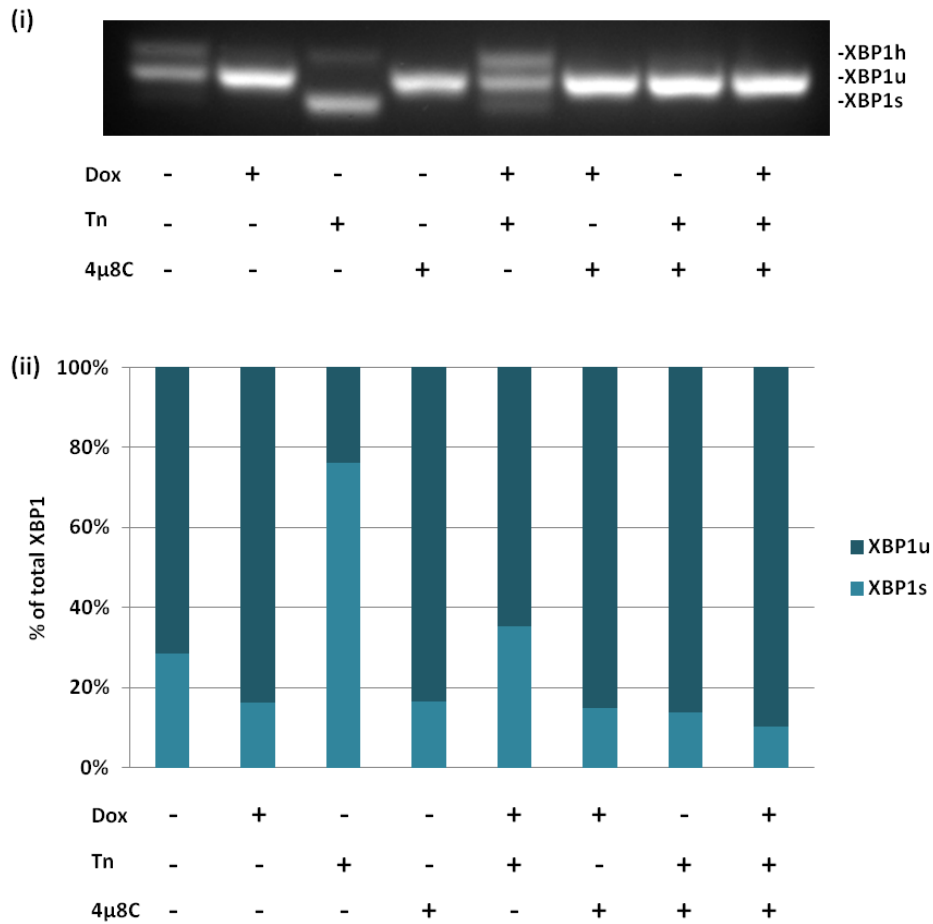


Figure 5-11 - Endogenous XBP1 splicing in X1-B cells treated with the IRE1 inhibitor 4 μ 8C.

(i) Agarose gel of PCR products resulting from primers that anneal to only endogenous XBP1, amplifying cDNA from cells treated with doxycycline, tunicamycin and/or 4 μ 8C, n=2. (ii) Quantification of the PCR products shown on the above gel.

To confirm that the presence of 4 μ 8C does not interfere with the exogenous expression of XBP1s from the pTetOne vector, the same CHO-S X1-B cDNA as used in the assay in Figure 5-11 was used in a splice assay with the endogenous/exogenous primer pair, shown in Figure 5-12. The pattern of splicing shown in the PCR products from this primer pair is unchanged from the endogenous only primers, except for the addition of a band for XBP1s in doxycycline treated cells that corresponds to exogenous XBP1s. As previously observed, X1-B cells show a small amount of exogenous XBP1s expression in the absence of doxycycline, which is thought to come from leaky expression from the pTetOne inducible vector. 4 μ 8C is shown to not influence the expression of exogenous XBP1s, only the XBP1s that is derived from XBP1u by IRE1-mediated splicing.

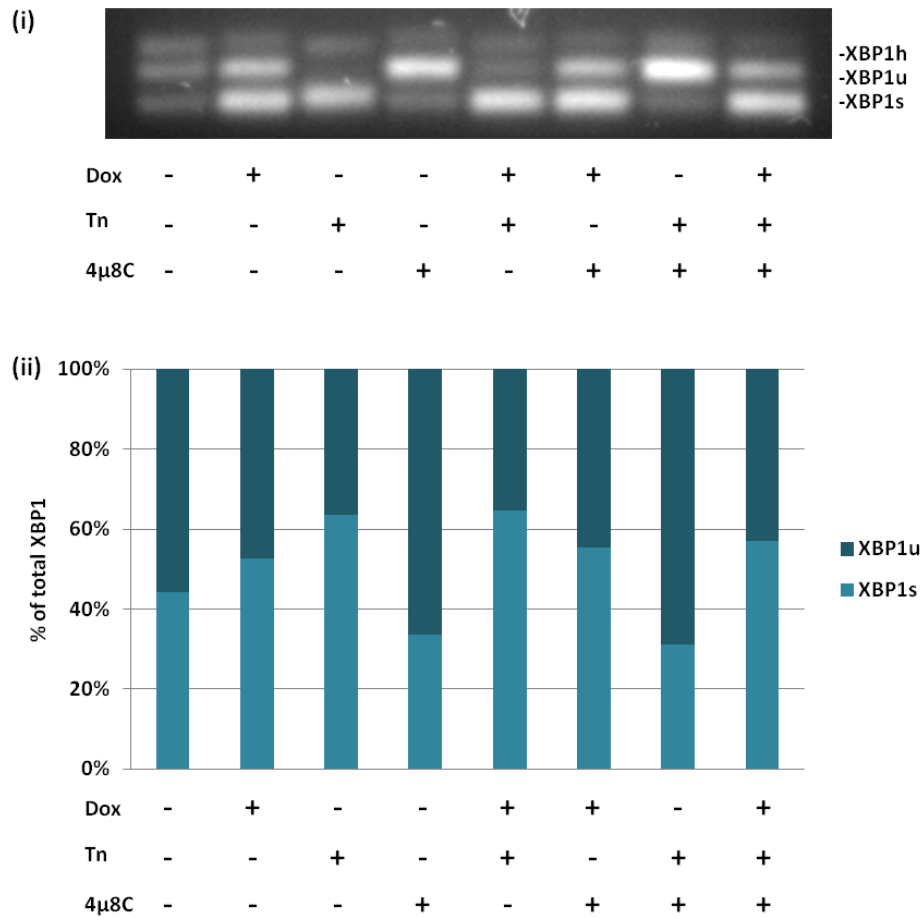


Figure 5-12 - Total XBP1 transcripts in X1-B cells treated with the IRE1 inhibitor 4 μ 8C.

(i) Agarose gel of PCR products resulting from primers that anneal to only endogenous XBP1, amplifying cDNA from cells treated with doxycycline, tunicamycin and/or 4 μ 8C, n=1. (ii) Quantification of the PCR products shown on the above gel.

5.2.8 Quantification of XBP1S protein in the presence of 4 μ 8C

After visualising the effect of 4 μ 8C on XBP1 transcript levels, the effect of the inhibitor on XBP1S protein levels was then determined. As 4 μ 8C is seen to block the generation of endogenous XBP1s, it could be predicted that the levels of XBP1S derived from endogenous XBP1s would drop as a consequence, but that XBP1S translated from exogenous XBP1s would be unaffected. To visualise XBP1S in the presence of 4 μ 8C, CHO-S and X1-B cells were treated with doxycycline and/or 4 μ 8C over three days and then lysed. Lysates were separated by SDS PAGE and blotted with anti-XBP1S.

A band corresponding to XBP1S protein can be seen in both CHO-S and X1-B samples. The intensity of this band was unexpected, as previous applications of this primary antibody did not reveal the endogenous protein, only the overexpressed, exogenous protein. The antibody used in this western blot was a fresh batch ordered from the same manufacturer, and there may have been variation in the efficacy of different batches of the same antibody. Induced X1-B cells are seen to have an abundance of XBP1S, as previously observed, and CHO-S and uninduced X1-B have relatively little. Interestingly, cells treated with 4 μ 8C show a reduction in XBP1S compared to their untreated counterparts, and even induced X1-B has less XBP1S when also treated with 4 μ 8C. This drop in protein levels is likely to be due to two reasons. Firstly, the inhibition of IRE1 by 4 μ 8C results in the blocking of XBP1 splicing, meaning that there are fewer XBP1s transcripts to be translated into XBP1S protein. Secondly, the corresponding increase in XBP1u transcripts results in more XBP1U being translated, which functions as a regulator of the levels of XBP1S by binding it and targeting it to the proteasome (Yoshida et al. 2006). Together, these two effects contribute to a drop in XBP1S.

In doxycycline treated X1-B cells, there appears to be two higher molecular weight species above XBP1S. Similar high molecular weight species have been previously observed on an anti-XBP1S blot (Chen and Qi 2010), and were proposed to represent XBP1S that had undergone SUMOylation. The activity of XBP1S as a transcription factor is known to be repressed by SUMOylation at K276 and K297 on the C terminal transactivation domain, and the band at approximately 65kDa was therefore identified as XBP1S that had undergone one SUMOylation event and the 80kDa band as XBP1S with two SUMO tags.

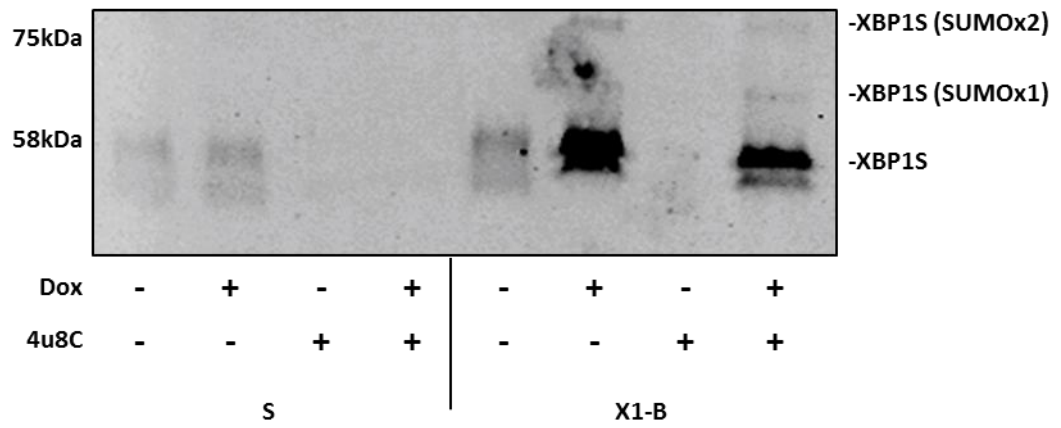


Figure 5-13 - XBP1S protein levels in cells treated with 4 μ 8C.

Western blot of crude lysates from CHO-S and CHO-S X1-B cells treated with doxycycline and/or 4 μ 8C over three days, separated by SDS PAGE under reduced conditions and blotted with anti-XBP1S, n=1.

5.2.9 ER amount in the presence of 4 μ 8C

As the presence of 4 μ 8C is shown to reduce the abundance of XBP1S, it was possible that this reduction would affect the amount of ER by preventing downstream XBP1S signalling. There were three potential consequences of 4 μ 8C treatment on ER size: firstly, that all 4 μ 8C treated cells would have less ER than their untreated counterparts due to the reduction in XBP1S; secondly, that the presence of 4 μ 8C would only block the expansion of the ER in X1-B cells triggered by exogenous XBP1S expression, but IRE1 inhibition in CHO-S would have no effect; and thirdly, that 4 μ 8C would have no effect on the amount of ER in any of the cells.

To test these hypothetical outcomes, a portion of cells from the CHO-S and X1-B samples that had been used for the western blot shown in Figure 5-13 were retained and treated with ER Tracker. After quenching and washing, the cells were analysed by flow cytometry to measure green fluorescence resulting from the ER specific stain. As previously seen in Figure 5-2, the amount of ER membrane in CHO-S cells does not change in response to doxycycline. However, a small degree of expansion can be seen in CHO-S cells treated only with 4 μ 8C. As the lysates from these cells shown in Figure 5-13 show that there are undetectable levels of XBP1S in these cells, it is not clear why the ER of these cells is seen to expand. The only conclusion that can be drawn is that this expansion is mediated by a mechanism independent of XBP1S.

CHO-S X1-B exhibits ER expansion in the presence of doxycycline, as previously observed in Figure 5-2. The addition of 4 μ 8C does not increase or decrease the amount of ER, either in doxycycline treated or untreated cells. This result would appear to correlate with the western blot data in Figure 5-13, which displays high levels of XBP1S in X1-B cells treated with doxycycline. As this abundance is only marginally reduced by the presence of 4 μ 8C, it appears that downstream XBP1S is not compromised and ER expansion is able to occur.

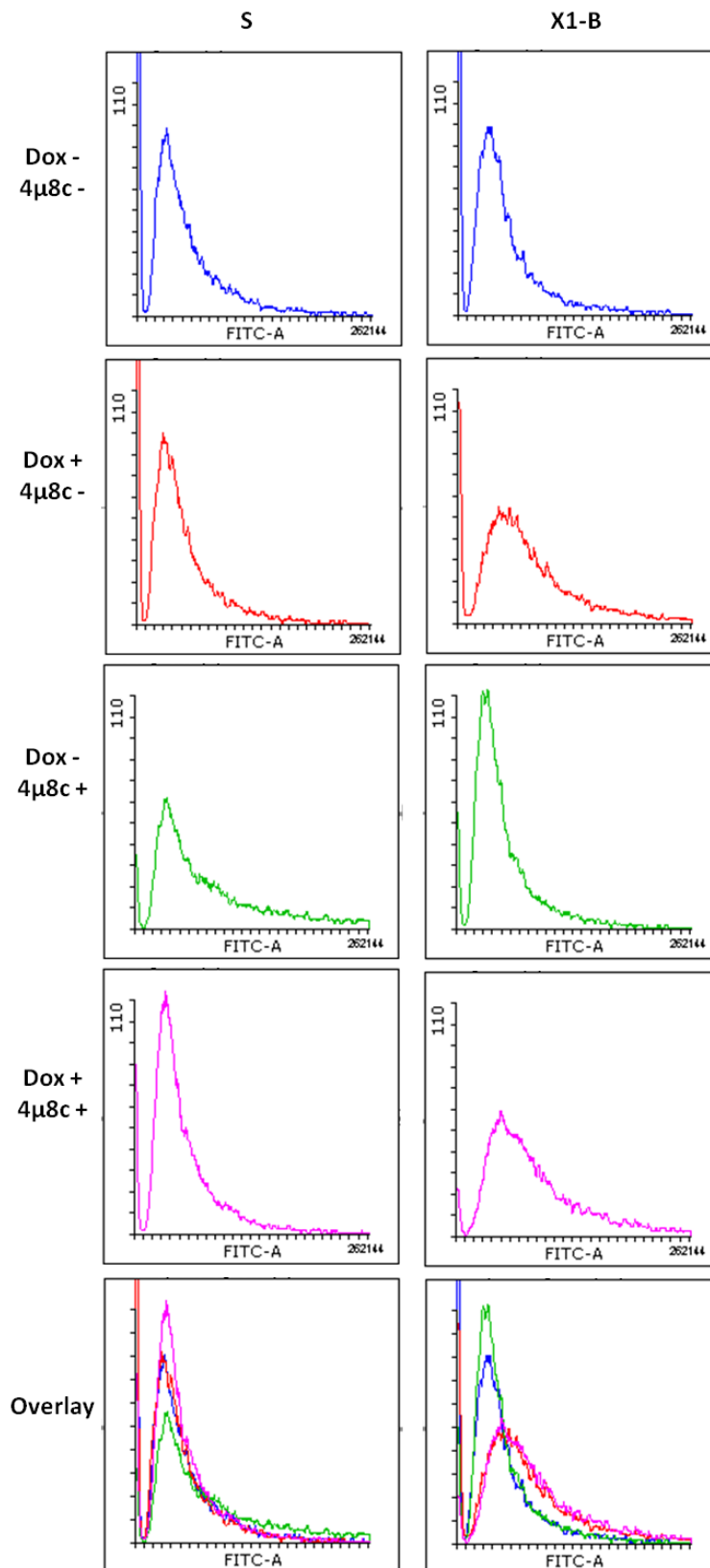


Figure 5-14 - ER size in 4μ8C treated cells.

Histograms of green fluorescence, as a representative of ER size, in CHO-S and CHO-S X1-B cells resulting from treatment with ER Tracker. Cells were treated with doxycycline and/or the IRE1 inhibitor 4μ8C over three days.

5.2.10 Antibody productivity in the presence of 4 μ 8C

The aim of the experiments involving 4 μ 8C was to find if the inhibition of IRE1 in induced X1-B, or any cell line with upregulated XBP1S, would improve cell viability during the transient production of recombinant protein by inhibiting IRE1-mediated proapoptotic pathways. As the induction of XBP1s overexpression has been shown to both improve antibody yield (Figure 4-14) and reduce viable cell density (Figure 4-11), it was hypothesised that the reduction in cell viability could be alleviated by the presence of 4 μ 8C while the secretion of antibody would be either unaffected or improved, leading to an overall enhancement in productivity.

In order to quantify the effect of 4 μ 8C on productivity, CHO-S X1-B cells were transiently transfected with antibody and then split evenly into eight flasks. Two of these flasks were induced with doxycycline, two were treated only with 4 μ 8C, two were treated with both doxycycline and 4 μ 8C and the final two were left untreated. The flasks were grown for three days in the presence of the treatments, and at the end of the experimental period the viable cell density of each flask was measured and the concentration of secreted antibody was calculated by antibody capture ELISA. The antibody concentration was normalised against the number of viable cells to calculate productivity, as shown in Figure 5-15.

CHO-S X1-B cells treated only with doxycycline are seen to have an increased concentration of secreted antibody compared to untreated cells, which is a result consistent to what was observed in Figure 4-14. The viability of these cells does not significantly decrease upon the addition of doxycycline. While consistent with the results in X1-B in Figure 4-14, this is a different result to the drop in viability seen in X1 in Figure 4-11. Cells treated only with 4 μ 8C have a statistically significant lower concentration of secreted antibody than untreated cells. The viability of these cells does not drop significantly, although it is not seen to improve either. The addition of 4 μ 8C with doxycycline does not improve antibody productivity beyond the improvements achieved through doxycycline treatment alone. Viable cell density is not improved in these cells compared to those only treated with doxycycline either and, in the case of experiment 3, viability is seen to drop significantly. Generally, there is no benefit to the productivity of X1-B provided by 4 μ 8C that could not have been achieved by doxycycline alone.

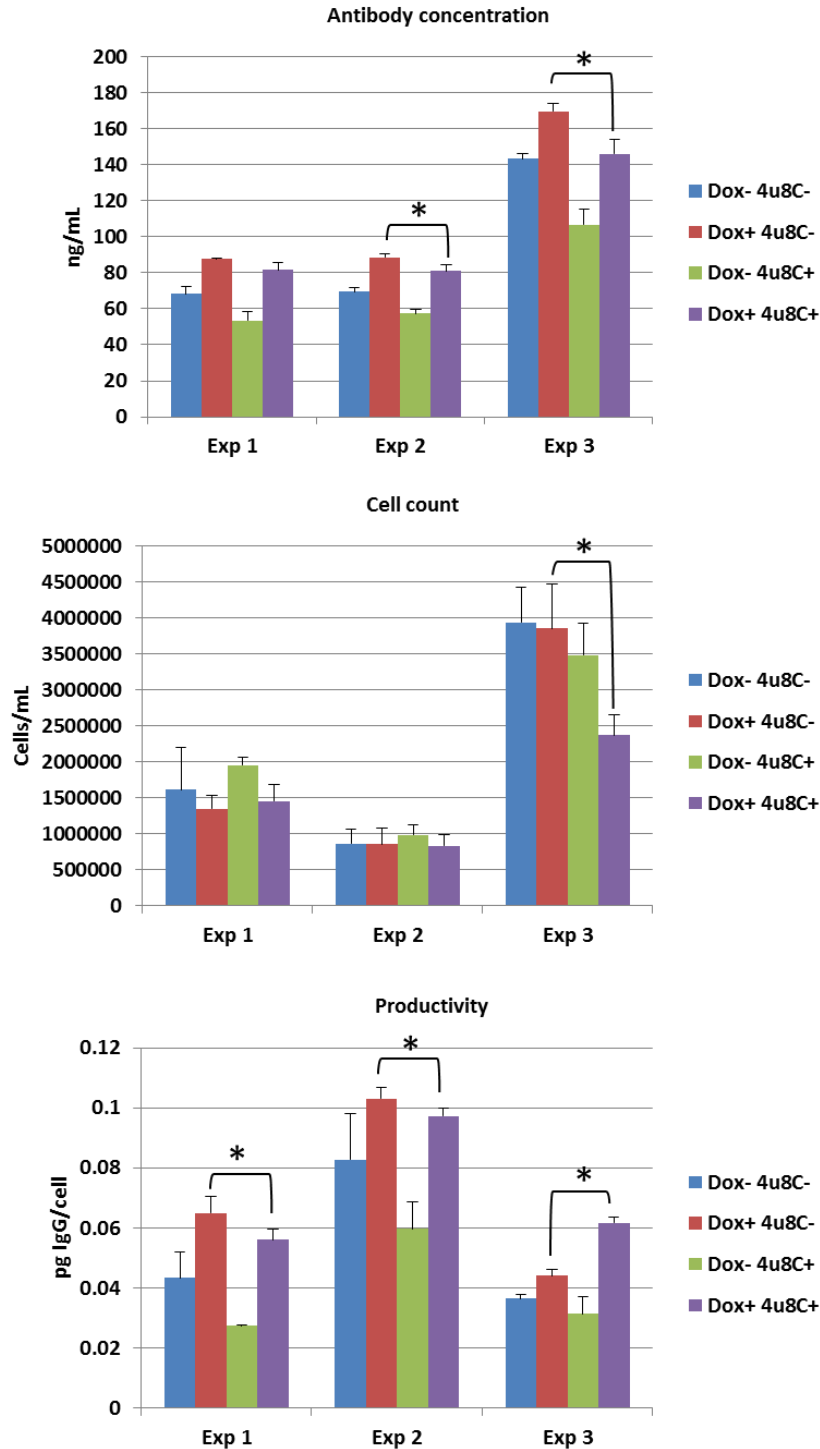


Figure 5-15 - Antibody productivity in CHO-S X1-B cells treated with 4 μ 8C.

CHO-S X1-B cells transiently transfected with antibody were cultured in duplicate with one of the four following conditions: untreated, doxycycline only, 4 μ 8C only, or doxycycline and 4 μ 8C together. At the end of the treatment period, the concentration of secreted antibody and viable cell density were recorded, and overall productivity was calculated. Each experiment represents a single initial transfection. Instances where Dox+ 4 μ 8C- (red) samples vary significantly from Dox+ 4 μ 8C+ (purple) samples ($p < 0.05$, as determined by Student's T Test) are indicated by *. Error bars represent standard deviation across duplicate flasks.

5.3 Discussion

The consequences of XBP1s overexpression on the phenotype of CHO-S X1 and CHO-S X1-B cells were further characterised in order to unravel the reasons behind the increase in antibody yield observed in CHO-S X1-B in Chapter 4, and CHO-S XE-D in Chapter 3, as well as to gain a greater understanding of XBP1s signalling as a whole. The effect of XBP1s overexpression on ER amount, XBP1 splicing, and the depletion of exogenously expressed BFP were examined as consequences that had the potential to be relevant to the production of recombinant protein. In addition to this, the impact of an inhibitor of IRE1 on antibody yield, the amount of ER and cell viability in cells with induced XBP1s was also investigated in order to find if further improvements to productivity could be obtained beyond what was achieved by XBP1s overexpression alone.

The induction of XBP1s by doxycycline treatment in CHO-S X1 and CHO-S X1-B was shown to result in an expansion of the ER. This correlates with what is known about the downstream effect of XBP1s signalling on lipid biogenesis (Shaffer et al. 2004). However, CHO-S XE-D, a cell line with constitutive XBP1s overexpression, was observed to have a smaller ER than either X1 or X1-B cells with induced XBP1s overexpression. One possible explanation for this discrepancy is that the extent of XBP1s expression in these cells is different. As observed in Chapter 4, western blot analysis shows that lysates of XE-D contain less XBP1S than lysates from doxycycline treated X1 or X1-B, so it is possible that a high degree of XBP1s expression is required for ER expansion.

CHO-S X1-B cells were also observed have a reduction in both BFP and blue fluorescence in the presence of upregulated XBP1s, either through doxycycline induction or through the activation of the UPR by tunicamycin. This depletion of BFP was not alleviated by treatment with the 26S proteasome inhibitor MG132 at a dose that was able to cause accumulation of XBP1S, which is known to have a high turn-over rate (Tirosh et al. 2006). This result indicated that the loss of BFP is mediated by a method other than proteasomal degradation. However, another possible explanation for the result is that BFP is depleted as part of the upregulated ERAD induced by XBP1s expression, but that the protein is merely rendered undetectable by either western blotting or flow cytometry before it reaches the proteasome for final degradation. The primary antibody used to probe for BFP may not be able to recognise ubiquitinated BFP, and likewise the addition of ubiquitin may also modify its tertiary structure in a manner that abolishes its fluorescence.

It has been previously published that some ER-localised fluorescent proteins are prone to aggregation, and oligomers of these proteins can be observed on a non-reducing

western blot (Aronson et al. 2011). The ER-BFP used in this project, also known as oxBFP, was engineered from EBFP2 specifically to overcome this shortcoming and adapt the protein to the oxidising environment of the ER by the addition of three amino acid substitutions: C48S, C70V and V163A (Costantini et al. 2015). The two cysteine substitutions were found to reduce the extent of oligomerisation, and the valine substitution was required to retain the fluorescence intensity of EBFP2. In addition to these three amino acid variations, the sequence of oxBFP also contains the eight amino acid substitutions responsible for blue fluorescence that distinguish EBFP2 from EGFP (Yang et al. 1998), and the six 'superfolder' GFP mutations, which improve the folding and maturation rate of the protein (Pédelacq et al. 2006). Two additional modifications made that distinguish oxBFP from EBFP2 were a prolactin signal sequence added to the N-terminus, upstream of the BFP sequence, to target the protein to the ER, and a KDEL motif was added to the C terminus to retain the protein in the ER (Costantini et al. 2015). As it has been published that oxBFP is less prone to form oligomers than EBFP2, the ability of oxBFP to form oligomers was not reexamined in this project and it was assumed that oxBFP exists solely as a monomer. Likewise, it should also be noted that the localisation of oxBFP to the ER was not examined beyond a cursory microscopy analysis, as this was also inferred from the original published data.

The possibility exists that the BFP in X1-B had a propensity to form oligomers, which were never observed visually as X1-B lysates were exclusively examined under reduced conditions, and that these hypothetical oligomers were bound by BiP and subjected to ERAD at a higher rate than the monomeric form of BFP. The upregulation of ERAD by induced XBP1s may increase the unfolding of aggregated BFP, in a manner that rendered the protein undetectable by flow cytometry or a reduced gel, but did not lead to the degradation of BFP in the proteasome. It is also possible that BFP does in fact exist solely as a monomer, and the loss of BFP is due to it being recognised by ER quality control mechanisms as an exogenous molecule. The mechanism for this recognition is unknown, but it could ultimately involve lysosomal degradation as opposed to proteasomal degradation as a method for BFP depletion, as this form of degradation is not affected by MG132 and it is a possibility that was not investigated. Regardless of the molecular mechanism and the specific site of degradation within the cell, the observation that the overexpression of XBP1s leads to an upregulation of BFP depletion indicates an enhancement of ERAD in induced X1-B. This may contribute to an increase in protein folding efficiency that in turn leads to an increased yield of antibody.

The results from the RT-PCR assay of XBP1 splicing revealed that induced X1-B cells, as well as XE-D cells, have downregulated XBP1 splicing and upregulated XBP1 transcription when compared to cells with physiological levels of XBP1s. This result

indicates that XBP1S has the ability to downregulate the endoribonuclease activity of IRE1, which reveals a novel aspect of the regulation of XBP1 signalling. The regulation of IRE1 has been the subject of a number of studies, and its activity and abundance are known to be controlled at both the protein and the transcript level. Firstly, IRE1 activity is at least in part modulated by Sec63, which works in complex with BiP to negatively regulate IRE1 autophosphorylation. A mouse Sec63 knockout cell line was shown to have constitutive activation of IRE1 phosphorylation, regardless of the presence of ER stress (Fedele et al. 2015). Intriguingly, this study also revealed that the overexpression of XBP1s in the Sec63 knockout cell line was able to abolish the activation of Ire1 almost entirely, even in the presence of tunicamycin, indicating that Sec63 and XBP1s work in concert to regulate IRE1 phosphorylation, and an abundance of XBP1s is able to block IRE1 activation. However, this study did not examine the effect of XBP1s overexpression on IRE1 activation in a cell line with physiological levels of Sec63; circumstances which would be closer to the phenotype of X1-B. It can be inferred from the XBP1 splicing assay in X1-B and XE-D, as well as the work of Fedele and colleagues, that an abundance of XBP1s is a potent inhibitor of IRE1 autophosphorylation.

Another level in the regulation of IRE1 activity is that the abundance of IRE1 is modulated by the E3 ubiquitin ligase synoviolin (SYVN1). The ubiquitination of IRE1 by SYVN1 leads to its dislocation from the ER and degradation in the proteasome (Gao et al. 2008). SYVN1 is upregulated in collagen induced arthritis, and it is thought that the increased degradation of IRE1 administered by SYVN1 is a causative factor in this disease via the downregulation of apoptotic functions of IRE1 in synovial fibroblasts, leading to abnormal proliferation of these cells and an increase in the severity of arthritic symptoms. As this study reveals that the amount of IRE1 protein, as well as its phosphorylation state, influences the extent of its downstream activity, it would be interesting to determine IRE1 protein abundance with and without the overexpression of XBP1s, as well as levels of autophosphorylation under these circumstances. This could be revealed by western blotting of induced and uninduced X1-B lysates with phosphospecific and non-phosphospecific primary antibodies to IRE1, similar to the probes used for western blotting in (Fedele et al. 2015). As transcripts for IRE1 are also known to be degraded by the IRE1 endoribonuclease domain as part of RIDD (Tirasophon et al. 2000), the quantification of IRE1 transcript levels by PCR with IRE1 specific primers would provide a complementary experiment to the western blot data obtained for IRE1 protein. These experiments would reveal whether the downregulation of XBP1 splicing observed in XBP1s overexpressing cells is due to a loss of IRE1 protein or transcripts, or a reduction in IRE1 activation by phosphorylation.

The chemical inhibitor of IRE1 endoribonuclease activity, 4 μ 8C (Cross et al. 2012), was used alongside the induction of XBP1s with the aim of potentially improving the viability of cells which could be compromised by pro-apoptotic functions of RIDD (Han et al. 2009; Hollien et al. 2009). 4 μ 8C was shown to block the XBP1 splicing function of IRE1 entirely, even in the presence of tunicamycin, and the exogenous XBP1s induced by doxycycline treatment was unaffected by the loss of IRE1 activity. The ability of 4 μ 8C to inhibit RIDD directly was not tested, but was inferred from its original publication (Cross et al. 2012). The addition of 4 μ 8C was shown not to alter the amount of ER in either CHO-S or X1-B; however, levels of endogenous XBP1S were depleted by 4 μ 8C treatment. When the productivity of antibody in induced X1-B cells was tested it was found that both the yield of antibody and the viable cell density were not improved by the presence of 4 μ 8C. While disappointing, this result could be attributed to the fact that 4 μ 8C is an inhibitor only of XBP1 splicing and RIDD, and does not affect the kinase functions of IRE1. It therefore does not affect its interactions with phosphorylation targets such as Jun Kinase, which has known apoptotic functions (Lei and Davis 2003; Putcha et al. 2003). To date, there is no inhibitor of IRE1 available that blocks its kinase functions, but hypothetically the inhibition of both the kinase and endoribonuclease activities of IRE1 alongside the overexpression of XBP1s could lead to an improvement of cell viability.

5.3.1 Summary

To summarise the observed consequences of XBP1s overexpression in X1-B cells:

- Antibody productivity improved by 30-40%
- Increased ER size
- Upregulated PDI expression
- Upregulated degradation of ER-localised BFP
- Upregulated XBP1u expression
- Downregulated XBP1 splicing

Chapter 6 Discussion

6.1 Summary of objectives

The work presented in the previous three chapters represents a series of experiments designed to achieve the following aims, as described in Chapter 1:

1. To identify genes or pathways that can be manipulated in order to improve antibody yield from CHO host cell lines.
2. To gain a greater understanding of the biochemistry of ER stress responses; in particular, the activity and regulation of XBP1.

The specific objectives of the project were:

- To characterise the high yield host cell line CHO-S XE-D.
- To generate a series of CHO-derived cell lines with inducible overexpression of the genes XBP1s, Ero1 α or GADD34.
- To find if the overexpression of these genes individually leads to an increase in antibody yield.
- To investigate the effect of co-overexpressing these genes on antibody yield.
- To find if a chemical inhibitor of IRE1 is able to improve viability and overall productivity of the XBP1s inducible cell line.
- To investigate the effect of exogenous XBP1s induction on endogenous XBP1 expression and splicing, and the regulation of IRE1 activity.

6.1.1 Characterisation of CHO-S XE-D

The first objective that was investigated was the characterisation of CHO-S XE-D. It was discovered early in the project that the CHO-S XE cells grown at the University of Glasgow differed in a number of ways from the CHO-S XE cells grown at UCB. It was assumed that these differences were due to a speciation event that had occurred, perhaps as a result of the change in culture environment or the method by which the cells were thawed. Due to these differences, the CHO-S XE cells grown at Glasgow were designated as CHO-S XE Derivative (CHO-S XE-D) and considered to be a separate cell line from the CHO-S XE1 clone described in (Cain et al. 2013). One key difference

between XE1 and XE-D was in their rate of growth: XE1 was reported to have a fast rate of growth and robust viability, whereas XE-D grew significantly slower than parental CHO-S cells and generally had poorer viability, particularly when transfected. It should be noted that a direct comparison of the secretory properties of CHO-S XE-D and CHO-S XE1 was not performed, and only the growth characteristics and viability were compared between these clones. Despite its poor growth rate, the secretory properties of CHO-S XE-D were very strong, and this cell line was shown to secrete more protein per cell than CHO-S cells. This high yield was observed for three model proteins: IgG1 antibody, a multi-domain protein with 16 disulphide bonds; tPA, which has 23 disulphide bonds; and α 1AT, which has no disulphide bonds in its native structure. This result appeared to indicate that the higher yield observed in CHO-S XE-D was not dependent on the structure or the relative complexity of the model protein being secreted, but was instead a general attribute of the cell that could be potentially applied to any exogenously expressed protein.

It was initially thought that the only difference between CHO-S and CHO-S XE, besides the differences in yield, would be the presence of overexpressed XBP1s and Ero1 α in XE, as well as an abundance of any gene upregulated by either of these overexpressed genes. However, work on the CHO-S XE-D lineage appeared to indicate that there was more variation than previously thought between these two cell lines, such as the differences in rate of growth and cell size, but the exact molecular nature of these differences was not known. CHO-S XE-D was shown to display higher levels of transiently transfected GFP, as measured by western blotting, and higher levels of green fluorescence resulting from this GFP, as measured by flow cytometry. This interesting result provided the first indication that XBP1s was not solely responsible for the strong secretory properties of CHO-S XE-D, as the folding of GFP, a single domain cytosolic protein with no disulphide bonds, should not logically have been improved by the presence of upregulated chaperones provided by XBP1s.

CHO-S XE-D was also found to have higher levels of many endogenous proteins than CHO-S. These proteins included chaperones and foldases, such as BiP and PDI, which have a known link to XBP1 signalling (Lee et al. 2003), but also the so-called 'housekeeping' proteins actin and GAPDH, which are not known to be affected by XBP1s. Again, this result indicates differences in CHO-S XE-D that are not related to XBP1s. The variations between CHO-S and CHO-S XE-D could have arisen as a result of spontaneous genomic mutation, possibly during clonal selection or cryopreservation. Transcriptomics analysis could be used to reveal a more complete picture of genes with altered expression in CHO-S XE-D compared to CHO-S. It could be predicted that a large number of genes would have varied expression levels between these cell lines, and the

identity of these genes could be determined by a transcriptomics method such as a gene array. Any identified gene with a predicted role in protein secretion could then be further analysed using an inducible system such as pTetOne to find the individual contribution of this gene towards the phenotype of CHO-S XE-D.

The differences between CHO-S and CHO-S XE-D could also be solely due to the activity XBP1s and Ero1 α , as initially hypothesised. In order to determine if this is the case, and to find the specific role of XBP1s and Ero1 α overexpression to the characteristics of CHO-S XE and XE-D, these genes could be knocked down or knocked out to find if this results in the high productivity characteristics being compromised. Knockdown by siRNA was attempted in (Page 2012), but only partial knockdown was achieved for Ero1 α and no reduction in XBP1 expression was observed at all. Targeting of XBP1 with siRNA appeared to induce XBP1 gene expression rather than repress it, therefore, another strategy for depleting XBP1 activity may be required. Genome editing by CRISPR/Cas9 may be able to remove the sequence of both the endogenous and exogenous forms of XBP1 from CHO-S XE-D. However, the limitation of this powerful technique is that it involves the generation of a new clonal cell line derived from the parental CHO-S XE-D population. As CHO cells are known to be prone to genomic mutation (Chasin and Urlaub 1975), the process of genome editing followed by clonal selection may result in a cell line that differs from CHO-S XE-D by more than simply the loss of either XBP1 or Ero1 α . This variation between cell lines may reduce the reliability of any direct comparisons made between the populations of cells, therefore, genome editing of CHO-S XE-D by CRISP/Cas9 may have limited value. Another possible method of comparing CHO-S and CHO-S XE-D would be to obtain full genomic sequences of these cell lines in order to undertake genomic analysis; however, this is likely to be prohibitively expensive.

6.1.2 Investigation of CHO-S cell lines with inducible gene overexpression

Following the characterisation of CHO-S XE-D, the next experimental strategy undertaken was to engineer cell lines with inducible overexpression of XBP1s, GADD34 or Ero1 α , as this would allow comparative analysis of populations of cells that differed in only the presence or absence of a single overexpressed gene. This would enable a more definitive assessment of the specific roles of each of these genes individually towards the secretory characteristics of CHO cells. Although the GADD34 and Ero1 α overexpressing cell lines, G1 and E1, did not display any increase in antibody yield with gene induction, the XBP1s inducible cell line, X1, and a derivative of this cell line with ER-localised blue fluorescent protein, X1-B, both displayed increased antibody productivity when XBP1s was overexpressed. X1 and X1-B were found to have an

expanded ER when XBP1s was induced, which correlates with what is known about the downstream effects of XBP1s (Lee et al. 2003; Shaffer et al. 2004), and they also appeared to have more ER than CHO-S XE-D. It was initially hypothesised that the amount of ER would directly correlate with the ability of that cell to secrete protein, in that the larger the ER, the higher yield of protein. The relative ER amounts of X1, X1-B and XE-D do not correlate directly with their yield of transiently transfected antibody, as XE-D had a far higher yield than X1 or X1-B, but had the least ER. Therefore, it appears that ER membrane size, as determined by uptake of ER Tracker dye, is not an appropriate marker of a high yield cell line. However, as the yield of X1 and X1-B improves with XBP1s overexpression, it is likely that another outcome of XBP1 signalling, such as chaperone upregulation, is responsible for improving the yield of antibody in these cell lines.

The Ero1 α inducing cell line, E1, was shown to have no increase in antibody yield when Ero1 α was overexpressed. This partially invalidates one hypothesis about the mechanism behind the high yield of CHO-S XE; that XBP1s and Ero1 α are individually capable of increasing yield when overexpressed, and their effects are cumulative when co-overexpressed. This hypothesis was based on work by UCB researchers, where a CHO-K1 cell line overexpressing Ero1 α , CHO-K1 E, had a higher yield of antibody than either wild-type CHO-S or CHO-K1 (Cain et al. 2013). The predecessor population to CHO-S XE, CHO-S X, which overexpresses only XBP1s, also had higher yield than either of these wild-type lineages (Cain et al. 2013). The variation in the results between E1 and CHO-K1 E could be attributed to inherent differences between CHO-S and CHO-K1, in that there may be a bottleneck in the CHO-K1 secretory pathway that can be alleviated by Ero1 α overexpression, whereas no such bottleneck exists in CHO-S and Ero1 α overexpression in this cell line has no discernible effect.

One potential area of future investigation into the effects of Ero1 α overexpression on protein yield would be to examine the effects of a mutant form of Ero1 α which is engineered to be constitutively active. This mutant has two regulatory cysteines, C104 and C131, mutated to alanines to abolish the formation of the regulatory disulphide that would normally block the activity of the Ero1 α active site (Baker et al. 2008). The C104,131A mutant would hypothetically have a greater ability to reoxidise PDI than wild-type; however, as this reoxidation reaction generates the reactive oxygen species hydrogen peroxide as a by-product (Gross et al. 2006), it could also be predicted that overexpression of this constitutively active form of Ero1 α would be damaging to cells. This detrimental effect has been shown in a HEK293 cell line with inducible overexpression of C104,131A Ero1 α , which displayed markers of the UPR when the mutant Ero1 α was induced (Hansen et al. 2012). Additional experiments in CHO-S to

find the effect of C104,131A Ero1 α on antibody production, and to confirm any drop in cell viability in this cell line, would be an interesting avenue of investigation. One strategy to offset any cellular damage caused by the abundance of hydrogen peroxide produced by C104,131A Ero1 α activity would be to co-overexpress the mutant Ero1 α with peroxiredoxin 4 (PRDX4), as this protein utilises hydrogen peroxide in the formation of *de novo* disulphide bonds (Tavender et al. 2010), and could reduce the extent of ER stress generated by Ero1 α (Tavender and Bulleid 2010). Co-overexpression of these two proteins in an antibody producing cell may result in an environment better optimised for producing high titres of secreted protein.

On the other hand, it could be argued that increased levels of Ero1 α would have a detrimental effect on protein folding. The primary purpose of controlling the activity of Ero1 α by regulatory disulphide bonds is to minimise the generation of hydrogen peroxide (Appenzeller-Herzog et al. 2008), but a second purpose is to ensure that a small amount of PDI remains in a reduced form in order to catalyse the reduction of non-native disulphides, an essential process for folding proteins to achieve their native structure (Frand and Kaiser 1998). The overexpression of Ero1 α could offset the balance of reduced and oxidised PDI, which could impede the overall efficiency of protein folding. Further investigation of the impact of wild-type Ero1 α and C104,131A Ero1 α overexpression on the secretory properties of the cell is required to determine whether this protein has a positive effect, a negative effect, or no discernible impact on antibody yield.

The GADD34 inducible cell line, G1, was hypothesised to display an improved rate of protein translation in the presence of overexpressed GADD34, as this would result in an increased ratio of the active, non-phosphorylated form of eIF2 α compared to the inactive, phosphorylated form. It was found that the overexpression of GADD34 did not improve antibody yield; however, the direct effect of GADD34 on eIF2 α phosphorylation was not determined due to the poor quality of the phosphospecific anti-eIF2 α primary antibody used in western blots of G1 lysates. Obtaining a functioning primary antibody and carrying out the appropriate western blot of induced and uninduced G1 cells would determine whether GADD34 overexpression caused the intended effect on cells.

Another strategy that could potentially improve the viability of the G1 cell line would be to treat these cells with a PERK inhibitor alongside the induction of GADD34 overexpression. By blocking the phosphorylation of eIF2 α by PERK, and subsequently overexpressing GADD34, it is hypothesised that this would improve the efficiency of protein translation and increase the yield of protein. However, this treatment would also prevent the translation of ATF4, a key UPR transcription factor with a range of both

adaptive and pro-apoptotic effects (Vattem and Wek 2004), and the outcome of PERK inhibition on induced G1 cells may be difficult to predict. Another approach that could be taken would be to generate a cell line derived from G1 that co-overexpresses GADD34 with XBP1s. This strategy was attempted and a cell line stably transfected with both GADD34-pTetOne and XBP1s-pTetOne was generated. The cell line was provisionally named GX1; however, early western blot screening showed an absence of XBP1s expression in the presence of doxycycline, and the cell line was discarded. Reattempting the generation of a cell line with this combination of inducible gene constructs may yield a host cell line with improved protein translation, from the effects of GADD34, and improved protein folding, from the effects of XBP1s.

In addition to GX1, another co-overexpressing cell line was made by stable integration of the XBP1s-pTetOne vector into the E1 cell line, which has inducible expression of Ero1 α . This cell line was named EX1 and should have had inducible expression of XBP1s and Ero1 α controlled by doxycycline, but unfortunately, EX1 was found to have lost expression of XBP1s over multiple passages. Experiments into the improvement of antibody yield in the EX1 cell line were performed, but these did not reveal an increase in antibody yield that was convincingly due to the co-overexpression of these genes. This disappointing conclusion meant that the intended experiments into the effect of co-overexpression of protein folding-related genes on antibody yield and viability could not be performed, but it remains an interesting potential avenue for future experiments.

Other UPR or protein folding related genes could be subcloned into pTetOne for controlled analysis of the effects of overexpression of these genes on antibody yield. One possibility for investigation is the ERAD component proteins EDEM2 and EDEM3, which catalyse the sequential trimming of mannose molecules from terminally misfolded proteins to induce their expulsion from the ER (Ninagawa et al. 2014). As these two cleavage events have been proposed to be rate limiting steps in mammalian ERAD (Ninagawa et al. 2014), co-overexpression of these proteins may have the effect of improving the efficiency and rate of ERAD and alleviating any ER stress caused by misfolded proteins, which could have a consequent effect on enhancing protein folding and secretion. Another possibility is to overexpress components of the Sec61 translocon using the pTetOne vector. This may have the effect of improving uptake of nascent chains into the ER, or it could also potentially result in overloading of the ER and triggering of the UPR. Co-overexpression of Sec61 components with proteins involved with export from the ER, such as COPII and/or SNAREs, could possibly compensate for this, but as Sec61, cargo proteins and SNAREs all function as part of complexes, this may be an overly simplistic approach.

On the other hand, the majority of published work on the effects of genetic manipulation of host cell lines on recombinant protein production relates to the consequences of overexpression of a single gene. Positive effects on protein titres have been observed from mammalian cells individually overexpressing genes such as XBP1s (Tigges and Fussenegger 2006), GADD34 (Omasa et al. 2008), calnexin (Chang et al. 1997), calreticulin (Chung et al. 2004), ATF4 (Ohya et al. 2008), CHOP (Nishimiya et al. 2013), ATF6 (Pybus et al. 2014) or BiP (Pybus et al. 2014), to name a few, but very few studies have combined these individual results and analysed the potential combinations of these genes. This interesting field of investigation could be explored by generating a library of pTetOne constructs, each containing a single gene. These constructs could be co-overexpressed in CHO cells and the effect of different combinations of genes on antibody titres could be examined by antibody capture ELISA, or perhaps a high throughput system such as ClonePix. This would allow for an unbiased identification of beneficial gene combinations, which could lead the generation of novel host cell lines optimised for increased protein production.

Another strategy to improve protein yield is in the use of chemical inhibitors of UPR related proteins. This possibility was explored using the compound 4 μ 8C, an inhibitor of IRE1 endoribonuclease activity. As IRE1 has a variety of roles in the UPR in addition to XBP1 splicing, including pro-apoptotic signalling (Urano et al. 2000a), it was hypothesised that inhibiting the endoribonuclease activity of IRE1 while inducing overexpression of XBP1s would result in a cell with favourable secretory properties conferred by XBP1s, but improved viability resulting from the inhibition of IRE1. This possibility was tested using 4 μ 8C on CHO-S X1-B cells with induced XBP1s. The induction of XBP1s in this cell line was already known to improve antibody yield, but it was subsequently found that the inhibition of IRE1 in addition to XBP1s overexpression did not improve antibody yield beyond XBP1s overexpression alone. An alternative approach would be to use an inhibitor of PERK instead of 4 μ 8C. This strategy could improve protein translation by preventing the phosphorylation of eIF2 α performed by PERK, while retaining the improvements in yield conferred by XBP1s. A third chemical inhibitor which could be employed is an inhibitor of the Sec61 translocon named eeyarestatin (Cross et al. 2009). While a strong dose of this inhibitor would block import of nascent chains into the ER and succeed only in killing the cell, a low dose of this inhibitor over multiple passages could prompt adaptation of cells with stably upregulated ER import and improved ER capacity.

6.1.3 Investigation into the biochemistry of XBP1 signalling

The overexpression of exogenous XBP1s was found to upregulate the expression of XBP1u transcripts, and also downregulate endogenous XBP1 splicing. Cells with overexpressed XBP1s that were subsequently treated with the ER stress inducing drug tunicamycin were found to have reduced XBP1 splicing, which indicated that IRE1 was able to sense the abundance of XBP1s in the cell and modulate its own endoribonuclease activity. The molecular mechanism of this downregulation of IRE1 is not known, but it could be determined if it is mediated through changes to IRE1 phosphorylation using a phosphospecific anti-IRE1 antibody. Western blotting using a non-phosphospecific IRE1 primary antibody would also reveal if IRE1 is degraded in the presence of an abundance of XBP1S. The levels of IRE1 transcripts in the presence and absence of XBP1S could also be determined by semi-quantitative PCR.

The effect of XBP1s overexpression on the overall viability and metabolism of cells could be determined through an MTS assay, or a similar cell viability assay. This assay uses a tetrazolium salt such as 3-(4,5-dimethylthiazol-2-yl)-5-(3-carboxymethoxyphenyl)-2-(4-sulfophenyl)-2H-tetrazolium (MTS) which is metabolised to a coloured formazan compound by viable cells (Cory et al. 1991). The resulting colour change is proportional to the number of viable cells in the population and the extent of metabolic activity of those cells, and any effect on viability resulting from an experimental treatment, such as the overexpression of XBP1s, can be measured through the extent of the colour change. This assay would allow for the quantification of any changes to overall cell metabolism caused by the treatment of an XBP1 inducible cell line with doxycycline and/or tunicamycin. As these treatments were shown to affect XBP1 splicing, IRE1 activity, and potentially the UPR as a whole, the impact of these treatments on cell viability would be interesting to quantify.

6.2 Concluding remarks

The scope of work in this project can be viewed from either an industrial perspective or an academic one, reflecting the origins of the project as an academic collaboration with industry. When viewed from an industrial, bioprocessing perspective, the most relevant aspect of the project is on improvements to antibody titres and overall protein yield from cells. The most promising direction for the future of this aspect of the project is in extensive genetic manipulation of host cell lines; in the co-overexpression of genes favourable to protein secretion, and downregulation of regulatory processes that lead to bottlenecks in production. Current published work in this area deals predominantly in the outcome of manipulation of a single gene, but a broader approach of co-overexpression may help to adapt the cells better towards an optimum secretory phenotype. The use of specific chemical inhibitors, such as the PERK inhibitor, or the slow adaptation of cells to drugs such as the Sec61 inhibitor, is another area with good potential for favourable results. These approaches may lead to advancements in host cell line generation, and subsequent improvements to industrial outputs of therapeutic proteins. This advancement would impact on the cost-of-goods involved with drug development and manufacture, and subsequently of the availability of these drugs to patients.

When the work of the project is examined from an academic perspective, the focus is shifted instead onto the broader biochemistry of ER stress responses. While these molecular interactions are relatively well understood, there are many details that are not yet unravelled. The XBP1s overexpressing cell line generated during this project allowed for the opportunity to study the consequences of an abundance of XBP1S on the regulation of XBP1 splicing and IRE1. These results indicated a downregulation in IRE1 activity, although the molecular nature of this downregulation is not known. Further experiments could further elucidate the interplay of XBP1 and IRE1 during the UPR, and potentially on other aspects of the UPR. A greater understanding of ER stress responses would impact on the understanding of how host cell lines cope with high levels of recombinant protein production, and also on the understanding the molecular basis of diseases known to involve dysregulating UPR signalling, such as Parkinson's disease (Mercado et al. 2016), inflammatory bowel disease (Kaser et al. 2010) and certain types of cancer (Koong et al. 2006; Romero-Ramirez et al. 2004).

Appendix

Purpose	Gene	Orientation	Sequence
Subcloning into pTetOne	GADD34	Forward	5'-GAATTTGCGGCCGCCACCATGGACTACAAG-3'
		Reverse	5'-GAACGCACCGGTTTCATTGGCTTGGGAAG-3'
	Ero1 α	Forward	5'-GATATATAAGCGGCCGCAAACATGGGCCGCGGC-3'
		Reverse	5'-GCGCGCACCGGTTTAATGAATATTCTG-3'
	XBP1 (Human sequence)	Forward	5'-GAAATTTGCGGCCGCCGAGATGGTGGTGGTG-3'
		Reverse	5'-GCGCGCACCGGTTTAGACACTAATCAGCTG-3'
XBP1 splicing assay	XBP1 (CHO sequence)	Forward	5'-CGCTTGGGAATGGATG-3'
		Reverse	5'-CAGGGTCCAAGTTGTCC-3'
	XBP1 (Human sequence)	Forward	5'-ACAGCGCTTGGGGATGGATG-3'
		Reverse	5'-TGACTGGGTCCAAGTTGTCC-3'

Table 2 - Primers

Sequences of primers used during the project.

List of References

- Acosta-Alvear D, Zhou Y, Blais A, Tsikitis M, Lents NH, Arias C, Lennon CJ, Kluger Y, Dynlacht BD. 2007. XBP1 controls diverse cell type- and condition-specific transcriptional regulatory networks. *Mol Cell* 27(1):53-66.
- Alt FW, Blackwell TK, Yancopoulos GD. 1987. Development of the primary antibody repertoire. *Science* 238(4830):1079-87.
- Anelli T, Alessio M, Bachi A, Bergamelli L, Bertoli G, Camerini S, Mezghrani A, Ruffato E, Simmen T, Sitia R. 2003. Thiol-mediated protein retention in the endoplasmic reticulum: the role of ERp44. *EMBO J* 22(19):5015-22.
- Appenzeller-Herzog C, Riemer J, Christensen B, Sørensen ES, Ellgaard L. 2008. A novel disulphide switch mechanism in Ero1alpha balances ER oxidation in human cells. *EMBO J* 27(22):2977-87.
- Appenzeller-Herzog C, Riemer J, Zito E, Chin KT, Ron D, Spiess M, Ellgaard L. 2010. Disulphide production by Ero1alpha-PDI relay is rapid and effectively regulated. *EMBO J* 29(19):3318-29.
- Aronson DE, Costantini LM, Snapp EL. 2011. Superfolder GFP is fluorescent in oxidizing environments when targeted via the Sec translocon. *Traffic* 12(5):543-8.
- Baker KM, Chakravarthi S, Langton KP, Sheppard AM, Lu H, Bulleid NJ. 2008. Low reduction potential of Ero1alpha regulatory disulphides ensures tight control of substrate oxidation. *EMBO J* 27(22):2988-97.
- Baumal R, Potter M, Scharff MD. 1971. Synthesis, assembly, and secretion of gamma globulin by mouse myeloma cells. 3. Assembly of the three subclasses of IgG. *J Exp Med* 134(5):1316-34.
- Belmont PJ, Tadimalla A, Chen WJ, Martindale JJ, Thuerauf DJ, Marcinko M, Gude N, Sussman MA, Glembotski CC. 2008. Coordination of growth and endoplasmic reticulum stress signaling by regulator of calcineurin 1 (RCAN1), a novel ATF6-inducible gene. *J Biol Chem* 283(20):14012-21.
- Bergman LW, Kuehl WM. 1979. Co-translational modification of nascent immunoglobulin heavy and light chains. *J Supramol Struct* 11(1):9-24.
- Bertolotti A, Zhang Y, Hendershot LM, Harding HP, Ron D. 2000. Dynamic interaction of BiP and ER stress transducers in the unfolded-protein response. *Nat Cell Biol* 2(6):326-32.
- Bibila TA, Flickinger MC. 1992. Use of a structured kinetic model of antibody synthesis and secretion for optimization of antibody production systems: I. Steady-state analysis. *Biotechnol Bioeng* 39(3):251-61.
- Borth N, Mattanovich D, Kunert R, Katinger H. 2005. Effect of increased expression of protein disulfide isomerase and heavy chain binding protein on antibody secretion in a recombinant CHO cell line. *Biotechnol Prog* 21(1):106-11.
- Brush MH, Weiser DC, Shenolikar S. 2003. Growth arrest and DNA damage-inducible protein GADD34 targets protein phosphatase 1 alpha to the endoplasmic reticulum and promotes dephosphorylation of the alpha subunit of eukaryotic translation initiation factor 2. *Mol Cell Biol* 23(4):1292-303.

- Bulleid NJ. 2012. Disulfide bond formation in the mammalian endoplasmic reticulum. *Cold Spring Harb Perspect Biol* 4(11).
- Bulleid NJ, Ellgaard L. 2011. Multiple ways to make disulfides. *Trends Biochem Sci* 36(9):485-92.
- Cabibbo A, Pagani M, Fabbri M, Rocchi M, Farmery MR, Bulleid NJ, Sitia R. 2000. ERO1-L, a human protein that favors disulfide bond formation in the endoplasmic reticulum. *J Biol Chem* 275(7):4827-33.
- Cain K, Peters S, Hailu H, Sweeney B, Stephens P, Heads J, Sarkar K, Ventom A, Page C, Dickson A. 2013. A CHO cell line engineered to express XBP1 and ERO1-L α has increased levels of transient protein expression. *Biotechnol Prog* 29(3):697-706.
- Calame K, Rogers J, Early P, Davis M, Livant D, Wall R, Hood L. 1980. Mouse Cmu heavy chain immunoglobulin gene segment contains three intervening sequences separating domains. *Nature* 284(5755):452-5.
- Cao Y, Kimura S, Park JY, Yamatani M, Honda K, Ohtake H, Omasa T. 2011. Chromosome identification and its application in Chinese hamster ovary cells. *BMC Proc* 5 Suppl 8:O8.
- Caramelo JJ, Castro OA, de Prat-Gay G, Parodi AJ. 2004. The endoplasmic reticulum glucosyltransferase recognizes nearly native glycoprotein folding intermediates. *J Biol Chem* 279(44):46280-5.
- Carvalho P, Stanley AM, Rapoport TA. 2010. Retrotranslocation of a misfolded luminal ER protein by the ubiquitin-ligase Hrd1p. *Cell* 143(4):579-91.
- Chakrabarti A, Chen AW, Varner JD. 2011. A review of the mammalian unfolded protein response. *Biotechnol Bioeng* 108(12):2777-93.
- Chakravarthi S, Bulleid NJ. 2004. Glutathione is required to regulate the formation of native disulfide bonds within proteins entering the secretory pathway. *J Biol Chem* 279(38):39872-9.
- Chambers JE, Tavender TJ, Oka OB, Warwood S, Knight D, Bulleid NJ. 2010. The reduction potential of the active site disulfides of human protein disulfide isomerase limits oxidation of the enzyme by Ero1 α . *J Biol Chem* 285(38):29200-7.
- Chang KH, Kim KS, Kim JH. 1999. N-acetylcysteine increases the biosynthesis of recombinant EPO in apoptotic Chinese hamster ovary cells. *Free Radic Res* 30(2):85-91.
- Chang W, Gelman MS, Prives JM. 1997. Calnexin-dependent enhancement of nicotinic acetylcholine receptor assembly and surface expression. *J Biol Chem* 272(46):28925-32.
- Chasin LA, Urlaub G. 1975. Chromosome-wide event accompanies the expression of recessive mutations in tetraploid cells. *Science* 187(4181):1091-3.
- Chen CY, Malchus NS, Hehn B, Stelzer W, Avci D, Langosch D, Lemberg MK. 2014. Signal peptide peptidase functions in ERAD to cleave the unfolded protein response regulator XBP1u. *EMBO J* 33(21):2492-506.

- Chen H, Qi L. 2010. SUMO modification regulates the transcriptional activity of XBP1. *Biochem J* 429(1):95-102.
- Chen X, Shen J, Prywes R. 2002. The luminal domain of ATF6 senses endoplasmic reticulum (ER) stress and causes translocation of ATF6 from the ER to the Golgi. *J Biol Chem* 277(15):13045-52.
- Chivers PT, Laboissière MC, Raines RT. 1996. The CXXC motif: imperatives for the formation of native disulfide bonds in the cell. *EMBO J* 15(11):2659-67.
- Chung BK, Yusufi FN, Mariati, Yang Y, Lee DY. 2013. Enhanced expression of codon optimized interferon gamma in CHO cells. *J Biotechnol* 167(3):326-33.
- Chung CH. 2008. Managing premedications and the risk for reactions to infusional monoclonal antibody therapy. *Oncologist* 13(6):725-32.
- Chung JY, Lim SW, Hong YJ, Hwang SO, Lee GM. 2004. Effect of doxycycline-regulated calnexin and calreticulin expression on specific thrombopoietin productivity of recombinant Chinese hamster ovary cells. *Biotechnol Bioeng* 85(5):539-46.
- Coonrod A, Li FQ, Horwitz M. 1997. On the mechanism of DNA transfection: efficient gene transfer without viruses. *Gene Ther* 4(12):1313-21.
- Cory AH, Owen TC, Barltrop JA, Cory JG. 1991. Use of an aqueous soluble tetrazolium/formazan assay for cell growth assays in culture. *Cancer Commun* 3(7):207-12.
- Costantini LM, Baloban M, Markwardt ML, Rizzo M, Guo F, Verkhusha VV, Snapp EL. 2015. A palette of fluorescent proteins optimized for diverse cellular environments. *Nat Commun* 6:7670.
- Cross BC, Bond PJ, Sadowski PG, Jha BK, Zak J, Goodman JM, Silverman RH, Neubert TA, Baxendale IR, Ron D and others. 2012. The molecular basis for selective inhibition of unconventional mRNA splicing by an IRE1-binding small molecule. *Proc Natl Acad Sci U S A* 109(15):E869-78.
- Cross BC, McKibbin C, Callan AC, Roboti P, Piacenti M, Rabu C, Wilson CM, Whitehead R, Flitsch SL, Pool MR and others. 2009. Eeyarestatin I inhibits Sec61-mediated protein translocation at the endoplasmic reticulum. *J Cell Sci* 122(Pt 23):4393-400.
- de Virgilio M, Kitzmüller C, Schwaiger E, Klein M, Kreibich G, Ivessa NE. 1999. Degradation of a short-lived glycoprotein from the lumen of the endoplasmic reticulum: the role of N-linked glycans and the unfolded protein response. *Mol Biol Cell* 10(12):4059-73.
- DeLaBarre B, Christianson JC, Kopito RR, Brunger AT. 2006. Central pore residues mediate the p97/VCP activity required for ERAD. *Mol Cell* 22(4):451-62.
- Dharshanan S, Chong H, Hung C, S, Zamrod Z, Kamal N. 2011. Rapid automated selection of mammalian cell line secreting high level of humanized monoclonal antibody using Clone Pix FL system and the correlation between exterior median intensity and antibody productivity. *Electronic Journal of Biotechnology*.
- DiMasi JA, Grabowski HG, Hansen RW. 2016. Innovation in the pharmaceutical industry: New estimates of R&D costs. *J Health Econ* 47:20-33.

- Early P, Huang H, Davis M, Calame K, Hood L. 1980. An immunoglobulin heavy chain variable region gene is generated from three segments of DNA: VH, D and JH. *Cell* 19(4):981-92.
- Ecker DM, Jones SD, Levine HL. 2015. The therapeutic monoclonal antibody market. *MAbs* 7(1):9-14.
- Ellgaard L, Riek R, Braun D, Herrmann T, Helenius A, Wüthrich K. 2001. Three-dimensional structure topology of the calreticulin P-domain based on NMR assignment. *FEBS Lett* 488(1-2):69-73.
- Fedeles SV, So JS, Shrikhande A, Lee SH, Gallagher AR, Barkauskas CE, Somlo S, Lee AH. 2015. Sec63 and Xbp1 regulate IRE1 α activity and polycystic disease severity. *J Clin Invest* 125(5):1955-67.
- Fedorov AN, Baldwin TO. 1997. Cotranslational protein folding. *J Biol Chem* 272(52):32715-8.
- Feige MJ, Groscurth S, Marcinowski M, Shimizu Y, Kessler H, Hendershot LM, Buchner J. 2009. An unfolded CH1 domain controls the assembly and secretion of IgG antibodies. *Mol Cell* 34(5):569-79.
- Feige MJ, Hendershot LM, Buchner J. 2010. How antibodies fold. *Trends Biochem Sci* 35(4):189-98.
- Feige MJ, Walter S, Buchner J. 2004. Folding mechanism of the CH2 antibody domain. *J Mol Biol* 344(1):107-18.
- Frand AR, Kaiser CA. 1998. The ERO1 gene of yeast is required for oxidation of protein dithiols in the endoplasmic reticulum. *Mol Cell* 1(2):161-70.
- Frangione B, Milstein C, Franklin EC. 1968. Intrachain disulphide bridges in immunoglobulin G heavy chains. The Fc fragment. *Biochem J* 106(1):15-21.
- Frickel EM, Riek R, Jelesarov I, Helenius A, Wüthrich K, Ellgaard L. 2002. TROSY-NMR reveals interaction between ERp57 and the tip of the calreticulin P-domain. *Proc Natl Acad Sci U S A* 99(4):1954-9.
- Gachon F, Gaudray G, Thébault S, Basbous J, Koffi JA, Devaux C, Mesnard J. 2001. The cAMP response element binding protein-2 (CREB-2) can interact with the C/EBP-homologous protein (CHOP). *FEBS Lett* 502(1-2):57-62.
- Gao B, Lee SM, Chen A, Zhang J, Zhang DD, Kannan K, Ortmann RA, Fang D. 2008. Synoviolin promotes IRE1 ubiquitination and degradation in synovial fibroblasts from mice with collagen-induced arthritis. *EMBO Rep* 9(5):480-5.
- Gardner BM, Walter P. 2011. Unfolded proteins are Ire1-activating ligands that directly induce the unfolded protein response. *Science* 333(6051):1891-4.
- Gebauer F, Hentze MW. 2004. Molecular mechanisms of translational control. *Nat Rev Mol Cell Biol* 5(10):827-35.
- Gorman CM, Howard BH, Reeves R. 1983. Expression of recombinant plasmids in mammalian cells is enhanced by sodium butyrate. *Nucleic Acids Res* 11(21):7631-48.
- Gossen M, Bujard H. 1992. Tight control of gene expression in mammalian cells by tetracycline-responsive promoters. *Proc Natl Acad Sci U S A* 89(12):5547-51.

- Gossen M, Freundlieb S, Bender G, Müller G, Hillen W, Bujard H. 1995. Transcriptional activation by tetracyclines in mammalian cells. *Science* 268(5218):1766-9.
- Gross E, Sevier CS, Heldman N, Vitu E, Bentzur M, Kaiser CA, Thorpe C, Fass D. 2006. Generating disulfides enzymatically: reaction products and electron acceptors of the endoplasmic reticulum thiol oxidase Ero1p. *Proc Natl Acad Sci U S A* 103(2):299-304.
- Gulis G, Simi KC, de Toledo RR, Maranhao AQ, Brigido MM. 2014. Optimization of heterologous protein production in Chinese hamster ovary cells under overexpression of spliced form of human X-box binding protein. *BMC Biotechnol* 14:26.
- Haas IG, Wabl M. 1983. Immunoglobulin heavy chain binding protein. *Nature* 306(5941):387-9.
- Hamanaka RB, Bobrovnikova-Marjon E, Ji X, Liebhaber SA, Diehl JA. 2009. PERK-dependent regulation of IAP translation during ER stress. *Oncogene* 28(6):910-20.
- Hammond C, Braakman I, Helenius A. 1994. Role of N-linked oligosaccharide recognition, glucose trimming, and calnexin in glycoprotein folding and quality control. *Proc Natl Acad Sci U S A* 91(3):913-7.
- Han D, Lerner AG, Vande Walle L, Upton JP, Xu W, Hagen A, Backes BJ, Oakes SA, Papa FR. 2009. IRE1alpha kinase activation modes control alternate endoribonuclease outputs to determine divergent cell fates. *Cell* 138(3):562-75.
- Hansen HG, Schmidt JD, Søltøft CL, Ramming T, Geertz-Hansen HM, Christensen B, Sørensen ES, Juncker AS, Appenzeller-Herzog C, Ellgaard L. 2012. Hyperactivity of the Ero1 α oxidase elicits endoplasmic reticulum stress but no broad antioxidant response. *J Biol Chem* 287(47):39513-23.
- Harding HP, Zhang Y, Zeng H, Novoa I, Lu PD, Calfon M, Sadri N, Yun C, Popko B, Paules R and others. 2003. An integrated stress response regulates amino acid metabolism and resistance to oxidative stress. *Mol Cell* 11(3):619-33.
- Hayes NV, Smales CM, Klappa P. 2010. Protein disulfide isomerase does not control recombinant IgG4 productivity in mammalian cell lines. *Biotechnol Bioeng* 105(4):770-9.
- Haze K, Yoshida H, Yanagi H, Yura T, Mori K. 1999. Mammalian transcription factor ATF6 is synthesized as a transmembrane protein and activated by proteolysis in response to endoplasmic reticulum stress. *Mol Biol Cell* 10(11):3787-99.
- Heath JK, White SJ, Johnstone CN, Catimel B, Simpson RJ, Moritz RL, Tu GF, Ji H, Whitehead RH, Groenen LC and others. 1997. The human A33 antigen is a transmembrane glycoprotein and a novel member of the immunoglobulin superfamily. *Proc Natl Acad Sci U S A* 94(2):469-74.
- Hebert DN, Garman SC, Molinari M. 2005. The glycan code of the endoplasmic reticulum: asparagine-linked carbohydrates as protein maturation and quality-control tags. *Trends Cell Biol* 15(7):364-70.
- Helenius A, Aebi M. 2004. Roles of N-linked glycans in the endoplasmic reticulum. *Annu Rev Biochem* 73:1019-49.
- Hetz C, Glimcher LH. 2009. Fine-tuning of the unfolded protein response: Assembling the IRE1alpha interactome. *Mol Cell* 35(5):551-61.

- Hollander MC, Zhan Q, Bae I, Fornace AJ. 1997. Mammalian GADD34, an apoptosis- and DNA damage-inducible gene. *J Biol Chem* 272(21):13731-7.
- Hollien J, Lin JH, Li H, Stevens N, Walter P, Weissman JS. 2009. Regulated Ire1-dependent decay of messenger RNAs in mammalian cells. *J Cell Biol* 186(3):323-31.
- Hollien J, Weissman JS. 2006. Decay of endoplasmic reticulum-localized mRNAs during the unfolded protein response. *Science* 313(5783):104-7.
- Hosokawa N, Kamiya Y, Kamiya D, Kato K, Nagata K. 2009. Human OS-9, a lectin required for glycoprotein endoplasmic reticulum-associated degradation, recognizes mannose-trimmed N-glycans. *J Biol Chem* 284(25):17061-8.
- Huber R, Deisenhofer J, Colman PM, Matsushima M, Palm W. 1976. Crystallographic structure studies of an IgG molecule and an Fc fragment. *Nature* 264(5585):415-20.
- Inaba K, Masui S, Iida H, Vavassori S, Sitia R, Suzuki M. 2010. Crystal structures of human Ero1 α reveal the mechanisms of regulated and targeted oxidation of PDI. *EMBO J* 29(19):3330-43.
- Jayapal K, Wlaschin K, Hu W. 2007. Recombinant Protein Therapeutics from CHO cells - 20 years and counting. *CHO Consortium*. p 40-47.
- Jeong H, Sim HJ, Song EK, Lee H, Ha SC, Jun Y, Park TJ, Lee C. 2016. Crystal structure of SEL1L: Insight into the roles of SLR motifs in ERAD pathway. *Sci Rep* 6:20261.
- Jessop CE, Chakravarthi S, Garbi N, Hämmerling GJ, Lovell S, Bulleid NJ. 2007. ERp57 is essential for efficient folding of glycoproteins sharing common structural domains. *EMBO J* 26(1):28-40.
- Jessop CE, Watkins RH, Simmons JJ, Tasab M, Bulleid NJ. 2009. Protein disulphide isomerase family members show distinct substrate specificity: P5 is targeted to BiP client proteins. *J Cell Sci* 122(Pt 23):4287-95.
- Jurkin J, Henkel T, Nielsen AF, Minnich M, Popow J, Kaufmann T, Heindl K, Hoffmann T, Buslinger M, Martinez J. 2014. The mammalian tRNA ligase complex mediates splicing of XBP1 mRNA and controls antibody secretion in plasma cells. *EMBO J* 33(24):2922-36.
- Kao FT, Puck TT. 1967. Genetics of somatic mammalian cells. IV. Properties of Chinese hamster cell mutants with respect to the requirement for proline. *Genetics* 55(3):513-24.
- Kaser A, Martínez-Naves E, Blumberg RS. 2010. Endoplasmic reticulum stress: implications for inflammatory bowel disease pathogenesis. *Curr Opin Gastroenterol* 26(4):318-26.
- Kaufman RJ, Scheuner D, Schroder M, Shen X, Lee K, Liu CY, Arnold SM. 2002. The unfolded protein response in nutrient sensing and differentiation. *Nat Rev Mol Cell Biol* 3(6):411-21.
- Kaufman RJ, Wasley LC, Spiliotes AJ, Gossels SD, Latt SA, Larsen GR, Kay RM. 1985. Coamplification and coexpression of human tissue-type plasminogen activator and murine dihydrofolate reductase sequences in Chinese hamster ovary cells. *Mol Cell Biol* 5(7):1750-9.

- Kaufmann H, Mazur X, Fussenegger M, Bailey JE. 1999. Influence of low temperature on productivity, proteome and protein phosphorylation of CHO cells. *Biotechnol Bioeng* 63(5):573-82.
- Kebache S, Cardin E, Nguyen DT, Chevet E, Larose L. 2004. Nck-1 antagonizes the endoplasmic reticulum stress-induced inhibition of translation. *J Biol Chem* 279(10):9662-71.
- Kim JY, Kim YG, Lee GM. 2012. CHO cells in biotechnology for production of recombinant proteins: current state and further potential. *Appl Microbiol Biotechnol* 93(3):917-30.
- Kimata Y, Ishiwata-Kimata Y, Ito T, Hirata A, Suzuki T, Oikawa D, Takeuchi M, Kohno K. 2007. Two regulatory steps of ER-stress sensor Ire1 involving its cluster formation and interaction with unfolded proteins. *J Cell Biol* 179(1):75-86.
- Kimata Y, Kimata YI, Shimizu Y, Abe H, Farcasanu IC, Takeuchi M, Rose MD, Kohno K. 2003. Genetic evidence for a role of BiP/Kar2 that regulates Ire1 in response to accumulation of unfolded proteins. *Mol Biol Cell* 14(6):2559-69.
- Kober FX, Koelmel W, Kuper J, Drechsler J, Mais C, Hermanns HM, Schindelin H. 2013. The crystal structure of the protein-disulfide isomerase family member ERp27 provides insights into its substrate binding capabilities. *J Biol Chem* 288(3):2029-39.
- Kokame K, Kato H, Miyata T. 2001. Identification of ERSE-II, a new cis-acting element responsible for the ATF6-dependent mammalian unfolded protein response. *J Biol Chem* 276(12):9199-205.
- Koong AC, Chauhan V, Romero-Ramirez L. 2006. Targeting XBP-1 as a novel anti-cancer strategy. *Cancer Biol Ther* 5(7):756-9.
- Kruh J. 1982. Effects of sodium butyrate, a new pharmacological agent, on cells in culture. *Mol Cell Biochem* 42(2):65-82.
- Ku SC, Ng DT, Yap MG, Chao SH. 2008. Effects of overexpression of X-box binding protein 1 on recombinant protein production in Chinese hamster ovary and NS0 myeloma cells. *Biotechnol Bioeng* 99(1):155-64.
- Lee AH, Iwakoshi NN, Glimcher LH. 2003. XBP-1 regulates a subset of endoplasmic reticulum resident chaperone genes in the unfolded protein response. *Mol Cell Biol* 23(21):7448-59.
- Lee K, Tirasophon W, Shen X, Michalak M, Prywes R, Okada T, Yoshida H, Mori K, Kaufman RJ. 2002. IRE1-mediated unconventional mRNA splicing and S2P-mediated ATF6 cleavage merge to regulate XBP1 in signaling the unfolded protein response. *Genes Dev* 16(4):452-66.
- Lei K, Davis RJ. 2003. JNK phosphorylation of Bim-related members of the Bcl2 family induces Bax-dependent apoptosis. *Proc Natl Acad Sci U S A* 100(5):2432-7.
- Lilie H, Rudolph R, Buchner J. 1995. Association of antibody chains at different stages of folding: prolyl isomerization occurs after formation of quaternary structure. *J Mol Biol* 248(1):190-201.
- Lu PD, Harding HP, Ron D. 2004. Translation reinitiation at alternative open reading frames regulates gene expression in an integrated stress response. *J Cell Biol* 167(1):27-33.

- Lyles MM, Gilbert HF. 1991. Catalysis of the oxidative folding of ribonuclease A by protein disulfide isomerase: dependence of the rate on the composition of the redox buffer. *Biochemistry* 30(3):613-9.
- Maki R, Traunecker A, Sakano H, Roeder W, Tonegawa S. 1980. Exon shuffling generates an immunoglobulin heavy chain gene. *Proc Natl Acad Sci U S A* 77(4):2138-42.
- Marciniak SJ, Yun CY, Oyadomari S, Novoa I, Zhang Y, Jungreis R, Nagata K, Harding HP, Ron D. 2004. CHOP induces death by promoting protein synthesis and oxidation in the stressed endoplasmic reticulum. *Genes Dev* 18(24):3066-77.
- Mason M, Sweeney B, Cain K, Stephens P, Sharfstein ST. 2012. Identifying bottlenecks in transient and stable production of recombinant monoclonal-antibody sequence variants in Chinese hamster ovary cells. *Biotechnol Prog* 28(3):846-55.
- Matlack KE, Mothes W, Rapoport TA. 1998. Protein translocation: tunnel vision. *Cell* 92(3):381-90.
- McCullough KD, Martindale JL, Klotz LO, Aw TY, Holbrook NJ. 2001. Gadd153 sensitizes cells to endoplasmic reticulum stress by down-regulating Bcl2 and perturbing the cellular redox state. *Mol Cell Biol* 21(4):1249-59.
- Mercado G, Castillo V, Soto P, Sidhu A. 2016. ER stress and Parkinson's disease: Pathological inputs that converge into the secretory pathway. *Brain Res.*
- Mohan C, Lee GM. 2010. Effect of inducible co-overexpression of protein disulfide isomerase and endoplasmic reticulum oxidoreductase on the specific antibody productivity of recombinant Chinese hamster ovary cells. *Biotechnol Bioeng* 107(2):337-46.
- Moore K, Hollien J. 2015. Ire1-mediated decay in mammalian cells relies on mRNA sequence, structure, and translational status. *Mol Biol Cell* 26(16):2873-84.
- Ninagawa S, Okada T, Sumitomo Y, Horimoto S, Sugimoto T, Ishikawa T, Takeda S, Yamamoto T, Suzuki T, Kamiya Y and others. 2015. Forcible destruction of severely misfolded mammalian glycoproteins by the non-glycoprotein ERAD pathway. *J Cell Biol* 211(4):775-84.
- Ninagawa S, Okada T, Sumitomo Y, Kamiya Y, Kato K, Horimoto S, Ishikawa T, Takeda S, Sakuma T, Yamamoto T and others. 2014. EDEM2 initiates mammalian glycoprotein ERAD by catalyzing the first mannose trimming step. *J Cell Biol* 206(3):347-56.
- Nishimiya D, Mano T, Miyadai K, Yoshida H, Takahashi T. 2013. Overexpression of CHOP alone and in combination with chaperones is effective in improving antibody production in mammalian cells. *Appl Microbiol Biotechnol* 97(6):2531-9.
- Novoa I, Zeng H, Harding HP, Ron D. 2001. Feedback inhibition of the unfolded protein response by GADD34-mediated dephosphorylation of eIF2alpha. *J Cell Biol* 153(5):1011-22.
- Oh HK, So MK, Yang J, Yoon HC, Ahn JS, Lee JM, Kim JT, Yoo JU, Byun TH. 2005. Effect of N-Acetylcystein on butyrate-treated Chinese hamster ovary cells to improve the production of recombinant human interferon-beta-1a. *Biotechnol Prog* 21(4):1154-64.

- Ohya T, Hayashi T, Kiyama E, Nishii H, Miki H, Kobayashi K, Honda K, Omasa T, Ohtake H. 2008. Improved production of recombinant human antithrombin III in Chinese hamster ovary cells by ATF4 overexpression. *Biotechnol Bioeng* 100(2):317-24.
- Oikawa D, Kimata Y, Kohno K, Iwawaki T. 2009. Activation of mammalian IRE1alpha upon ER stress depends on dissociation of BiP rather than on direct interaction with unfolded proteins. *Exp Cell Res* 315(15):2496-504.
- Oka OB, Pringle MA, Schopp IM, Braakman I, Bulleid NJ. 2013. ERdj5 is the ER reductase that catalyzes the removal of non-native disulfides and correct folding of the LDL receptor. *Mol Cell* 50(6):793-804.
- Okumura M, Kadokura H, Inaba K. 2015. Structures and functions of protein disulfide isomerase family members involved in proteostasis in the endoplasmic reticulum. *Free Radic Biol Med* 83:314-22.
- Omasa T, Takami T, Ohya T, Kiyama E, Hayashi T, Nishii H, Miki H, Kobayashi K, Honda K, Ohtake H. 2008. Overexpression of GADD34 enhances production of recombinant human antithrombin III in Chinese hamster ovary cells. *J Biosci Bioeng* 106(6):568-73.
- Otsu M, Bertoli G, Fagioli C, Guerini-Rocco E, Nerini-Molteni S, Ruffato E, Sitia R. 2006. Dynamic retention of Ero1alpha and Ero1beta in the endoplasmic reticulum by interactions with PDI and ERp44. *Antioxid Redox Signal* 8(3-4):274-82.
- Pagani M, Fabbri M, Benedetti C, Fassio A, Pilati S, Bulleid NJ, Cabibbo A, Sitia R. 2000. Endoplasmic reticulum oxidoreductin 1-lbeta (ERO1-Lbeta), a human gene induced in the course of the unfolded protein response. *J Biol Chem* 275(31):23685-92.
- Page C. 2012. Investigating the consequences of exogenous expression of unfolded protein response components in recombinant Chinese hamster ovary cells: University of Manchester.
- Palermo DP, DeGraaf ME, Marotti KR, Rehberg E, Post LE. 1991. Production of analytical quantities of recombinant proteins in Chinese hamster ovary cells using sodium butyrate to elevate gene expression. *J Biotechnol* 19(1):35-47.
- Phi-Van L, von Kries JP, Ostertag W, Strätling WH. 1990. The chicken lysozyme 5' matrix attachment region increases transcription from a heterologous promoter in heterologous cells and dampens position effects on the expression of transfected genes. *Mol Cell Biol* 10(5):2302-7.
- Pink JR, Milstein C. 1967. Inter heavy-light chain disulphide bridge in immune globulins. *Nature* 214(5083):92-4.
- Promlek T, Ishiwata-Kimata Y, Shido M, Sakuramoto M, Kohno K, Kimata Y. 2011. Membrane aberrancy and unfolded proteins activate the endoplasmic reticulum stress sensor Ire1 in different ways. *Mol Biol Cell* 22(18):3520-32.
- Puck TT, Sanders P, Petersen D. 1964. Life cycle analysis of mammalian cells. II. Cells from the Chinese hamster ovary grown in suspension culture. *Biophys J* 4:441-50.
- Putcha GV, Le S, Frank S, Besirli CG, Clark K, Chu B, Alix S, Youle RJ, LaMarche A, Maroney AC and others. 2003. JNK-mediated BIM phosphorylation potentiates BAX-dependent apoptosis. *Neuron* 38(6):899-914.

- Pybus LP, Dean G, West NR, Smith A, Daramola O, Field R, Wilkinson SJ, James DC. 2014. Model-directed engineering of "difficult-to-express" monoclonal antibody production by Chinese hamster ovary cells. *Biotechnol Bioeng* 111(2):372-85.
- Pédelacq JD, Cabantous S, Tran T, Terwilliger TC, Waldo GS. 2006. Engineering and characterization of a superfolder green fluorescent protein. *Nat Biotechnol* 24(1):79-88.
- Qi W, Ding D, Salvi RJ. 2008. Cytotoxic effects of dimethyl sulphoxide (DMSO) on cochlear organotypic cultures. *Hear Res* 236(1-2):52-60.
- Reinhart D, Damjanovic L, Kaisermayer C, Kunert R. 2015. Benchmarking of commercially available CHO cell culture media for antibody production. *Appl Microbiol Biotechnol* 99(11):4645-57.
- Reinhart D, Sommeregger W, Debreczeny M, Gludovacz E, Kunert R. 2014. In search of expression bottlenecks in recombinant CHO cell lines--a case study. *Appl Microbiol Biotechnol* 98(13):5959-65.
- Riemer J, Hansen HG, Appenzeller-Herzog C, Johansson L, Ellgaard L. 2011. Identification of the PDI-family member ERp90 as an interaction partner of ERFAD. *PLoS One* 6(2):e17037.
- Romero-Ramirez L, Cao H, Nelson D, Hammond E, Lee AH, Yoshida H, Mori K, Glimcher LH, Denko NC, Giaccia AJ and others. 2004. XBP1 is essential for survival under hypoxic conditions and is required for tumor growth. *Cancer Res* 64(17):5943-7.
- Ron D, Walter P. 2007. Signal integration in the endoplasmic reticulum unfolded protein response. *Nat Rev Mol Cell Biol* 8(7):519-29.
- Ronzoni R, Anelli T, Brunati M, Cortini M, Fagioli C, Sitia R. 2010. Pathogenesis of ER storage disorders: modulating Russell body biogenesis by altering proximal and distal quality control. *Traffic* 11(7):947-57.
- Roth RA, Pierce SB. 1987. In vivo cross-linking of protein disulfide isomerase to immunoglobulins. *Biochemistry* 26(14):4179-82.
- Safdari Y, Farajnia S, Asgharzadeh M, Khalili M. 2013. Antibody humanization methods - a review and update. *Biotechnol Genet Eng Rev* 29:175-86.
- Satoh T, Chen Y, Hu D, Hanashima S, Yamamoto K, Yamaguchi Y. 2010. Structural basis for oligosaccharide recognition of misfolded glycoproteins by OS-9 in ER-associated degradation. *Mol Cell* 40(6):905-16.
- Scheinfeld N. 2003. Adalimumab (HUMIRA): a review. *J Drugs Dermatol* 2(4):375-7.
- Schellenberger EA, Weissleder R, Josephson L. 2004. Optimal modification of annexin V with fluorescent dyes. *Chembiochem* 5(3):271-4.
- Schneider CA, Rasband WS, Eliceiri KW. 2012. NIH Image to ImageJ: 25 years of image analysis. *Nat Methods* 9(7):671-5.
- Schrag JD, Bergeron JJ, Li Y, Borisova S, Hahn M, Thomas DY, Cygler M. 2001. The Structure of calnexin, an ER chaperone involved in quality control of protein folding. *Mol Cell* 8(3):633-44.

- Schroder M, Friedl P. 1997. Overexpression of recombinant human antithrombin III in Chinese hamster ovary cells results in malformation and decreased secretion of recombinant protein. *Biotechnol Bioeng* 53(6):547-59.
- Schroder M, Korner C, Friedl P. 1999. Quantitative analysis of transcription and translation in gene amplified Chinese hamster ovary cells on the basis of a kinetic model. *Cytotechnology* 29(2):93-102.
- Schäuble N, Lang S, Jung M, Cappel S, Schorr S, Ulucan Ö, Linxweiler J, Dudek J, Blum R, Helms V and others. 2012. BiP-mediated closing of the Sec61 channel limits Ca²⁺ leakage from the ER. *EMBO J* 31(15):3282-96.
- Sevier CS, Qu H, Heldman N, Gross E, Fass D, Kaiser CA. 2007. Modulation of cellular disulfide-bond formation and the ER redox environment by feedback regulation of Ero1. *Cell* 129(2):333-44.
- Shaffer AL, Shapiro-Shelef M, Iwakoshi NN, Lee AH, Qian SB, Zhao H, Yu X, Yang L, Tan BK, Rosenwald A and others. 2004. XBP1, downstream of Blimp-1, expands the secretory apparatus and other organelles, and increases protein synthesis in plasma cell differentiation. *Immunity* 21(1):81-93.
- Shang J, Lehrman MA. 2004. Discordance of UPR signaling by ATF6 and Ire1p-XBP1 with levels of target transcripts. *Biochem Biophys Res Commun* 317(2):390-6.
- Shen J, Chen X, Hendershot L, Prywes R. 2002. ER stress regulation of ATF6 localization by dissociation of BiP/GRP78 binding and unmasking of Golgi localization signals. *Dev Cell* 3(1):99-111.
- Shepherd C, Oka OB, Bulleid NJ. 2014. Inactivation of mammalian Ero1 α is catalysed by specific protein disulfide-isomerases. *Biochem J* 461(1):107-13.
- Shusta EV, Raines RT, Pluckthun A, Wittrup KD. 1998. Increasing the secretory capacity of *Saccharomyces cerevisiae* for production of single-chain antibody fragments. *Nat Biotechnol* 16(8):773-7.
- Sriburi R, Jackowski S, Mori K, Brewer JW. 2004. XBP1: a link between the unfolded protein response, lipid biosynthesis, and biogenesis of the endoplasmic reticulum. *J Cell Biol* 167(1):35-41.
- Stansfield SH, Allen EE, Dinnis DM, Racher AJ, Birch JR, James DC. 2007. Dynamic analysis of GS-NS0 cells producing a recombinant monoclonal antibody during fed-batch culture. *Biotechnol Bioeng* 97(2):410-24.
- Surani MA. 1979. Glycoprotein synthesis and inhibition of glycosylation by tunicamycin in preimplantation mouse embryos: compaction and trophoblast adhesion. *Cell* 18(1):217-27.
- Szegezdi E, Logue SE, Gorman AM, Samali A. 2006. Mediators of endoplasmic reticulum stress-induced apoptosis. *EMBO Rep* 7(9):880-5.
- Tavender TJ, Bulleid NJ. 2010. Peroxiredoxin IV protects cells from oxidative stress by removing H₂O₂ produced during disulphide formation. *J Cell Sci* 123(Pt 15):2672-9.
- Tavender TJ, Springate JJ, Bulleid NJ. 2010. Recycling of peroxiredoxin IV provides a novel pathway for disulphide formation in the endoplasmic reticulum. *EMBO J* 29(24):4185-97.

- Thompson LH, Baker RM. 1973. Isolation of mutants of cultured mammalian cells. *Methods Cell Biol* 6:209-81.
- Tigges M, Fussenegger M. 2006. Xbp1-based engineering of secretory capacity enhances the productivity of Chinese hamster ovary cells. *Metab Eng* 8(3):264-72.
- Tirasophon W, Lee K, Callaghan B, Welihinda A, Kaufman RJ. 2000. The endoribonuclease activity of mammalian IRE1 autoregulates its mRNA and is required for the unfolded protein response. *Genes Dev* 14(21):2725-36.
- Tirosh B, Iwakoshi NN, Glimcher LH, Ploegh HL. 2006. Rapid turnover of unspliced Xbp-1 as a factor that modulates the unfolded protein response. *J Biol Chem* 281(9):5852-60.
- Tjio JH, Puck TT. 1958. Genetics of somatic mammalian cells. II. Chromosomal constitution of cells in tissue culture. *J Exp Med* 108(2):259-68.
- Travers KJ, Patil CK, Wodicka L, Lockhart DJ, Weissman JS, Walter P. 2000. Functional and genomic analyses reveal an essential coordination between the unfolded protein response and ER-associated degradation. *Cell* 101(3):249-58.
- Trombetta ES. 2003. The contribution of N-glycans and their processing in the endoplasmic reticulum to glycoprotein biosynthesis. *Glycobiology* 13(9):77R-91R.
- Tu BP, Weissman JS. 2002. The FAD- and O(2)-dependent reaction cycle of Ero1-mediated oxidative protein folding in the endoplasmic reticulum. *Mol Cell* 10(5):983-94.
- Urano F, Bertolotti A, Ron D. 2000a. IRE1 and efferent signaling from the endoplasmic reticulum. *J Cell Sci* 113 Pt 21:3697-702.
- Urano F, Wang X, Bertolotti A, Zhang Y, Chung P, Harding HP, Ron D. 2000b. Coupling of stress in the ER to activation of JNK protein kinases by transmembrane protein kinase IRE1. *Science* 287(5453):664-6.
- Urlaub G, Chasin LA. 1980. Isolation of Chinese hamster cell mutants deficient in dihydrofolate reductase activity. *Proc Natl Acad Sci U S A* 77(7):4216-20.
- Ushioda R, Hoseki J, Araki K, Jansen G, Thomas DY, Nagata K. 2008. ERdj5 is required as a disulfide reductase for degradation of misfolded proteins in the ER. *Science* 321(5888):569-72.
- van Huizen R, Martindale JL, Gorospe M, Holbrook NJ. 2003. P58IPK, a novel endoplasmic reticulum stress-inducible protein and potential negative regulator of eIF2alpha signaling. *J Biol Chem* 278(18):15558-64.
- Vattem KM, Wek RC. 2004. Reinitiation involving upstream ORFs regulates ATF4 mRNA translation in mammalian cells. *Proc Natl Acad Sci U S A* 101(31):11269-74.
- Venetianer P. 1966. New assay of the ribonuclease-reactivating enzyme based on disulphide exchange. *Nature* 211(5049):643-4.
- Walsh G. 2014. Biopharmaceutical benchmarks 2014. *Nat Biotechnol* 32(10):992-1000.
- Wang HG, Pathan N, Ethell IM, Krajewski S, Yamaguchi Y, Shibasaki F, McKeon F, Bobo T, Franke TF, Reed JC. 1999. Ca²⁺-induced apoptosis through calcineurin dephosphorylation of BAD. *Science* 284(5412):339-43.

- Wang Y, Shen J, Arenzana N, Tirasophon W, Kaufman RJ, Prywes R. 2000. Activation of ATF6 and an ATF6 DNA binding site by the endoplasmic reticulum stress response. *J Biol Chem* 275(35):27013-20.
- Wang Y, Xing P, Cui W, Wang W, Cui Y, Ying G, Wang X, Li B. 2015. Acute Endoplasmic Reticulum Stress-Independent Unconventional Splicing of XBP1 mRNA in the Nucleus of Mammalian Cells. *Int J Mol Sci* 16(6):13302-21.
- Witzig TE. 2000. The use of ibritumomab tiuxetan radioimmunotherapy for patients with relapsed B-cell non-Hodgkin's lymphoma. *Semin Oncol* 27(6 Suppl 12):74-8.
- Wong SP, Argyros O, Harbottle RP. 2015. Sustained expression from DNA vectors. *Adv Genet* 89:113-52.
- Wurm F. 2013. CHO Quasispecies—Implications for Manufacturing Processes. *Processes*. p 296-311.
- Wurm FM. 2004. Production of recombinant protein therapeutics in cultivated mammalian cells. *Nat Biotechnol* 22(11):1393-8.
- Wurm FM, Hacker D. 2011. First CHO genome. *Nat Biotechnol* 29(8):718-20.
- Xu P, Raden D, Doyle FJ, 3rd, Robinson AS. 2005. Analysis of unfolded protein response during single-chain antibody expression in *Saccharomyces cerevisiae* reveals different roles for BiP and PDI in folding. *Metab Eng* 7(4):269-79.
- Xu X, Nagarajan H, Lewis NE, Pan S, Cai Z, Liu X, Chen W, Xie M, Wang W, Hammond S and others. 2011. The genomic sequence of the Chinese hamster ovary (CHO)-K1 cell line. *Nat Biotechnol* 29(8):735-41.
- Yamamoto K, Ichijo H, Korsmeyer SJ. 1999. BCL-2 is phosphorylated and inactivated by an ASK1/Jun N-terminal protein kinase pathway normally activated at G(2)/M. *Mol Cell Biol* 19(12):8469-78.
- Yamamoto K, Sato T, Matsui T, Sato M, Okada T, Yoshida H, Harada A, Mori K. 2007. Transcriptional induction of mammalian ER quality control proteins is mediated by single or combined action of ATF6alpha and XBP1. *Dev Cell* 13(3):365-76.
- Yang TT, Sinai P, Green G, Kitts PA, Chen YT, Lybarger L, Chervenak R, Patterson GH, Piston DW, Kain SR. 1998. Improved fluorescence and dual color detection with enhanced blue and green variants of the green fluorescent protein. *J Biol Chem* 273(14):8212-6.
- Yerganian G. 1972. History and cytogenetics of hamsters. *Prog Exp Tumor Res* 16:2-34.
- Yoshida H, Okada T, Haze K, Yanagi H, Yura T, Negishi M, Mori K. 2000. ATF6 activated by proteolysis binds in the presence of NF-Y (CBF) directly to the cis-acting element responsible for the mammalian unfolded protein response. *Mol Cell Biol* 20(18):6755-67.
- Yoshida H, Oku M, Suzuki M, Mori K. 2006. pXBP1(U) encoded in XBP1 pre-mRNA negatively regulates unfolded protein response activator pXBP1(S) in mammalian ER stress response. *J Cell Biol* 172(4):565-75.
- Yoshida H, Uemura A, Mori K. 2009. pXBP1(U), a negative regulator of the unfolded protein response activator pXBP1(S), targets ATF6 but not ATF4 in proteasome-mediated degradation. *Cell Struct Funct* 34(1):1-10.

- Zagari F, Jordan M, Stettler M, Broly H, Wurm FM. 2013. Lactate metabolism shift in CHO cell culture: the role of mitochondrial oxidative activity. *N Biotechnol* 30(2):238-45.
- Zahn-Zabal M, Kobr M, Girod PA, Imhof M, Chatellard P, de Jesus M, Wurm F, Mermod N. 2001. Development of stable cell lines for production or regulated expression using matrix attachment regions. *J Biotechnol* 87(1):29-42.
- Zboray K, Sommeregger W, Bogner E, Gili A, Sterovsky T, Fauland K, Grabner B, Stiedl P, Moll HP, Bauer A and others. 2015. Heterologous protein production using euchromatin-containing expression vectors in mammalian cells. *Nucleic Acids Res* 43(16):e102.
- Zhang B. 2009. Ofatumumab. *MAbs* 1(4):326-31.
- Zhou X, Vink M, Klaver B, Berkhout B, Das AT. 2006. Optimization of the Tet-On system for regulated gene expression through viral evolution. *Gene Ther* 13(19):1382-90.
- Zito E, Chin KT, Blais J, Harding HP, Ron D. 2010. ERO1-beta, a pancreas-specific disulfide oxidase, promotes insulin biogenesis and glucose homeostasis. *J Cell Biol* 188(6):821-32.
- Züнкler BJ, Wos-Maganga M, Panten U. 2004. Fluorescence microscopy studies with a fluorescent glibenclamide derivative, a high-affinity blocker of pancreatic beta-cell ATP-sensitive K⁺ currents. *Biochem Pharmacol* 67(8):1437-44.